NONLINEAR CONTROL OF AN AUTONOMOUS UNICYCLE ROBOT: PRACTICAL ISSUES

by

David William Vos

Hons. B. Ing. (Aeronautics), University of Stellenbosch,
South Africa (1983)
S.M., Aeronautics and Astronautics, Massachusetts Institute of Technology
(1989)

Submitted to the Department of Aeronautics and Astronautics
in Partial Fulfillment of the Requirements for the Degree of

DOCTOR OF PHILOSOPHY

at the

MASSACHUSETTS INSTITUTE OF TECHNOLOGY
June, 1992

Signature of Author _____
Department of Aeronautics and Astronautics
May 4, 1992

Certified by _____
Professor Andreas H. von Flotow
Thesis Supervisor, Associate Professor of Aeronautics and Astronautics

Certified by _____
Professor Lena Valavani
Associate Professor of Aeronautics and Astronautics

Certified by _____
Professor Christopher G. Atkeson
Associate Professor of Brain and Cognitive Science

Certified by _____
Professor Marc H. Raibert
Professor of Electrical Engineering and Computer Science

Certified by _____
Professor Jean–Jacques E. Slotine
Associate Professor of Mechanical Engineering

Accepted by _____
Professor Harold Y. Wachman
Chairman, Department Graduate Committee

NONLINEAR CONTROL OF AN AUTONOMOUS UNICYCLE ROBOT: PRACTICAL ISSUES

by

David William Vos

Submitted to the Department of Aeronautics and Astronautics on May 4, 1992
in Partial Fulfillment of the Requirements for the Degree of
Doctor of Philosophy

ABSTRACT

The control of linear and nonlinear systems with time–varying parameters is formally addressed with derivation of the correct gain scheduling control laws for guaranteed stability. Successful adaptive control of systems with uncertain friction nonlinearities is also discussed with application to compensation of destabilizing friction in a unicycle robot. The work is focused by a case study on the autonomous unicycle robot.

The effect of the nonlinear friction is to negate the stabilizing efforts of the unicycle lateral controllers. Artificial neural network friction modeling, as well as Model Reference Adaptive Control strategies are employed to cancel the friction. The MRAC methods, since these are stability based and offer structured methods of controller synthesis and tuning, prove the better approach to achieving suitable friction compensation with the important secondary effect of good stiffness in roll modes. Many alterations on the original MRAC system design are required for successful implementation. These include: Bounding of friction model parameters; Tracking error resetting; Adaptive dither signals for overpowering friction; Adding structure to the friction parameter estimation for stability under fast parameter variation.

Gain scheduling is addressed in the setting of feedback linearization, extended to feedback LTI'zation. This defines the correct gain scheduling procedure and control law for guaranteed stability with arbitrary parameter values and rates of change. Stability conditions for slowly varying *closed loop* dynamics, as well as conditions for dropping parameter rate of change dependent terms in the control law, are determined for parameters varying as fast as the system is capable. For output feedback, a single point observer, which runs in transformed coordinates, is used in an LQG controller setting. The gain scheduled controller requires only a single point design, which yields stable control of the parameter dependent system over the full operating envelope with arbitrary parameter variation.

All of the techniques are successfully implemented on the unicycle robot and demonstrated in simulation and/or experiment.

Thesis Supervisor:	Professor Andreas H. von Flotow
Title:	Associate Professor in Aeronautics and Astronautics

ACKNOWLEDGEMENTS

This idea for PhD research became reality primarily through the efforts of Andy. Many thanks are due for the hours of discussion and advice and undying enthusiasm for the work. The pleasure of working with and learning Andy's approach to problem solving, both in the academic environment as well as extramural, stands out in my review of the last five years at MIT. To Lucia and the little Flotows, thank you too.

Thanks to the rest of my committee members for their guidance and constructive crticism. To Lena for her enthusiasm, support and positive response to ideas. To Chris for his collaborated effort with Andy in obtaining the primary source of funding for this research, as well as his energetic support. To Marc for the great environment, the Leg Lab, which became home to the unicycle. To Jean–Jacques for his support and advice.

To Walt Baker and Draper Laboratory, thanks for the final injection of financial aid which carried me through completion of this work.

Thanks also to Professor Hattingh of the BMI, Stellenbosch, South Africa for his continued support and friendship. To my parents in Cape Town, South Africa, for their huge roll in my achieving these goals, I owe very much. To Norm, Mathieu, Darryll and Siggy, thanks for the friendship and many discussions in our years at MIT.

Finally, to Trix, Billy, Zingo and Umbala, thanks for always being there for me.

TABLE OF CONTENTS

CHAPTER 1. LITERATURE SURVEY AND INTRODUCTION

INTRODUCTION

The unicycle robot offers an example of applied control theory with which people can identify: most having at some stage in their lives contemplated or attempted the art of unicycling. Whether successful or not, appreciation of the difficulty of the task very quickly becomes well established.

To the best knowledge of the author, the first unicycle robot was constructed at Stanford University [*Schoonwinkel*] circa 1986 and initial efforts at computer stabilizing the unstable, non minimum phase system were demonstrated. Due to, amongst other reasons, unsuitable sensors and time constraints on completion of the work, limited success was achieved, in fact only the longitudinal control, which is the inverted pendulum problem, was successfully implemented. The unusual and highly challenging nature of the project served as motivation for the design, construction and testing of a similar unicycle robot at MIT, which lead to the body of work presented in this thesis. The work attempts to balance two important aspects of control research: namely, theoretical development (the gain scheduling problem), as well as practical development (modifying the MRAC friction cancellation strategies for successful implementation).

How Useful is a Unicycle Robot?

At first sight, the unicycle robot does not appear to have any practical use other than being an extremely good educational project for learning the details of interfacing

hardware with theoretical issues in dynamics and control. A closer look, however, reveals the (fortunate) point of view that the unicycle robot is a dynamic system which exhibits many of the control issues that both practicing control engineers and researchers have to overcome in the process of realizing a workable control strategy for many varied applications (not the least of which is a unicycle robot). For example, the system is characterized by unstable, non minimum phase behavior in both lateral and longitudinal axes. Lateral dynamics and specifically, controllability of the roll dynamics, are a strong function of wheelspeed (the roll dynamics are uncontrollable at zero wheelspeed). Nonlinear friction yaw torques, present between the wheel and surface, are important and dependent on both wheelspeed and other exogenous parameters (e.g. tire pressure, surface friction characteristics). Addressing these issues in the light of the real world limitations on theoretical solutions together with all the hardware details, presents an exciting and invigorating research environment and yields many interesting solutions which may be difficult to conceive of without such an application.

Possibly one of the leading advantages of such application oriented research, is the elimination of all doubt as to the validity of the "simulation" upon which the various control strategies are tested. Nature does not err in modeling the unicycle perfectly and in highlighting any shortcomings of the controllers.

The Unicycle: Exemplifying Specific Problems in Control of Many Systems

Many systems to be controlled exhibit dynamics which are well captured by linear time invariant (LTI) models for fixed operating conditions. Dependence of the dynamics on some time–varying parameter(s) broadens the class of systems considerably. Aircraft dynamics usually depend significantly on dynamic pressure and

angle of attack; bicycles, motor vehicles, boats and unicycles are all examples of forward speed dependent dynamic systems; the perturbational behavior of a robotic manipulator depends on both configuration and payload properties; and the list is endless.

The dynamic behaviour of the unicycle is surprisingly similar to the high frequency dynamic behaviour of an aircraft unstable in both longitudinal (short period mode) and lateral (dutch roll mode) axes. A forward swept wing aircraft such as the X–29, with only elevator and rudder actuators (as may arise in the case of aileron failure), and with friction present in the rudder actuator is one such example: the non minimum phaseness in the roll dynamics manifesting in requiring e.g. right rudder to induce roll to the left. In addition, the dynamics of an aircraft are strongly dependent on dynamic pressure and angle of attack [*McRuer, Ashkenas, Graham*], prescribing that a stabilizing controller usually needs to be scheduled according to operating condition in order to maintain good performance throughout the flight envelope; not unlike the requirement for the forward speed dependent dynamics of the unicycle. The scheduling technique may be in the form of fixed gain scheduling, fully adaptive control or a hybrid combination employing elements of both fixed point scheduling and adaptation.

The unicycle dynamics are well described by a model linearized in roll, pitch and yaw about the vertical (balanced) position [*Vos – S.M., Schoonwinkel*] facilitating application of the control engineer's favorite linear control design technique to a difficult system. The forward speed dependence of the lateral dynamics require some form of adaptation or gain scheduling [*Vos*]. Furthermore, nonlinear friction present between the tire and surface negate the efforts of the linear (gain scheduled) control system and, if not accounted for, lead to unsuccessful control of the lateral dynamics.

Combining control authority limitations with these interesting characteristics, yields a system with many of the ingredients constituting a challenging control problem.

The linear control theory literature is substantial and many synthesis techniques exist for designing linear control systems for suitable linear systems. Control synthesis techniques are not as abundant in the nonlinear control literature, although a number of extremely useful methods have been developed [*e.g. feedback and input–output linearization; sliding mode control; adaptive control. See e.g.: Isidori, Nijmeijer and van der Schaft, Aström and Wittenmark, Slotine and Li*].

Much insight to the problem of control of linear parameter dependent systems, traditionally solved by gain scheduling, is gained by viewing the problem in the framework of feedback linearization, with extension to account for the parameter variation. This thesis defines a gain scheduling design approach, which requires only a single design and which guarantees stability for arbitrary parameter values and variation of parameters. A second aspect of this thesis addresses ,by example of the unicycle robot, some of the issues necessary to yield a satisfactorily functional adaptive friction compensation strategy.

Techniques Demonstrated

A baseline controller [*chapter 2*], based on the LQR optimal control design methodology [e.g. *Bryson*] forms the backbone of the unicycle controllers. The longitudinal controller is a fixed gain LQ servo controller yielding integral servo control action on wheelspeed with inner loop stabilization of the unstable pitch dynamics. Lateral control is via a continuously gain scheduled LQ servo controller with nonlinear compensation of the yaw friction nonlinearity, with the friction

compensation parameters, in the case of the baseline controller, well tuned to a given range of wheel speeds and floor surfaces. These controllers allow commanding of heading and forward speed with full stability augmentation.

Since the baseline controller is only well tuned to specific operating conditions, adaptive control is used to overcome this limitation [*chapter 3*]. Many friction models [e.g. *Canudas, Maron, Papadopoulos, Radcliffe*] exist for various systems, such that the friction nonlinearity may be viewed in the setting of a parameter dependent nonlinearity with the parameters unknown and dependent on the operating condition. This structure is very amenable to applying Model Reference Adaptive Control (MRAC) techniques to, since the linear control design plant (ignoring the friction nonlinearity) is a natural and obvious choice for a reference model which is both achievable, and representative of the behavior expected by the controllers designed for the linear wheelspeed dependent system. Both more traditional parameter estimation laws as determined through Lyapunov analysis, and Neural Network techniques are applied to the Model Reference Adaptive Control strategy.

On occasion, use has been made of learning techniques (non–parametric regression techniques) to obtain a full forward or inverse model of the system for control [e.g. *Atkeson, Nguyen, Guez*]. In the case of the unstable, non minimum phase unicycle robot, this is not regarded a practical proposition and the MRAC and Neural network compensation in hybrid adaptive/linear gain scheduled settings are implemented as two possible friction compensation strategies. The difference being that the network is used to learn only the friction model (not the entire plant) which is invertible and static (in the sense of the functional dependence on the operating condition easily represented on a graph independent of time), thus suitable for learning by a neural network.

In the MRAC implementations, direct application of the controller as designed yields instability. A number of implementation issues thus need to be addressed for successful application. Bounding of the adaptation *parameters* is enforced to ensure that stability is maintained by not allowing large (physically meaningless) deviations of these parameters. In order to prevent propagation of model errors and sensor biases, the reference model state is periodically reset (such that the tracking error=0 at time of reset) in order to maintain a meaningful process. Without this strategy, instability occurs remarkably quickly. In addition, the typical performance of the friction compensating MRAC system, was determined to be erring on the low side, i.e. the friction compensating term is usually slightly *smaller* than the required (actual) value. The result is poor performance in roll, as these dynamics depend critically on the friction effect being *overpowered.* Use of (classical) dithering of the signals by suitable switching strategies dramatically improves the situation. Finally, for fast parameter changes, the condition $\frac{\partial(\text{parameter})}{\partial t} \approx 0$ assumed in the MRAC parameter update law, is violated. The resulting instability is prevented by defining a nominal parameter model and then only adapting on the parameter error, since $\frac{\partial(\delta\text{parameter})}{\partial t} \approx 0$ is a much more valid assumption. These are simply means of enforcing knowledge of the system onto the adaptation process, which makes good physical sense and yields much improved performance and stability.

The second major area of work of this thesis is the problem of gain scheduled control of parameter dependent systems [*chapter 4*]. As mentioned previously, many systems exhibit known parameter dependence with the parameter variation also well known or measured. The classical example is an aircraft operating at various dynamic pressures. The unicycle is another such system, with obvious favor in this work. The gain scheduling problem has traditionally been approached very much on a rule of thumb basis, and very little work has been done to define more formal strategies in

the design of such controllers. The work of [*Shamma*] is the only major contribution in this field, where extensive studying of the conditions for stability of such systems is made. The work is essentially an analysis of the traditional design approach, with the conclusions that, as assumed by rule of thumb in practice, the system may be slowly time varying and the dependence of the system on the parameter must be reflected in the control law to guarantee stability.

Some attempt at defining a framework of gain scheduling analysis is given by [*Rugh*], and the literature abounds with application of input–output or feedback linearizing techniques to obtaining adaptive control laws [e.g. *Kokotovic, Kanellakopoulos, Teel, Marino, Praly*] for the parameter dependent system, but to the best of the author's knowledge, no connection with the gain scheduling problem is made. This section of work shows that for suitable systems (feedback LTI'able), with the correct gain scheduling strategy, stability may be maintained independent of the rate of change of the parameters upon which the system dynamics depend. The control law is determined from the feedback linearizing control law, with added terms which enforce the transformed (feedback linearized) system to be both *linear* and *time invariant* (in transformed space). The gain scheduled control design strategy is extended to the case where slowly varying *closed loop system dynamics* are desired and a simple test is given (evaluated in transformed space) for evaluating stability in this case.

In addition, the case of output feedback is discussed, with application of LQG control of the system in *transformed* space. The resulting control laws are implemented in system space, with an observer which runs in transformed space. The essence of this section is the need for only a single design point observer which runs in transformed coordinates and which is driven directly by the system space sensor signals to yield estimates of the unknown states for use in the control law. This controller, designed

at only one operating parameter value is valid for operation over the entire envelope for arbitrary parameter variation.

CHAPTER 2. UNICYCLE DYNAMICS, BASELINE CONTROLLERS AND EXPERIMENTAL SETUP

UNICYCLE DYNAMICS

Introduction

The autonomous unicycle presents a novel example in the study of multibody dynamics and control. Autonomy is achieved by replacing the human unicyclist with a turntable reaction mass for lateral control and a wheel torque actuator for longitudinal control. The system consists of three connected rigid bodies; the wheel, frame and turntable (see figure 2.1). Actuation is via two DC motors which are used as torque actuators. The pitch actuator drives the unicycle wheel through a belt drive of gear ratio 72:1 and the yaw motor, driving the turntable through a spur gear drive of ratio 25:1, facilitates yaw actuation.

The linearized equations of motion are readily determined using Kane's formalism [*Vos*]. These equations, for nominal turntable velocity set to zero, yield decoupled lateral and longitudinal dynamics, hence a model well suited to linear control design techniques. The linearized longitudinal dynamics are time invariant, while the lateral dynamics depend on wheelspeed, thus requiring a gain scheduled lateral controller. Sensors are available for measuring all seven states: yaw, roll and pitch rates; roll and pitch angles as well as turntable and wheel angular velocities.

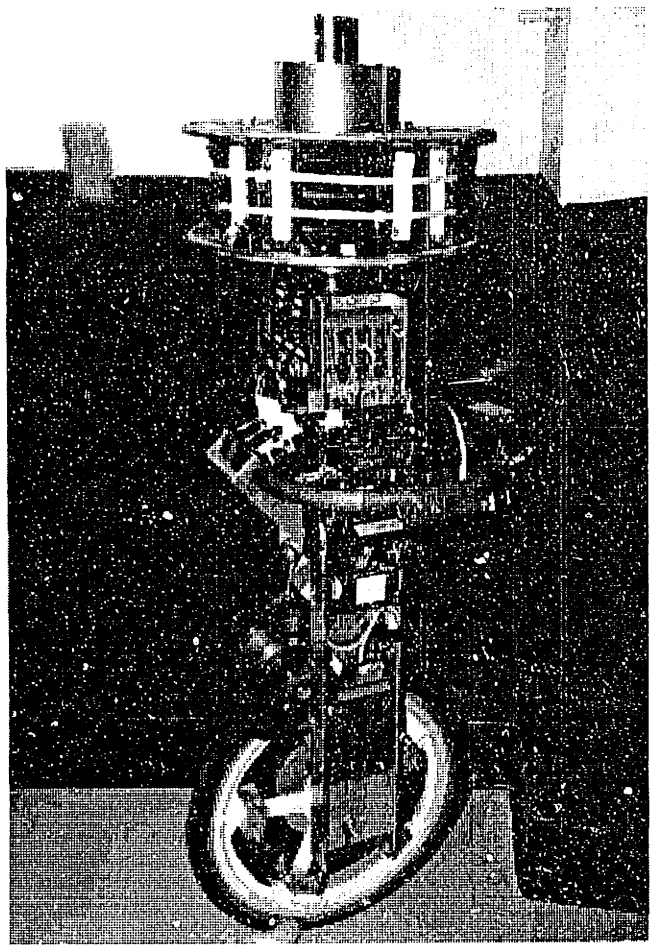

Figure 2.1. Autonomous unicycle robot. Pitch actuator drives wheel through a belt drive of gear ratio 72:1 and yaw actuator drives turntable reaction mass through spur gear of ratio 25:1.

The presence of nonlinear friction between the wheel and the surface, which is implicitly assumed a perfect non–slip condition in the rolling constraint of the wheel, contributes the non–holonomic nature of the system. Of course, the longitudinal controller depends on this for actuation, but the lateral controller is heavily handicapped by the resulting friction between the wheel and surface in yaw. This is exacerbated since the yaw friction is poorly known and stiction or breakaway friction

compounds the problem into a highly nonlinear effect, which is also dependent on wheelspeed. The proposed means of solving this problem is implementation of an adaptive friction controller which complements the lateral gain scheduled controller. Compensation of the friction problem in the lateral dynamics is the focus of *chapter 3.*

From the control point of view, these dynamics present a particularly challenging problem in that all of the following adjectives apply: unstable, non minimum phase, time varying and nonlinear.

Open Loop Longitudinal Dynamics

The longitudinal dynamics may be viewed as the inverted pendulum dynamics imposed upon a moving base, which arises as an integrator (or a slow, stable, real pole in the case of frame/wheel viscous friction included) representing the wheel rolling mode. These linearized dynamics are LTI, and well suited to linear control design techniques. Figure 2.2 illustrates the s–plane plot of the open lop dynamics, where the unstable/stable pole pair represent the inverted pendulum mode. Note the non minimum phase zero at the mirror image (about the imaginary axis) of the minimum phase zero. These zeros arise in the loop transfer function from wheel torque input to wheelspeed output, with the frequency on the same order of magnitude as the pole frequencies, thus placing fundamental limits on achievable closed loop bandwidth of the wheelspeed servo loop.

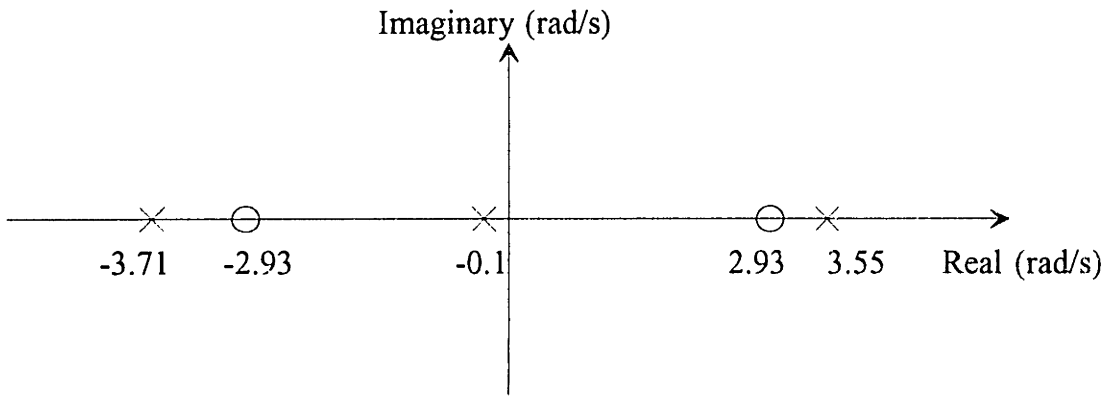

LONGITUDINAL. Zeros in torque-wheelspeed Transfer Function

Figure 2.2. Open loop longitudinal dynamics. The zeros arise in the loop transfer function from wheel torque to wheelspeed.

The longitudinal inverted pendulum poles (ignoring viscous rolling friction) are given by the expression

$$\lambda_{1,2}_{long} = \pm \left\{ \frac{((m_w+m_f+m_t)\, r_w^2+I_2^w)(m_f r_f+m_t l_t)g}{\Delta_{long}} \right\}^{1/2} \qquad (1)$$

with

$$\Delta_{long}=(m_f r_f^2+m_t l_t^2+I_2^t+I_2^f)v$$

and

$$v=((m_w+m_f+m_t)r_w^2+I_2^w)-(m_f r_f+m_t l_t)^2 r_w^2$$

with

g	Acceleration due to gravity	
Ω_0	Nominal wheelspeed (rad/s)	
I_j^k	Inertia of element k, about j'th axis	
m_i	Mass of element i	
subscript	t	refers to turntable
	f	refers to unicycle frame
	w	refers to wheel

Note that the longitudinal dynamics are independent of wheelspeed (Ω).

Lateral Dynamics

For the lateral case (ignoring viscous friction in yaw, for this simplified analysis), the inverted pendulum modal frequency is given by the expression

$$\lambda_{lat}^2 = \pm \left\{ \frac{-I_2^w \Omega_0^2((m_w r_w+m_f(r_w+r_f)+m_t(r_w+l_t))r_w+I_2^w)}{\Delta} + \frac{(m_w r_w+m_f(r_w+r_f)+m_t(r_w+l_t))g(I_3^w+I_3^f)}{\Delta} \right\}^{1/2} \qquad (2)$$

with

$$\Delta=(m_w r_w^2+m_f(r_w+r_f)^2+m_t(r_w+l_t)^2+I_1^w+I_1^f+I_1^t)(I_3^w+I_3^f)$$

and

r_w Wheel radius

r_f Reference frame mass center location

l_t Reference turntable mass center location

The presence of the product with wheelspeed (Ω_0) in the first term, which represents *gyroscopic* contribution to the eigenvalue, indicates the dependence of the inverted pendulum mode on this parameter. The second term represents the contribution due to gravity in the eigenvalue. Clearly there exists a speed for which the gyroscopic (negative) term is the more significant and the poles become oscillatory, which loosely speaking, occurs when the gyroscopic moments generated by the wheel are at least equal to the gravitational "inverted pendulum" moments. This speed depends on the relative magnitudes of the wheel and turntable–frame inertias.

Figure 2.3 shows how the open loop eigenvalues of the lateral system vary with wheelspeed. In this root locus vs wheelspeed, viscous friction between the tire and surface in yaw is modeled, resulting in the yawing mode arising as a stable real pole and not an integrator as in the frictionless case.

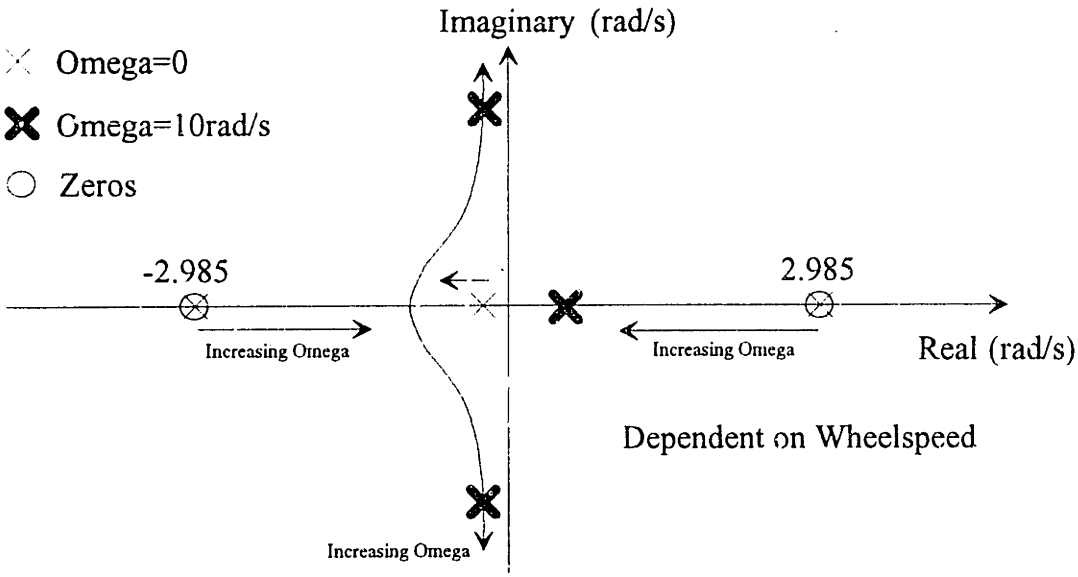

Figure 2.3. Lateral dynamics vs wheelspeed. At zero wheelspeed, the slow real pole represents the yaw dynamics and the roll dynamics are represented by the stable/unstable real pair. The zeros arise in the loop transfer function from turntable torque command to yaw rate ouput. At zero wheelspeed, the roll mode poles are canceled by the zeros, an artifact of the uncontrollability of the roll dynamics in this condition.

Since the pendulum moment arm in longitudinal motion is smaller than in lateral motion and the wheel rolls from under the frame as it falls longitudinally, this inverted pendulum modal instability is slightly faster than for the lateral case, for small wheel speeds (Ω_0 less than speed for which modes are oscillatory).

Friction in the Unicycle Robot

Friction effects include wheel–surface friction in both forward and yawing motion and friction in the drive trains of the pitch and yaw actuators. The forward rolling friction (at the tire–surface interface) is modeled in the sense of the rolling constraint

(forward speed=Ωr_w). Drive train friction is modeled as a viscous effect proportional to angular velocity of the wheel or turntable. The surface friction in yaw is strongly nonlinear and is modeled as such. *Chapter 3* concentrates on this problem and discusses the various models which may be assumed and that which was found to be most representative.

BASELINE CONTROLLERS

The baseline lateral and longitudinal controllers which are well tuned to a specific set of operating conditions, namely testing in the laboratory environment, are given here. Note that the longitudinal and lateral gain scheduled controllers may be operated in various conditions, but the friction compensation strategy given for the baseline controllers is tuned to operation at nominal forward speed of Ω=4 rad/s, tire pressure of 55psi and the tiled laboratory floor. *Chapter 3* successfully deals with the problem of designing and implementing adaptive friction compensation, thus allowing operation over a large range of surface conditions, wheelspeeds and tire pressures.

Longitudinal Controller

The longitudinal control system is a standard LQ servo structure including a lead network to improve the loop shape, with servo control on the wheelspeed. The open loop dynamics with wheelspeed error integrator (e) and lead network (v=lead network state) appended, are given as (discrete time model for sample rate of 18.2 Hz)

$$\begin{bmatrix} v \\ \Omega \\ \dot{\theta} \\ \theta \\ e \end{bmatrix}_{k+1} = \begin{bmatrix} 0.64 & 0 & 0 & 0 & 0 \\ -6.16 & 0.99 & -0.002 & -0.44 & 0 \\ 3.50 & 0.006 & 1.014 & 0.72 & 0 \\ 9.63 & 0.0002 & 0.055 & 1.02 & 0 \\ 0 & 0.055 & 0 & 0 & 1 \end{bmatrix} \begin{bmatrix} v \\ \Omega \\ \dot{\theta} \\ \theta \\ e \end{bmatrix}_k + \begin{bmatrix} 0.0445 \\ 1.2317 \\ -0.7008 \\ -0.0193 \\ 0 \end{bmatrix} \Gamma_{w_k} \quad (3)$$

with feedback control law

$$\Gamma_{w_k} = -\left[-5.5183 \; -0.0904 \; -1.0170 \; -3.5493 \; -0.0051\right] \begin{bmatrix} v \\ \Omega \\ \dot{\theta} \\ \theta \\ e \end{bmatrix}_k \quad (4)$$

The system block diagram and Bode plots for the loop transfer function of the closed loop system from commanded wheelspeed to achieved wheelspeed, are given in figure 2.4.

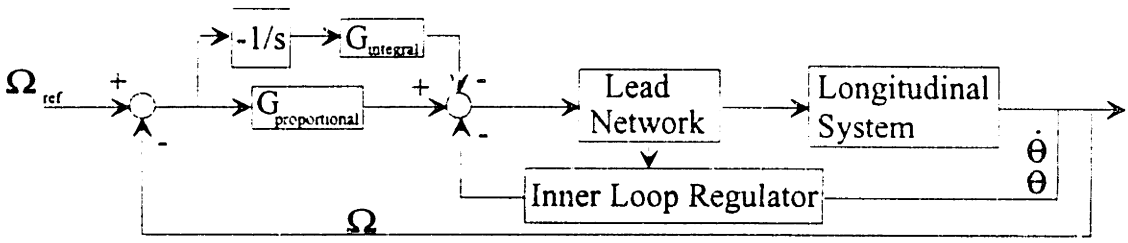

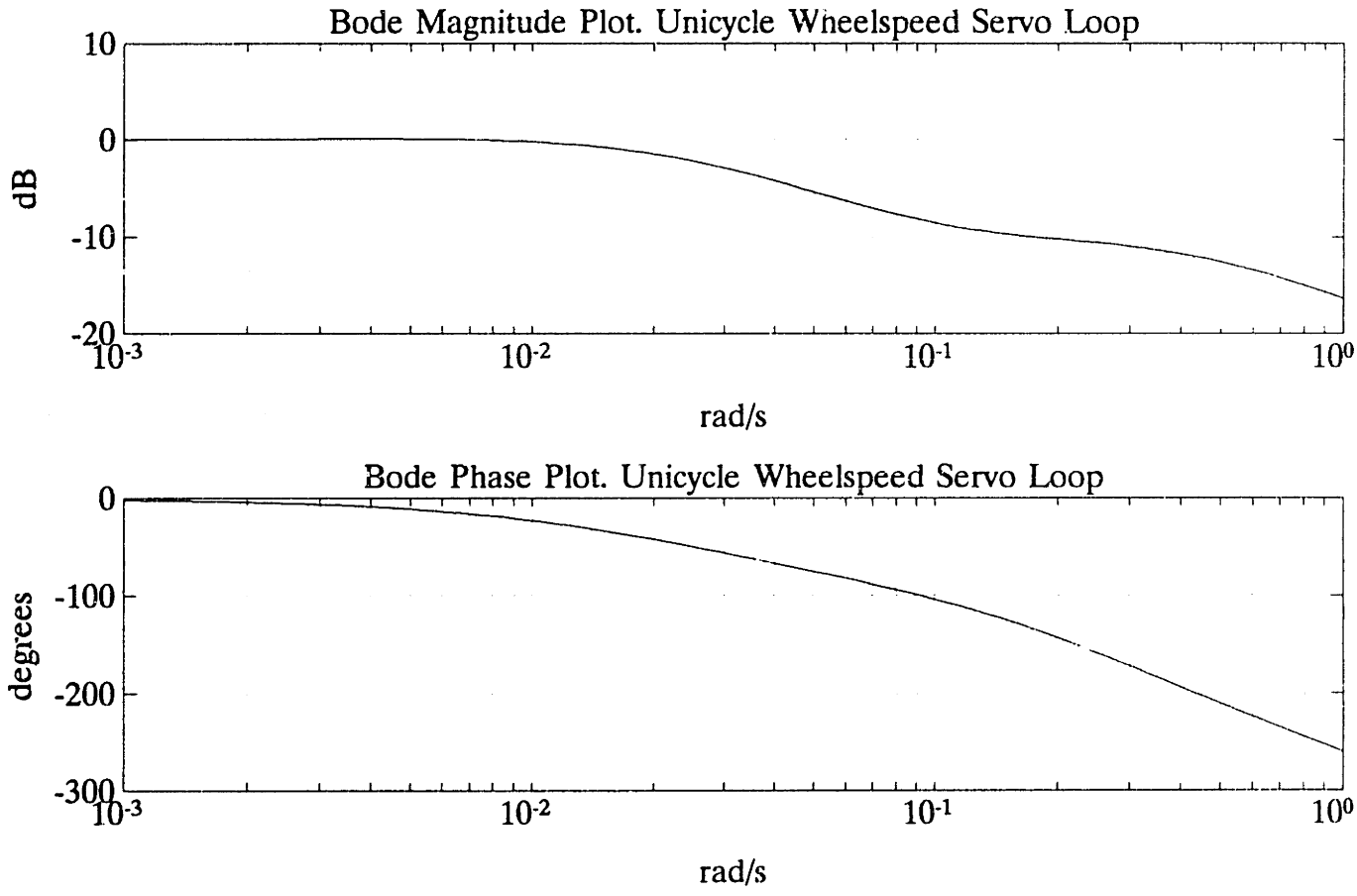

Figure 2.4. Longitudinal controller block diagram and Bode plots for wheelspeed control loop. Lead network is used to achieve desired frequency response loop transfer function shape.

Lateral Controller

The lateral dynamics are dependent on wheelspeed and the model is derived in [*Vos*, S.M.]. *Chapter 4* includes the wheelspeed dependent lateral dynamics model, which is not repeated here. The controller structure is a gain scheduled LQ servo, with block diagram similar to the longitudinal controller, but with heading as an outer loop servo function and no lead network.

Due to the wheelspeed dependence of the system, it is not possible to design a suitable LTI controller which maintains both good performance and stability over the operating range of wheelspeeds. For example, applying the feedback gains for the lateral controller designed at wheelspeed Ω=0.6rad/s, to the system at wheelspeed Ω=0.4rad/s, yields the unstable system of closed loop eigenvalues

$$\lambda_1 = -13.5 \text{ rad/s} \qquad \lambda_2 = -2.98 \text{ rad/s} \qquad \lambda_3 = -0.26 \text{ rad/s}$$
$$\lambda_{4,5} = 0.1362 \pm j\, 2.3 \text{ rad/s} \tag{5}$$

This problem is easily dealt with by gain scheduling the lateral control system. *Chapter 4* defines conditions under which this strategy will guarantee stability as well as means of evaluating the gain scheduled controller to check for stability with arbitrary parameter values and variation rates.

The feedback gains are polynomial curve fits to the gains of the designs done at various points for wheelspeeds between 0.5 and 10 rad/s. The polynomials are

$$K_{phi}(\Omega) = -1.1591e{-}4\Omega^7 + 4.717e{-}3\Omega^6 - 7.8746e{-}2\Omega^5 + 0.6954\Omega^4 - 3.4934\Omega^3$$
$$+ 9.9971\Omega^2 - 15.441\Omega + 11.3171 \tag{6}$$

$$K_{phidot}(\Omega) = -3.4595e{-}4\Omega^7 + 1.408e{-}2\Omega^6 - 0.235\Omega^5 + 2.0755\Omega^4 - 10.427\Omega^3 + 29.838\Omega^2 - 46.077\Omega + 33.778 \quad (7)$$

$$K_{psidot}(\Omega) = 1.3197e{-}12\Omega^7 - 7.5214e{-}10\Omega^6 + 3.1598e{-}8\Omega^5 - 4.6734e{-}7\Omega^4 + 5.2971e{-}7\Omega^3 + 4.8544e{-}5\Omega^2 - 6.6675E{-}7\Omega + 0.08932 \quad (8)$$

$$K_{psi}(\Omega) = -4.7625e{-}5\Omega^2 - 9.8481e{-}5\Omega - 0.1296 \quad (9)$$

$$K_{integrator}(\Omega) = 3.1675e{-}6\Omega^2 + 2.5314e{-}5\Omega - 0.29965 \quad (10)$$

Figure 2.5 shows these gains vs wheelspeed, as well as the equivalent transformed space gains vs wheelspeed (see *chapter 4*). Note that these gains vary less significantly with wheelspeed than the example given in *chapter 4*, and also that these easily satisfy the stability tests discussed therein, i.e. the gradients of each gain, evaluated at the nominal wheelspeed of Ω=2.5rad/s, satisfy the stability bounds of equation (114) in *chapter 4*, thus

$$\frac{\partial K_0}{\partial \Omega} \leq 8.1 \leq 38.0 \text{ (from equation (114a), } \textit{chapter 4}) \quad (11)$$

$$\frac{\partial K_1}{\partial \Omega} \leq 3.25 \leq 34.5 \text{ (from equation (114b), } \textit{chapter 4}) \quad (12)$$

$$\frac{\partial K_2}{\partial \Omega} \leq 0.21 \leq 10.3 \text{ (from equation (114c), } \textit{chapter 4}) \quad (13)$$

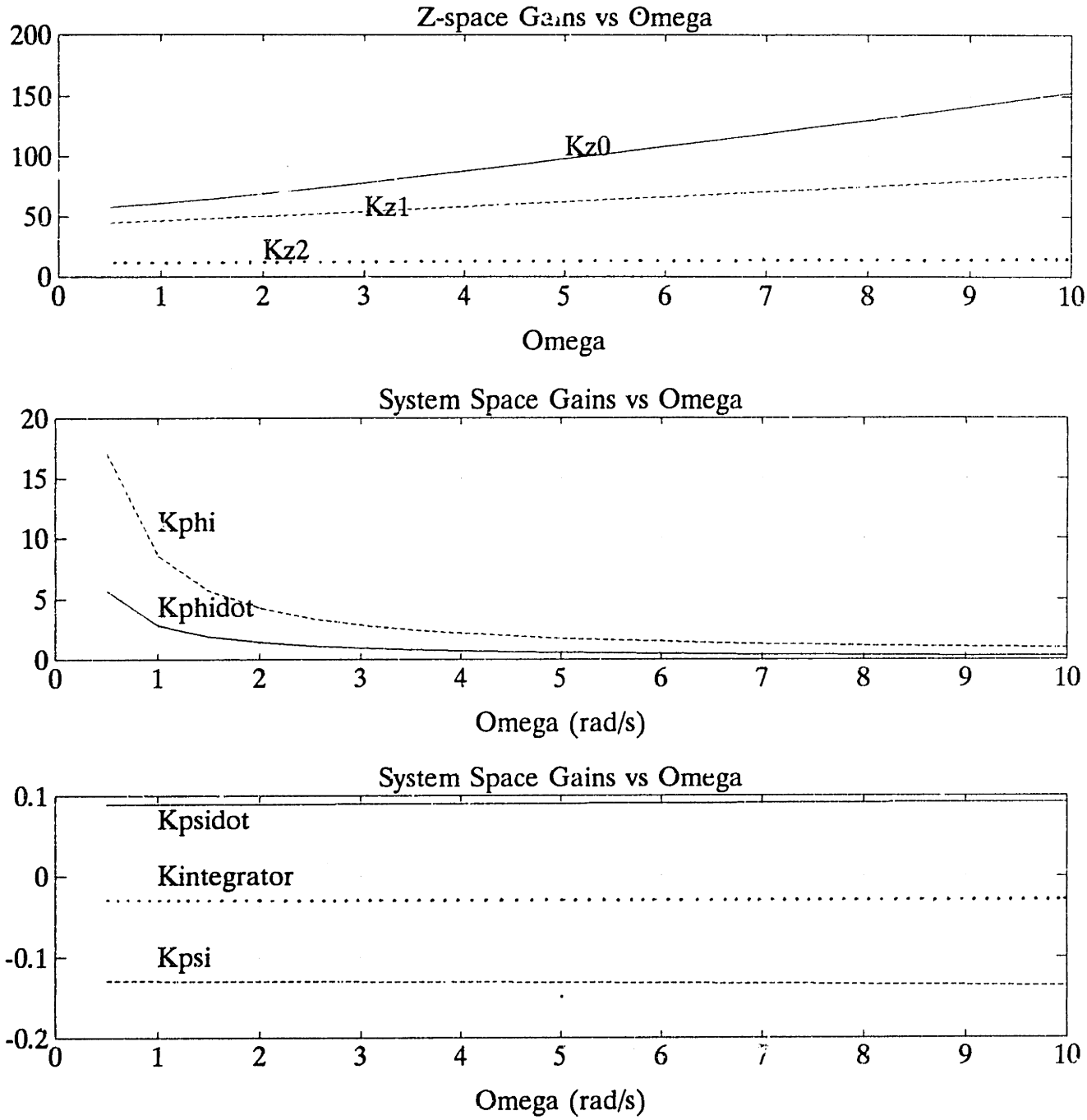

Figure 2.5. Gain scheduled lateral system feedback gains vs wheelspeed for system space as well as transformed space (for the third order model excluding heading and heading error integrator).

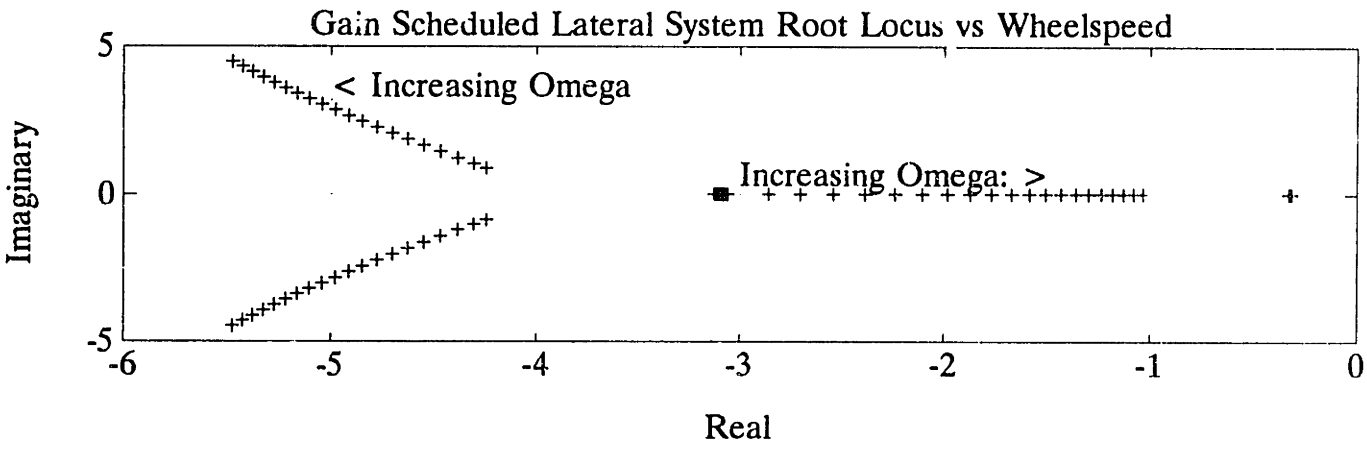

Figure 2.6. Root locus of closed loop gain scheduled (roll and yaw modes) eigenvalues vs wheelspeed. Notice that for increasing wheelspeed, the roll mode pole tracks toward the origin.

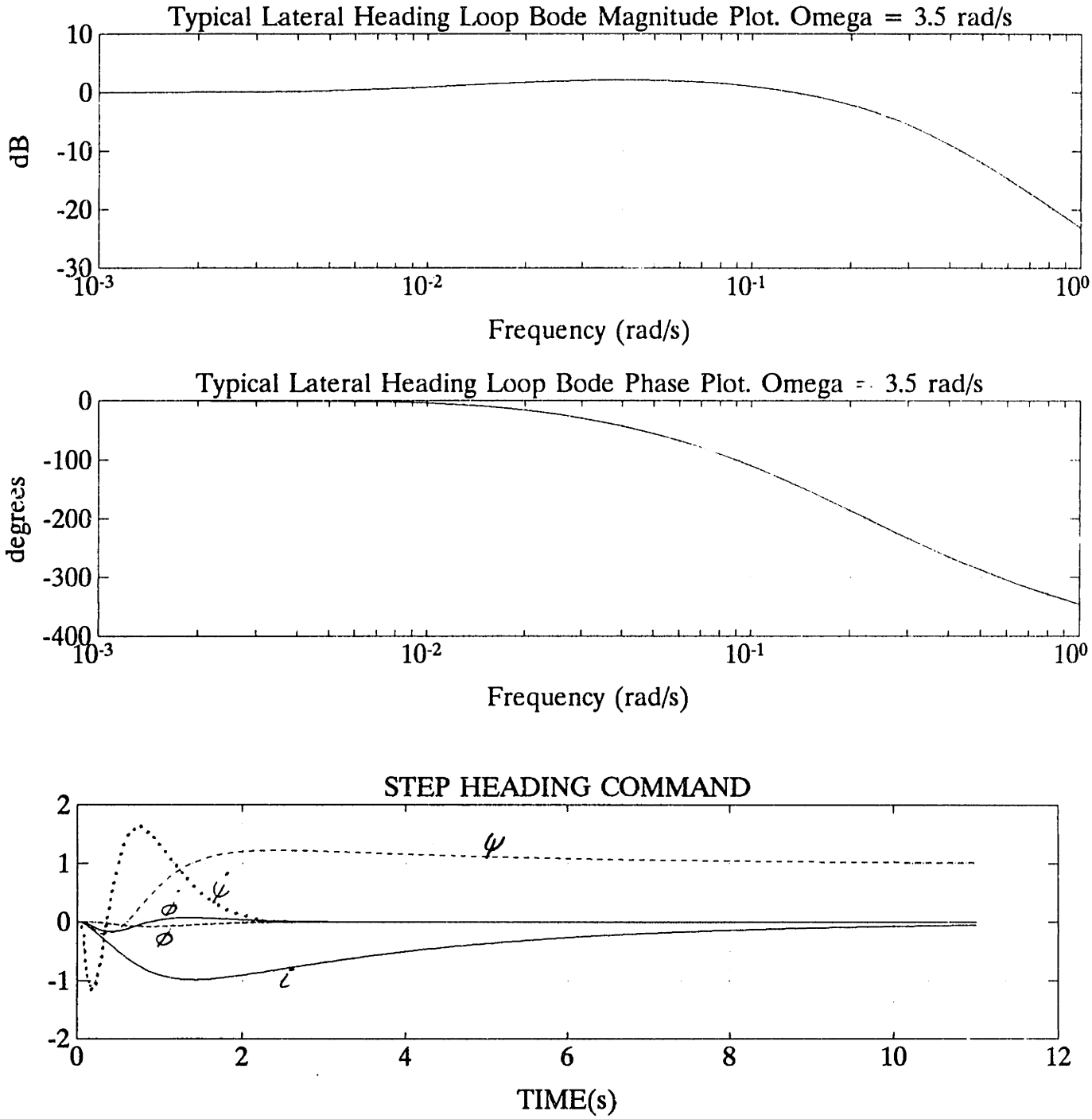

Figure 2.7. Bode plots and typical step heading command response for lateral closed loop (integral heading servo loop) system.

Friction compensation.

The friction compensation for the baseline controller is of the form

$$\Gamma = \Gamma_{gs} + C/n_t \, \mathrm{sgn}(\Gamma_{gs}) \tag{14}$$

where Γ_{gs} is the lateral gain scheduled controller command

$$\Gamma_{gs} = -[K_{phidot} \; K_{phi} \; K_{psidot} \; K_{psi} \; K_{integrator}] \begin{bmatrix} \dot{\psi} \\ \phi \\ \psi \\ \psi \\ e_{\psi} \end{bmatrix} \tag{15}$$

This ensures that the control command is always large enough to overpower the friction effects between the wheel and surface, as well as in the turntable drive train. This strategy works extremely well if carefully tuned. For C=1.25 (Nm), at steady wheelspeed of Ω=4 rad/s, for operation over the laboratory floor and the tire inflated to 55psi, performance is good. Note all the parameters which define the friction compensating value, hence the desire for adaptive friction compensation as discussed in *chapter 3.*

These control laws form the baseline controllers from which the adaptive friction compensating controllers are developed.

EXPERIMENTAL SETUP

The unicycle robot is a combination of off–shelf and self (by the author) constructed parts. Figure 2.1 shows the completed fully autonomous unicycle with onboard power

supplies (sealed lead acid batteries) and onboard CPU, with communication to the operator via R/C radio. The operator commands servo set–points, wheelspeed and heading, whilst inner loop stability augmentation takes care of the unicycle dynamics.

Piezoelectric solid state rate sensors (Watson industries ARS–C131–1A) are used for three axis angular rate information and a vertical gyroscope (Humphrey VG24) is used as roll and pitch angle sensor. Tachometers, integrated into the DC motor actuators, sense wheel and turntable angular velocities.

All sensor lines are low pass filtered via second order Butterworth filters of bandwidth 8 Hz for anti–aliasing (sample frequency of 18.2Hz) and the output lines (torque commands) are low pass filtered via 50 Hz second order Butterworth filters to ensure smooth output commands. Since the anti–aliasing filters are approximately one decade higher frequency than closed loop system bandwidth, the phase penalty incurred is approximately 6 degrees and the 50 Hz filters contribute only approximately 1 degree phase loss, which is tolerable.

Mavilor DC motors by Infranor Inc. are used for actuators: MO301 (316 Watt) motor for pitch actuator and MO80 (155 Watt) for yaw actuator. These are controlled through pulse width modulated amplifier cards, ESA–10–75 by Galil Motion Control Inc, which are implemented as current amplifiers.

Onboard power is through two sets of sealed lead acid (rechargeable) cells by Gates. A 32Volt set is used to power all electronics (sensors, anti–aliasing filters, onboard CPU) and a 48Volt set drives the actuators. Slip rings (8) capable of carrying 30 Amp loads are used to transfer power from the (rotating) turntable where the batteries are stored, to the unicycle frame. Two switching DC–DC power supplies by

International Power Devices are used to generate the correct DC power requirements of the onboard CPU and AT--Bus.

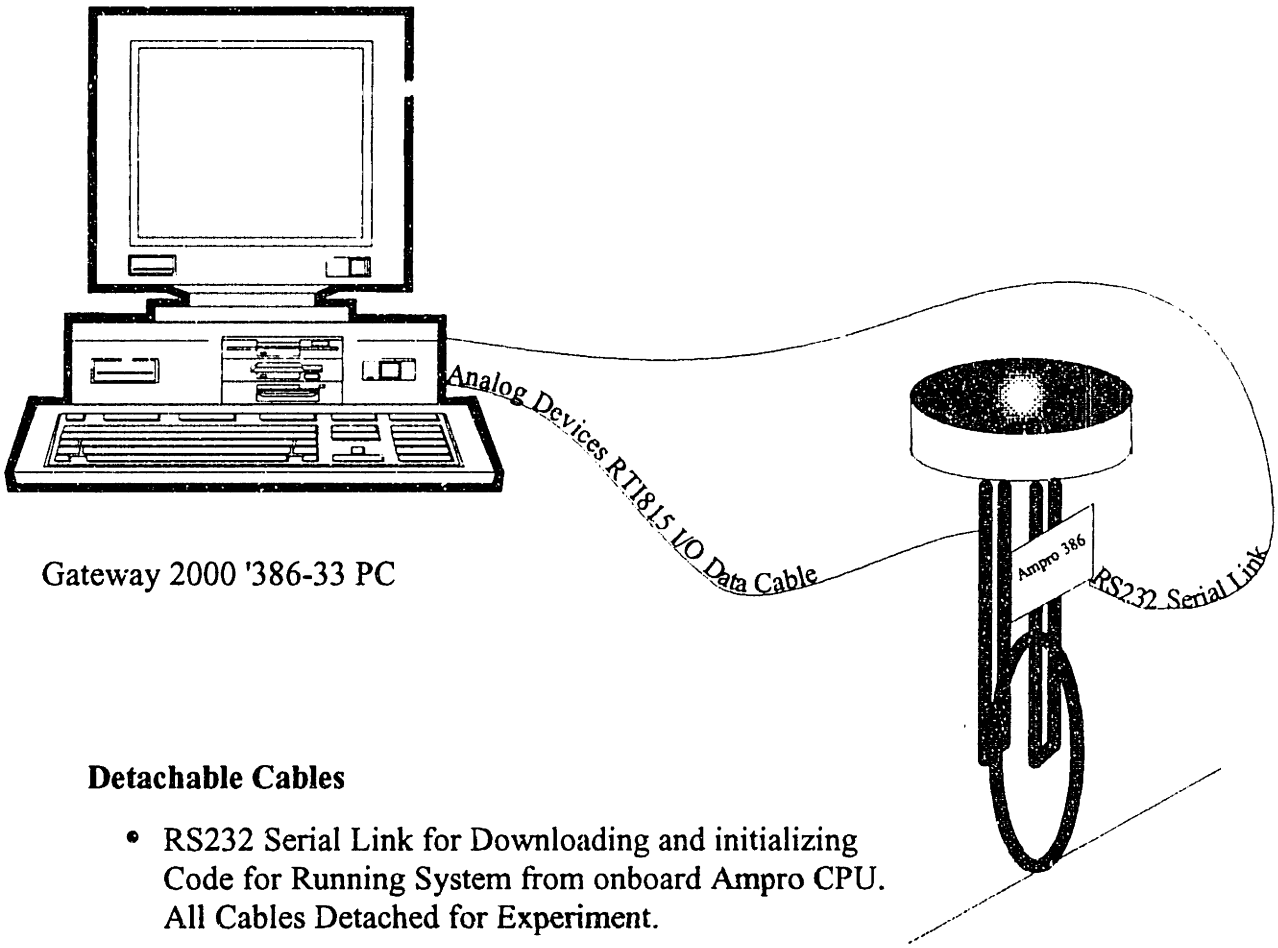

Figure 2.8. Unicycle control system development environment.

The development system consists of a Gateway 2000 386–33 PC with Analog Devices RTI–815 I/O (8 A/D, 2 D/A, 16 Digital ports) card for remote data acquisition and control via an umbilical. The target (onboard CPU) system is an Ampro 386–on–a–card CPU (20 Mhz) with Real Time Devices RTD402 I/O card with similar capabilities to the RTI–815 card. Target system development is done using the PC as a host, communicating over RS232 serial link with the Ampro CPU, and using Datalight C–Thru–Rom development software for remote development on the target (Ampro) CPU. When development is complete, code is simply downloaded and initialized over the RS232 link before disconnecting to yield a completely autonomous system. Figure 2.8 illustrates the development environment. All Coding is in Microsoft C (and MS QuickC) and Microsoft Assembler.

This experimental setup has proven an extremely good and inexpensive development environment with seamless transition from remote data acquisition and control via PC to onboard autonomous control via Ampro card.

CHAPTER 3. NONLINEAR FRICTION COMPENSATION IN LATERAL DYNAMICS

INTRODUCTION

Although well suited to fixed point linear control design techniques, and subsequent gain scheduling of the lateral controller with forward speed, the unicycle lateral dynamics require further compensation to overcome the destabilizing effects of nonlinear friction torque arising between the tire and surface in yawing motion, as well as stiction in the yaw actuator gear train. The baseline controller of *chapter 2* successfully employs an ad hoc friction cancellation tuned to particular operating conditions. This scheme assumes the friction torque, due to both the actuator and the tire, of such a nature as to always oppose the torque command required by the gain scheduled lateral controller; i.e. the friction torque is a signum function of the linear control command torque. The amplitude of this signum function is empirically determined, which yields good performance for the speed, surface and tire conditions at which this friction compensator is tuned. This, however, allows satisfactory operation at only one operating condition, while it is desirable to have stability and equally good performance for all forward speeds and various surfaces. In addition to the tire friction being yaw rate and forward speed dependent, thus partially state dependent, it is also dependent upon exogenous parameters such as tire pressure and surface condition. The unknown and indeterminable (are not measured in real time by the robot) nature of these exogenous parameters contributes to the need for adaptive on–line compensation of these effects to ensure stable operation of the robot.

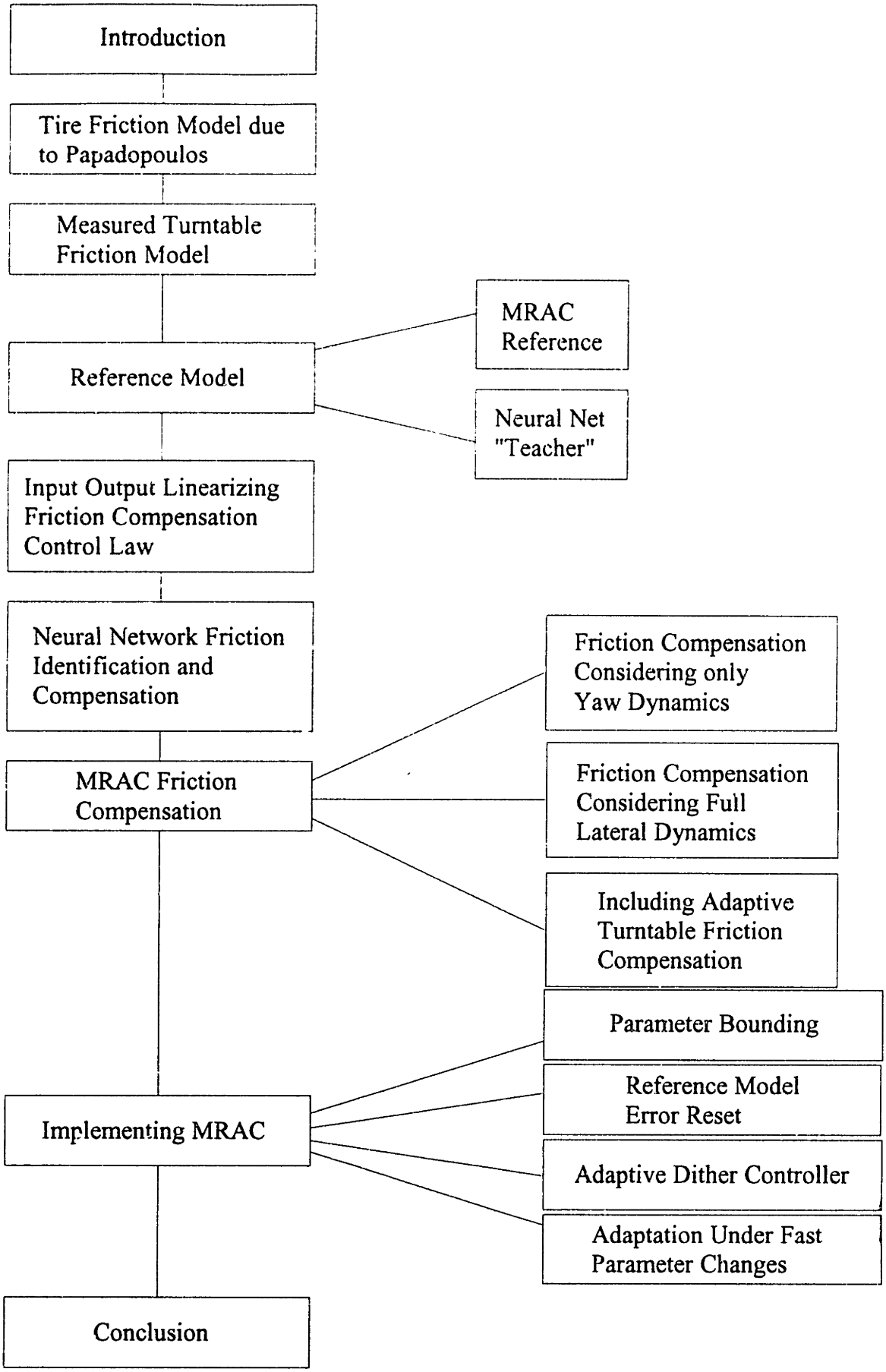

Figure 3.1. Chapter Roadmap.

The typical friction models of figure 3.2, for various systems, are either one (Coulomb friction only), two (Coulomb and viscous) or more parameter dependent [*Canudas, Maron, Radcliffe*]. While the gear train friction of the yaw torque reaction mass may be characterized by Coulomb plus viscous friction effects, the rolling tire has friction torques arising in yawing while in forward motion due to a number of effects, differing from the typical models. [*Papadopoulos*] proposes a bicycle tire friction model based predominantly on two effects. Initial lateral deformation of the tire tread due to the tire tracking a heading which is instantaneously at some "sideslip" angle with the heading of the tire–surface footprint, causes a moment proportional to the sideslip angle as a result of the lateral stress in the tread blocks: an effective spring effect proportional to sideslip angle and dependent on forward speed. The second effect, called *scrubbing*, arises when traversing a curved path, due to the torsional stiffness of the tire tread blocks. This effect is proportional to the rate of change of heading (yaw rate) and inversely proportional to forward speed. At high yaw rates relative to forward speed, a plateau is reached in both of these effects and the friction simply becomes Coulomb.

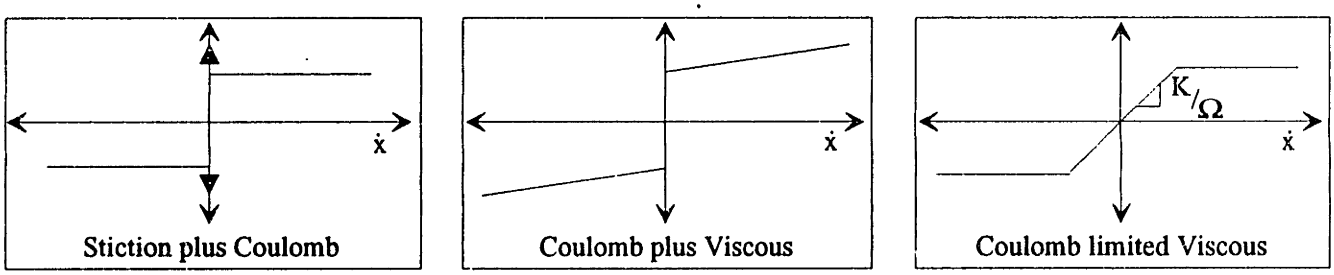

Figure 3.2. Typical friction models in mechanical systems. Linear viscous friction often arises with a transition to a plateau for rates above some maximum value. Other models are simply Coulomb models with stiction induced switching at the origin.

Depending on the operating condition of the system, one of these friction models' effects dominates and with this assumed friction model it is then possible to define an adaptive control law which continuously adapts the unknown friction model parameters to attempt to eliminate the effect of the friction from the response of the system. Adapting the parameters such that performance according to a desired model is striven for, casts the design strategy into a model reference setting [see e.g. *Landau*].

This approach of effectively input output (I/O) linearizing the nonlinearity is the obvious one to take and is reported in a number of cases [*Maron, Canudas* and others] where the unknown parameters for the assumed friction model are then estimated on–line, usually by least squares or recursive least squares regression [see e.g. *Aström and Wittenmark*]. The adaptation laws used in this chapter, however, are determined directly from the Model Reference Adaptive Control (MRAC) setting. As in the referenced literature, I/O or feedback linearization offers a well structured means of determining the feedback control law which cancels the nonlinearity, if the nonlinearity is perfectly known. Since the parameters of the assumed model are unknown and dependant on variable operating and environmental conditions, adaptive estimation of these is necessary for implementation.

For the system controlled by the gain scheduled controller, the only element which is not accounted for in the control law is the friction problem. In this section, only the relevant equations of motion (i.e. in which the friction effect appears explicitly) are considered for applying I/O linearization to cancel these effects and yield the system "apparently linear" as far as the rest of the controller sees the system. Figure 3.3 shows a block diagram representation of the gain scheduled lateral controller with the friction estimation and compensation loop. The friction compensation scheme tries to

make unity the transfer function across the friction nonlinearity, as this is the characteristic the gain scheduled lateral controller expects.

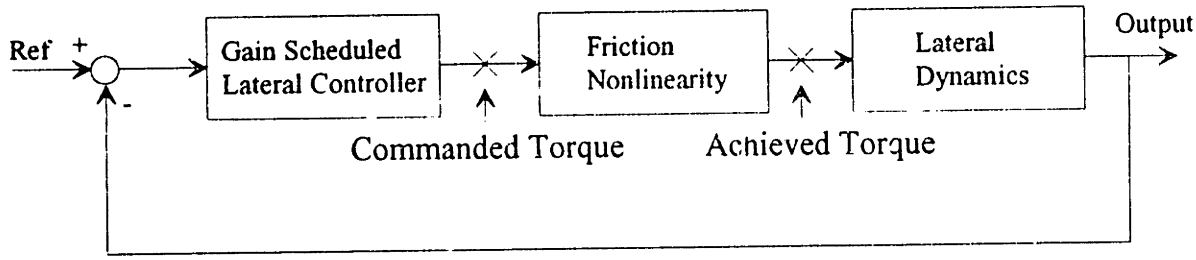

Figure 3.3. Lateral control system block diagram. The friction nonlinearity appears as a series concatenation in the yaw rate loop, with the rest of the plant being linear. The transfer function through the friction nonlinearity should ideally be unity, as this is the plant for which the lateral gain scheduled controller was designed.

An artificial neural network is used as another means of determining the friction compensating control term in the control law. A model reference setting similar to that of the MRAC strategy is used to determine the friction estimate, where this differs from the MRAC system in that the full friction compensating model is learnt, not only the parameter of an *assumed* model as in the MRAC case. The network is initially trained on experimental data acquired in testing of the baseline controller of *chapter 2*. By training a sufficiently complex network on the actual experimental data and subsequent pruning of nodes having small network weights, a network structure able to capture the relevant map between the system states and the present friction value is obtained. Once a reduced order network is determined in this fashion, it is implemented on the unicycle robot for further on–line training. The implemented neural network used an input layer (two inputs), a hidden layer and an output (single output) layer with biases at each neuron.

This chapter discusses use of both the neural network and MRAC techniques applied to the friction cancellation problem.

TIRE FRICTION MODEL

The bicycle tire friction model proposed by [*Papadopoulos*] may be written as

$$\mathcal{F} = \left\{ \begin{array}{ll} K_1(\cdot)a + K_2(\cdot)(\varphi + \kappa R) & \text{if } |\mathcal{F}| < |\mathcal{F}_{coulomb}| \\ \mathcal{F}_{coulomb} & \text{otherwise} \end{array} \right\} \qquad (1)$$

with K_1 the *sideslip* coefficient, and K_2 the *scrubbing* coefficient and

$\mathcal{F}$ = Friction Torque

a = sideslip angle

φ = angle of wheel from upright (roll angle)

κ = curvature of circular path traversed by wheel

R = wheel radius

Both sideslip and scrubbing effects are dependent on the wheel geometry and speed as well as tire characteristics including torsional and lateral stiffness of the tread elements. The sideslip term, K_1a, represents a spring effect due to the lateral stress in the tire tread blocks as the tire moves in a direction at some sideslip angle (α) to the heading of the footprint.

The scrubbing term $K_2(\cdot)(\varphi + \kappa R)$ may be viewed as a viscous damping effect. Consider the second term, which depends on the effective relative yawing rotation of the tire about the vertical axis per unit forward distance traveled. For the wheel

assumed nominally vertical ($\varphi \approx 0$) and a nominal steady forward speed of ΩR, the curvature of the circle traversed may be written as

$$\kappa = \frac{\dot{\psi}_{fp}}{\Omega R} \tag{2}$$

with

Ω wheel angular velocity in forward rolling motion

$\dot{\psi}_{fp}$ footprint yaw rate (rate of pivot about vertical axis) which in steady state is assumed equal to the wheel yaw rate $\dot{\psi}$

This term may thus be written as $K_2\frac{\dot{\psi}_{fp}}{\Omega R}$, which indicates the dependence on yaw rate (thus an effect of a viscous nature) and inverse proportionality to wheelspeed.

For the sideslip term, the effective sideslip angle may be expressed as the difference between wheel heading and footprint heading ($\psi - \psi_{fp}$), resulting in a friction model which is a second order oscillatory system. It is, however, not practicable to track the footprint heading (ψ_{fp}) although actual heading (ψ) may easily be measured. The effective length of the footprint may then be used to obtain an estimate of the sideslip angle.

Assume the effective footprint length to be the length of that section of the footprint which does not slide across the surface when the tire is in sideslip. Denoting this by l_{fp}, with the tire radius R and the angular velocity of the tire Ω, then the time spent by a tread block in contact with the surface (not sliding) is

$$t_l = \frac{l_{fp}}{\Omega R} \tag{3}$$

Since this tread block is on the same heading as the tire when initial contact with the surface is made, and remains on this heading while the lateral stress is smaller than the friction coefficient projection of the normal stress of the tread block onto the surface (i.e. sliding across the surface does not yet occur), the sideslip angle may be estimated as the difference between the headings of the tread block at initial contact with the ground and the heading when the same tread element breaks contact with the ground. This is effectively the change in heading of the tire over the time period t_l, thus

$$\hat{\alpha}(t) = \psi(t) - \psi(t-t_l) \tag{4}$$

For the sample period ΔT of the digital implementation of the controllers, the sideslip is determined as the difference between the present heading and the integer number (n) of sample periods in t_l

$$\hat{\alpha}(k) = \psi(k) - \psi(k-n) \tag{5}$$

with $\mathbb{Z}$ the set of integers, then

$$n = \max_z \{z = \frac{t_l}{\Delta T} \mid z \in \mathbb{Z}, z \geq 1\}$$

$$= \max_z \{z = \frac{l_{fp}}{\Omega R \, \Delta T} \mid z \in \mathbb{Z}, z \geq 1\} \tag{6}$$

The friction model may be then be written in terms of known system states as

$$\mathcal{T}(k) \quad = K_1(\cdot)(\psi(k) - \psi(k-n)) + K_2(\cdot)\frac{\dot{\psi}(k)}{\Omega(k)} \tag{7}$$

thus proportional to yaw rate, where the footprint yaw rate is assumed represented by the unicycle frame yaw rate, with the gradient $(K_2(\cdot)/\Omega(k))$ inversely proportional to forward speed. Note that the "sideslip" coefficient, $K_1(\cdot)$, is defined by the geometric and material characteristics of the tire, and the sideslip angle $(\hat{\alpha}(k)=\psi(k) - \psi(k-n))$ is inversely proportional to forward speed (Ω) (consider equations (3), (5) and (6)). For torsional loads greater than the region in which this linear relation holds (equivalently: $|\dot{\psi}_{fp}| > \dot{\psi}_{linear}$), it is assumed that the friction behaves according to a Coulomb friction model. Figure 3.4 represents the assumed model schematically.

The model assumed here is heuristically validated by a crude experiment. Figure 3.5 shows time histories of the actual unicycle in steady forward motion at constant wheelspeeds, with impulse yaw torque applied whilst maintaining the unicycle vertical in both pitch and roll. The lateral control system is inactive, with lateral support provided by a bearing mounted on the turntable. The response is typical of a second order system with the damping dependent on forward speed, thus qualitatively corroborating the model.

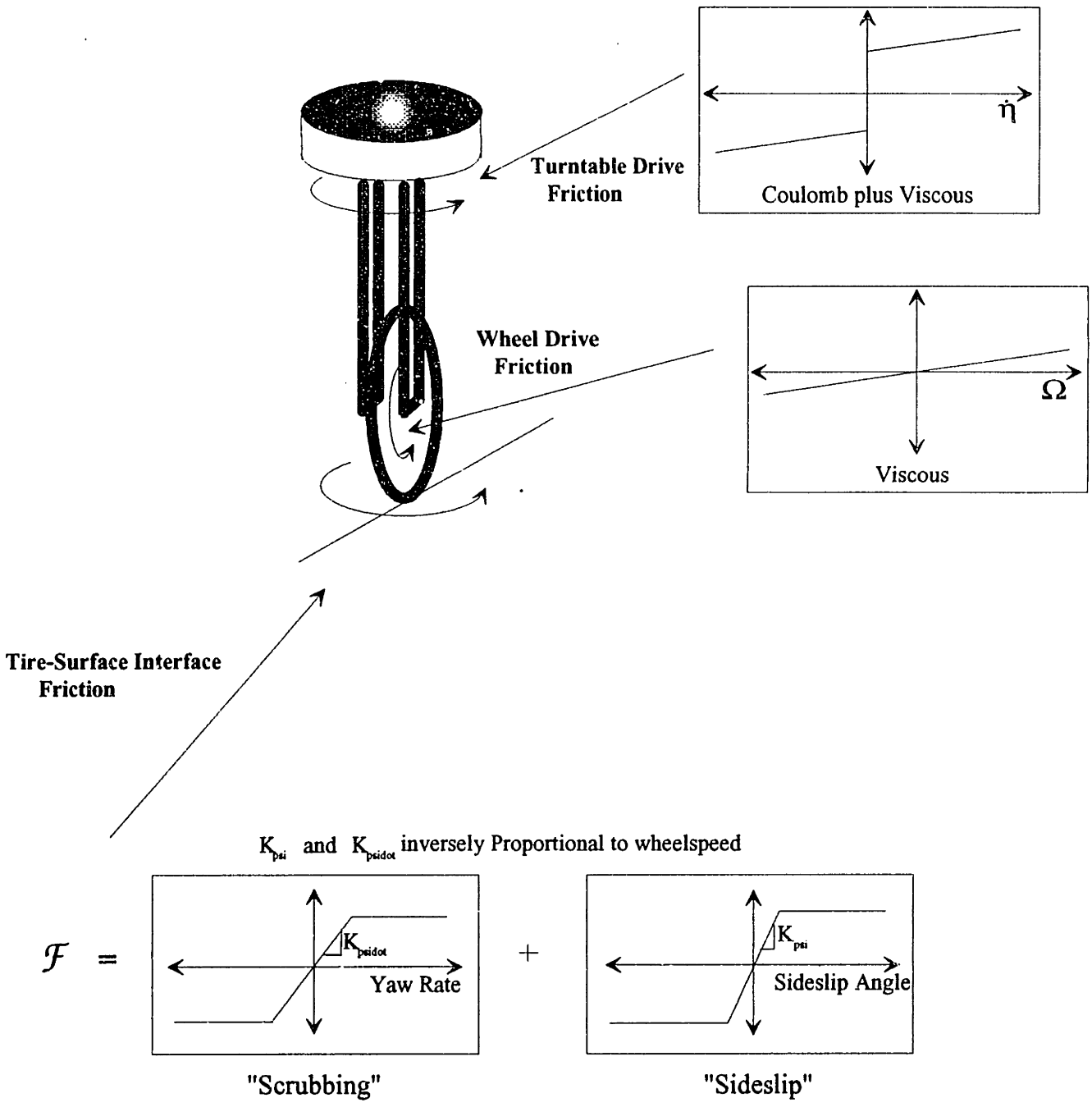

Figure 3.4. Unicycle friction problem. Turntable and wheel/frame friction are easily measured and compensated. For friction between tire and surface in yaw, assume the model according to [*Papadopoulos*], with linear dependence on "sideslip": error between footprint and tire heading, and "scrubbing": friction proportional to yaw rate for low enough rates where the footprint is not sliding across the surface. Both coefficients exhibit inversely proportional dependence on wheel forward speed. For large yaw rates, Coulomb friction is assumed.

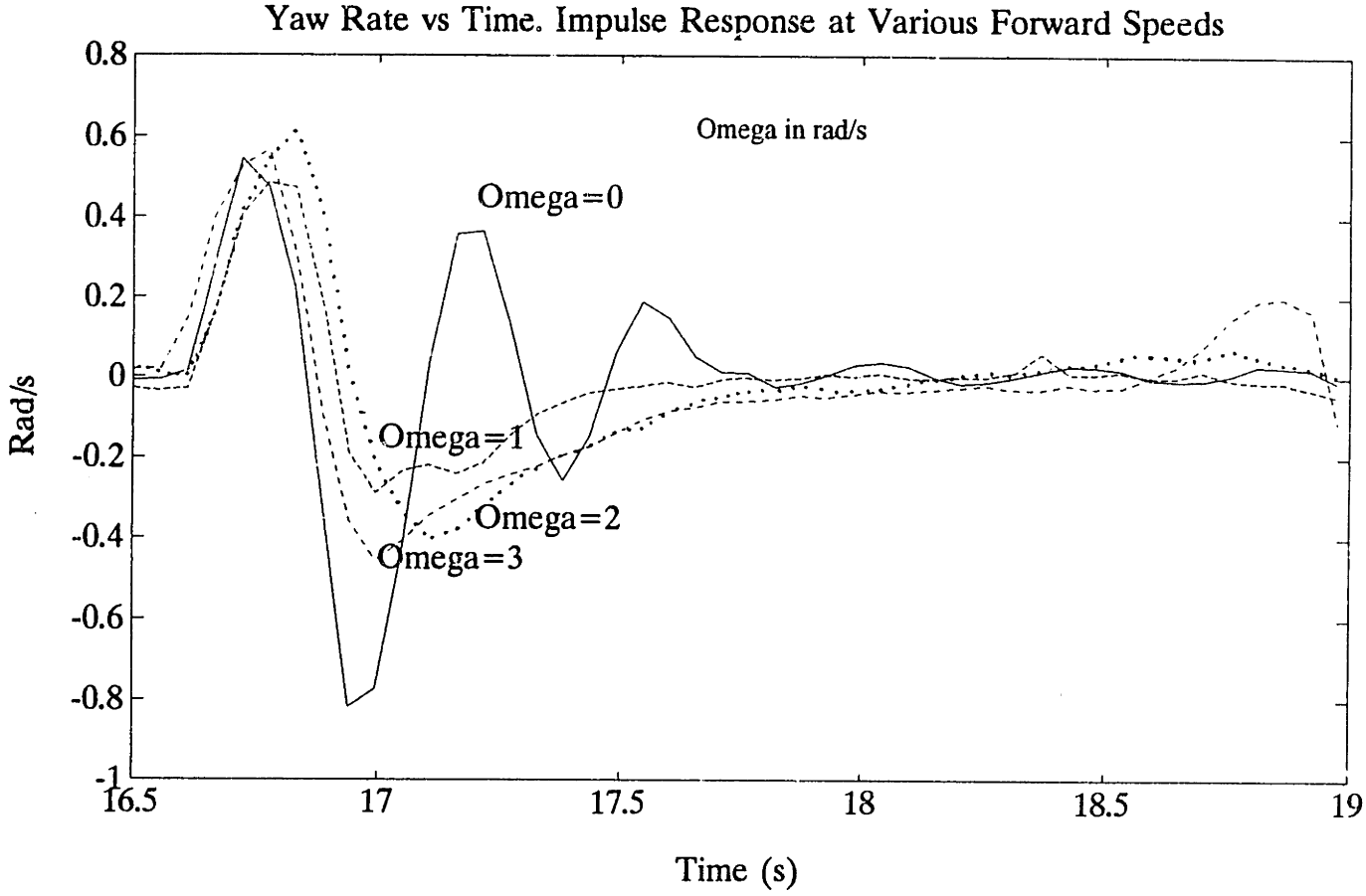

Figure 3.5. Time histories of yaw rate response to impulse torque commands at various forward speeds with unicycle robot maintained vertical. Behavior is typical of second order system with effective damping ratio dependent on forward speed.

YAW ACTUATOR DRIVE TRAIN FRICTION

The yaw actuator is in the form of a torque reaction mass driven through a 25:1 reduction gear train. The gears are spur gears and as such do not have very good meshing characteristics. In fact there is a significant high spot, resulting in drive train friction dependent upon rotation angle. Figure 3.6 shows a plot of measured output torque at the turntable versus commanded turntable torque with the drive train stationary at the high spot. Note the deadband of approximately 2.5 Nm, which represents the minimum torque required to rotate the reaction mass in either

direction. If the torque motor does not generate torque greater than this value, the power is simply dissipated in heating the motor and no torque is applied to the unicycle frame.

The two curves generated represent the stall torque of the actuator in opposite directions. For example, for a commanded torque of 10 Nm, the stall torque (minimum torque required to prevent turntable turning) in the direction of the torque command is 8.75 Nm and 13 Nm in the opposite direction (minimum torque required to overpower the actuator, i.e. move actuator in direction opposite to commanded torque direction).

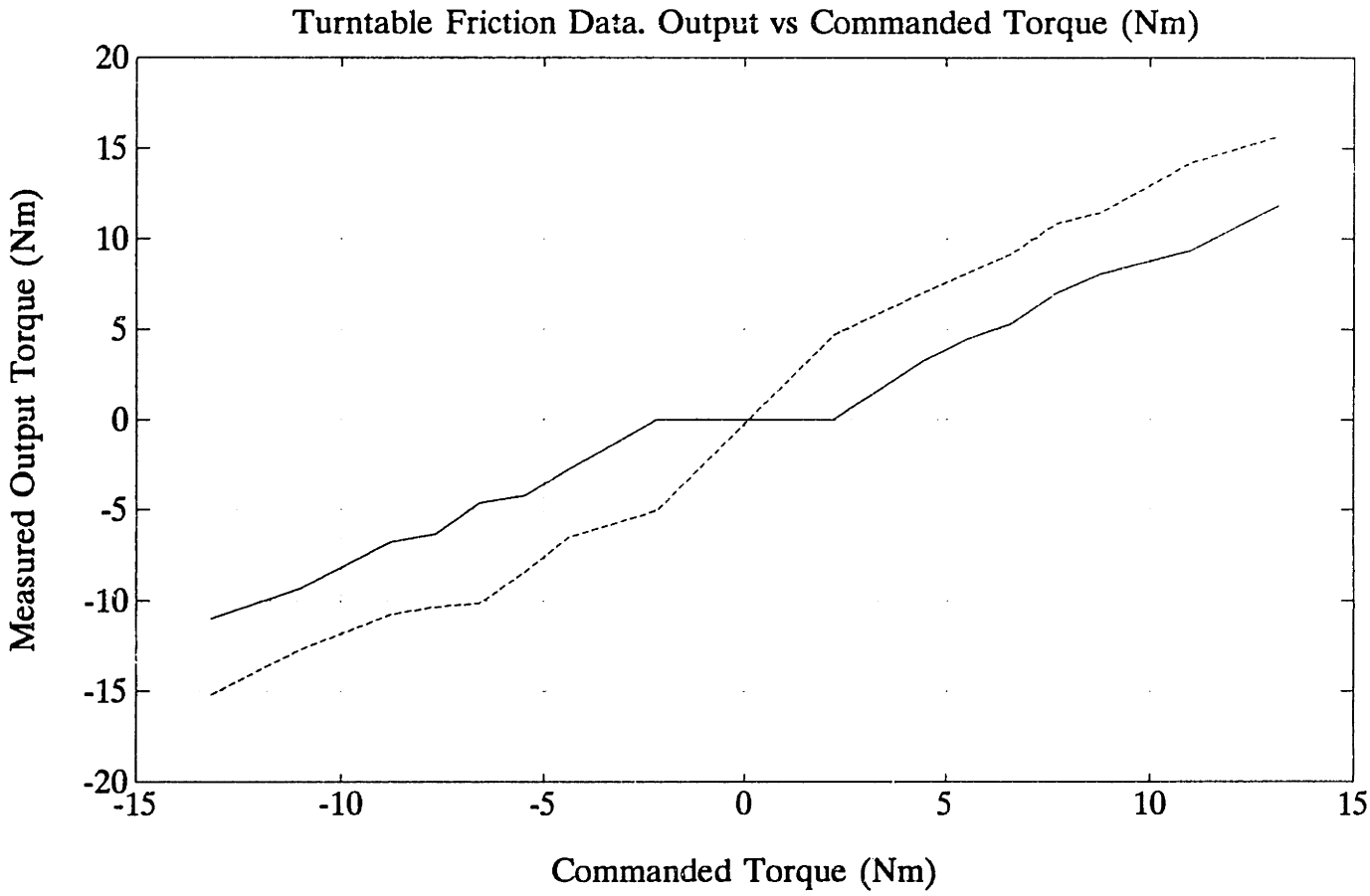

Figure 3.6. Measured versus commanded turntable torque. The two curves represent stall (minimum overpowering torques) torques in direction of commanded torque and

in opposite direction to commanded torque, respectively. Note the ±2.5 Nm deadband. This is a significant effect since the linear controller constantly requires small correcting torques to maintain balance. The magnitude of these correcting torques often falls within this deadband, so without some enhancement of the lateral controller with a friction compensating term, poor performance or instability results.

Since this friction is easily measured, such that a reasonably accurate model is obtainable, simple cancellation without adaptation is easily achieved. Figure 3.7 shows the assumed model and measured parameters, with essentially stiction plus a small viscous friction effect defining the structure of the turntable friction. The viscous term is measured by applying a known torque command and monitoring the average steady state turntable speed reached.

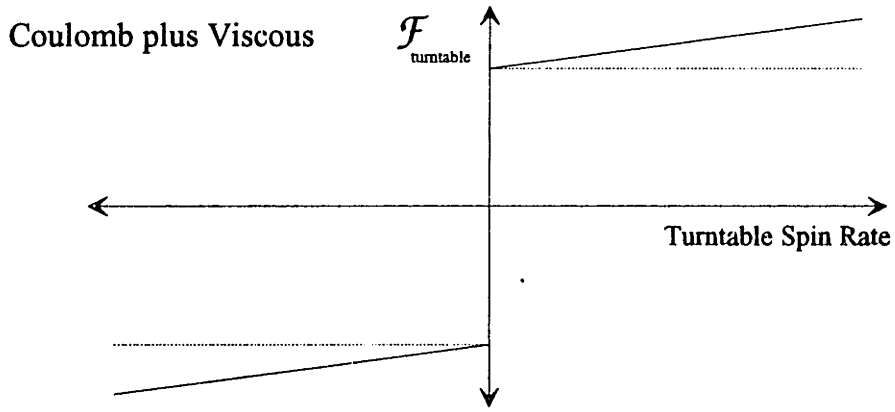

Figure 3.7. Turntable friction model. The parameters are easily measured and the model does not vary substantially in time, so that simple constant cancellation is implemented in the form $\Gamma=\Gamma_a+(\hat{\mathcal{F}}_{\text{turntable}})/n_t$.

LINEAR REFERENCE MODEL FOR TRAJECTORY FOLLOWING

The gain scheduled controller is designed using the wheel speed dependent *linear* equations of motion (see *chapter 4*). These equations of motion thus describe the response of the system to inputs as expected by the (linear) gain scheduled controller. The friction nonlinearities which exist in the turntable drive train and between the wheel and the surface result in a quite different response to that expected by the linear system. If the unicycle can be forced to follow the expected behavior for a given input, then the gain scheduled lateral controller will perform according to design specifications. The actual linear equations of motion are thus a natural reference model for the MRAC system.

The reference model for trajectory following, is determined from the linear equations of motion of the unicycle [*Vos*] with the relevant equation being that describing the yaw dynamics without the nonlinear friction effect. Since these are well representative of the actual system dynamics (within parameter errors, apart from the friction effects) in the region of linearization about the nominal vertical condition, it is a reasonable model to select as the reference model since the system should easily be able to track it (i.e. it is an *achievable* model for the system) if successful cancellation of the friction nonlinearity is achieved.

The yaw equation of motion is

$$-\mathcal{F}(\dot{\psi},\Omega) + n_t\Gamma = f_{\dot{\psi}}\dot{\psi} + I_2^W\Omega\dot{\varphi} + (I_3^f + I_3^W)\ddot{\psi} \qquad (8)$$

where

$\mathcal{F}(\dot{\psi},\Omega)$ = friction torque model (Nm)

n_t = yaw actuator gear ratio

Γ = yaw actuator torque (Nm)

$f_{\dot{\psi}}$ = yaw viscous friction coefficient (Nms/rad) (>0)

$\dot{\psi}$ = yaw rate (rad/s)

I_q^p = mass moment of inertia of p'th element about q'th axis (kgm^2)

Ω = wheel speed (rad/s)

$\dot{\varphi}$ = roll rate (rad/s)

$\ddot{\psi}$ = yaw acceleration (rad/s^2)

Notice that since the viscous friction coefficient is positive, A is Hurwitz for the reference model in standard form: $\dot{x}(t) = Ax(t) + Bu(t)$; with the other terms (not containing ψ or any derivatives thereof) considered exogenous inputs or disturbances to the stable system.

For training a neural network to learn the friction model, where the only information regarding the effect of the friction is in the measured yaw rate, an estimate of the friction acting on the system at the present time is required in order to define a "teacher" according to which the network output may be compared and the error used for updating the network weights. A simple means of achieving this estimate is by discrete differentiation of the system response as follows [*von Flotow*].

Implementing the discrete time controller (of sample period Δt) with a zero order hold, the torque impulse to the system over one sample period is given by the product $(\mathcal{F} + n_t\Gamma_t)\Delta t$, so that at the k'th time step

$$-\mathcal{F}_k\Delta t = (-n_t\Gamma + f_{\dot{\psi}}\dot{\psi} + I_2^w\Omega\dot{\varphi} + (I_3^f + I_3^w)\ddot{\psi})_k\Delta t \qquad (9)$$

allowing the yaw rate at time t_{k+1} to be determined by e.g. Euler integration as

$$\begin{aligned}\dot{\psi}_{k+1} &= \dot{\psi}_k + \ddot{\psi}_k \Delta t \\ &= \dot{\psi}_k + \frac{(-\mathcal{F} + n_t\Gamma - f_{\dot{\psi}}\dot{\psi} - I_2^w \Omega \dot{\varphi})_k}{(I_3^f + I_3^w)} \Delta t \end{aligned} \tag{10}$$

The gain scheduled linear controller expects the system to respond according to equation (10) *without* the friction term, $\mathcal{F}$, so that a discrete time *reference* model is then

$$(\dot{\psi}_{k+1})_{des} = \dot{\psi}_k + \frac{(n_t\Gamma - f_{\dot{\psi}}\dot{\psi} - I_2^w \Omega \dot{\varphi})_k}{(I_3^f + I_3^w)} \Delta t \tag{11}$$

Ω_k, $\dot{\varphi}_k$ And $\dot{\psi}_k$ are known through measurement so the desired yaw rate $(\dot{\psi}_{k+1})_{des}$ may be calculated from equation (11). Since $\dot{\psi}_{k+1}$ is measured, an estimate of the equivalent constant friction force active over one sample period is given by

$$\mathcal{F}_k \approx (I_3^f + I_3^w)\left(\frac{(\dot{\psi}_{k+1})_{des} - (\dot{\psi}_{k+1})_{measured}}{\Delta t}\right) \tag{12}$$

In the case of the unicycle robot digital controller implementation, the sample rate is set at 18.2 Hz and since the open loop dynamics are on the order of 1/2 Hz (time constants on the order of 1/3 seconds), Euler integration with this relatively small time step (1/18.2s) is an acceptable method of discretization. If sample rates closer to the system open loop natural frequency were used, a more suitable discretization algorithm such as Newton or Runge–Kutta would be necessary.

INPUT–OUTPUT LINEARIZATION OF FRICTION NONLINEARITY

It is often possible to write the relevant equations of motion for a nonlinear system in

a form which is amenable to feedback or I/O linearization [see e.g. *Isidori; Nijmeijer and Van der Schaft; Slotine and Li; Cro Granito, Valavani and Hedrick*]. The general strategy is to try and achieve a description of the system in a form where the nonlinearity appears linearly with the control terms. By a suitable number of differentiations of the output until the input appears explicitly, it then becomes possible to define the linearizing control law.

More formally [*Cro Granito, Valavani and Hedrik*], consider a system of the form

$$\begin{aligned} \dot{\mathbf{x}}(t) &= \mathbf{f}(\mathbf{x}(t)) + \mathbf{B}(\mathbf{x}(t))\mathbf{u}(t) \\ \mathbf{y}(t) &= \mathbf{C}\mathbf{x}(t) \end{aligned} \tag{13}$$

with $\mathbf{x}(\cdot)\in\mathbf{R}^n$, $\mathbf{y}(\cdot)\in\mathbf{R}^m$, $\mathbf{u}(\cdot)\in\mathbf{R}^m$, $\mathbf{C}:\mathbf{R}^n\rightarrow\mathbf{R}^m$, $\mathbf{B}(\cdot):\mathbf{R}^m\rightarrow\mathbf{R}^n$, $\mathbf{f}(\cdot):\mathbf{R}^n\rightarrow\mathbf{R}^n$

Take derivatives of the i'th output, $y_i(t)$, along $\mathbf{f}(\cdot)$ and $\mathbf{B}(\cdot)$, with the Lie derivative defined as (the directional derivative)

$$\mathcal{L}_f\lambda(\mathbf{x}) \equiv \nabla\lambda(\mathbf{x})\cdot f(\mathbf{x}) \tag{14}$$

Determine the smallest l_i for which any input (b_j: j=1,2,...m) appears explicitly in the l_i'th derivative of y_i. This may be more rigorously phrased as determining the smallest l_i; l_i being the relative degree of the system from u_j to y_i, such that

$$\begin{aligned} \mathcal{L}_{b_j}(\mathcal{L}_f^k(y_i(t))) &= 0 \qquad \text{for } k=0,1,\ldots,l_i-2, \text{ some } j\in[1,2,\ldots,m] \\ \mathcal{L}_{b_j}(\mathcal{L}_f^{l_i-1}(y_i(t))) &\neq 0 \qquad \forall\, \mathbf{x}\in\mathbf{R}^n \end{aligned} \tag{15}$$

The l_i'th derivative of y_i is then

$$\dot{y}_i^{l_i} = \mathcal{L}_f^{l_i}(y_i(t)) + \sum_{j=1}^{m} \mathcal{L}_{b_j}(\mathcal{L}_f^{l_i-1}(y_i(t)))\, u_j \tag{16}$$

for each $i \in [1,2,...m]$. Grouping the system into matrix form with

$$\mathbf{A}(\mathbf{x}) = \begin{bmatrix} \mathcal{L}_f^{l_1}(y_1(t)) \\ \vdots \\ \mathcal{L}_f^{l_m}(y_2(t)) \end{bmatrix} \tag{17}$$

$$\mathbf{B}(\mathbf{x}) = \begin{bmatrix} \mathcal{L}_{b_1}(\mathcal{L}_f^{l_1-1}(y_1(t))) & \cdots & \mathcal{L}_{b_m}(\mathcal{L}_f^{l_1-1}(y_1(t))) \\ \vdots & \ddots & \vdots \\ \mathcal{L}_{b_1}(\mathcal{L}_f^{l_m-1}(y_m(t))) & \cdots & \mathcal{L}_{b_m}(\mathcal{L}_f^{l_m-1}(y_m(t))) \end{bmatrix} \tag{18}$$

the control law for I/O linearization may be written as

$$\mathbf{u} = \mathbf{B}^{-1}(\mathbf{x}) \left[-\mathbf{A}(\mathbf{x}) + \nu \right] \tag{19}$$

where $\mathbf{B}(\mathbf{x})$ is assumed invertible. This yields the set of decoupled systems

$$\frac{d^{l_i} y_i}{dt} = \nu_i \qquad \forall\, i \in [1,2,...,m] \tag{20}$$

For the case of the unicycle robot, an extremely simple control law results, since the control term arises explicitly in the yaw equation of motion, which is the output of concern, hence no further differentiation is required.

In equation (8), the term $I_2^w \Omega \dot{\psi}$ may be considered an exogenous disturbance of bounded magnitude, assuming that successful control of the wheel dynamics (Ω) in longitudinal, and roll rate ($\dot{\psi}$) in lateral, is achieved. Select the control law

$$\Gamma(t) = \left(\frac{1}{n_t}\right) \mathcal{F}(\dot{\psi},\Omega) + \Gamma_{gs} \tag{21}$$

which yields the resulting linearized dynamics (ignoring the "disturbances")

$$\dot{\psi} = \frac{n_t \Gamma_{gs}}{((I_3^f + I_3^w)s + f_{\dot{\psi}})} \tag{22}$$

where

s = Laplace operator

Γ_{lc} = Control command generated e.g. by linear controller

Since the viscous friction coefficient $f_{\dot{\psi}}$ and the inertias $(I_3^f + I_3^w)$ are strictly positive, the I/O output linearized system with $\mathcal{F}(\dot{\psi},\Omega)$ perfectly known and canceled, is strictly stable. This linearizing control law (equation (21)) is to be used in the adaptive friction compensation algorithms discussed in this chapter.

NEURAL NETWORK FRICTION IDENTIFICATION AND COMPENSATION

Introduction

Non–parametric regression techniques have in recent years seen a revival in interest as tools where learning through experience is the primary means of generating a

model. In this section this approach is applied to the friction compensation problem of the unicycle robot.

These techniques would in general have great difficulty learning an inverse model of the unicycle lateral dynamics for compensation and elimination of the friction effect, as a result of the system being both non minimum phase and unstable, as well as dynamic. The nature of the friction nonlinearity which is to be canceled, however, being a series concatenation with the linear actuator and easily written as a parametric model, lends itself well to localized learning of the unknown ("static") parameters and subsequent cancellation of the friction nonlinearity.

Figure 3.8 illustrates the block diagram structure for the neural network friction compensator. The network is continuously trained using a reference signal generated by a model (may be linear or nonlinear) which depends on the state of the system. The reference model in this case is that given by equation (8), specifying at each state $\mathbf{x}(t_k)$ and control command issued by the linear controller Γ_{lc}, an expected response of the system as if it were linear. The error (at time t_{k+1}) between the system actual response and the expected response is used to determine an estimate of the friction acting over the k'th sample period according to equation (12). This is then the training value for the neural network at the (k+1)'th time step.

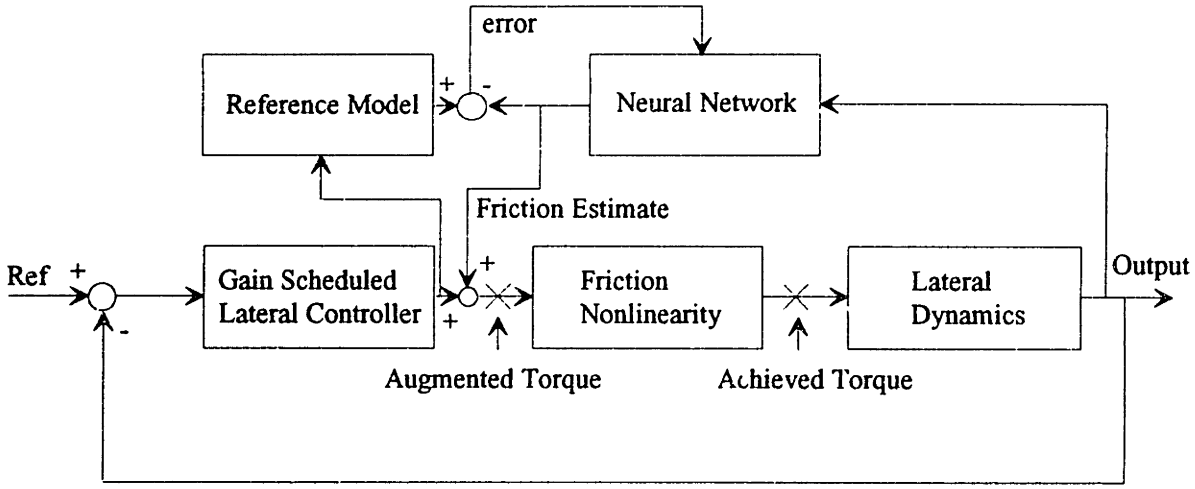

Figure 3.8. Neural network applied to nonlinear friction cancellation using a reference model for training. The transfer function between points x–x should ideally be 1.

The controller denoted "linear controller" in Figure 3.8, is the continuously gain scheduled controller (*chapter 2*) necessitated by the forward speed dependence of the lateral dynamics. In fact, lateral controllability varies strongly with forward speed and is completely lost at zero wheelspeed. Small deviations (change in wheelspeed by as little as 10%) from design points of the linear controllers can yield instability, which is easily overcome by the gain scheduling procedure.

Use of experimental data and pruning of an initial network structure with three inputs and a single hidden layer yields the structure of Figure 3.9. All inputs to the network are normalized and pruning is done by eliminating those weights which are orders of magnitude smaller than the rest.

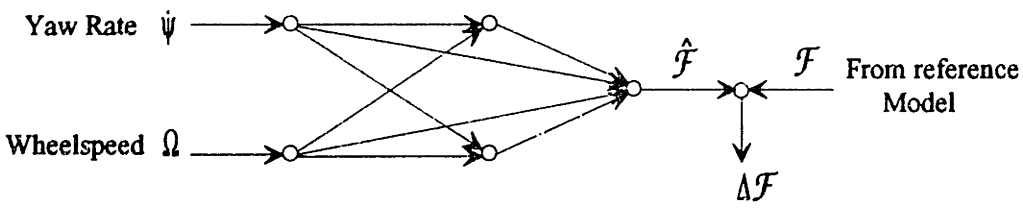

Figure 3.9. 3–Layer neural network structure determined by pruning an initial more complex structure and training on experimental data.

Use of a hidden layer is motivated by the friction model of figure 3.4, which indicates dependence of the friction on a combination of yaw rate and wheelspeed. The weights of the network (after training), however, placed less emphasis on this coupling than on direct dependence on wheelspeed and yaw rate.

The error $\Delta\mathcal{F}=\hat{\mathcal{F}}_k-\mathcal{F}_k$ where $\hat{\mathcal{F}}_k$ is the neural network estimated value and $\mathcal{F}_k$ is as determined by equation (12), is used for error back propagation to train the network. Note that the training value $\mathcal{F}_k$ is only obtained at time t_{k+1} and could thus not be used for compensation at time t_k.

The control command from the lateral gain scheduled controller (Γ_{gs}) is then augmented with the present estimate of the friction correction term according to equation (21) to yield the control command to the unicycle robot as (at time t_k)

$$\Gamma_k = (\Gamma_{gs}) + \hat{\mathcal{F}}_k/n_t \tag{23}$$

with $\hat{\mathcal{F}}_k/n_t$ the friction estimate scaled by the gear ratio (n_t) of the actuator.

Activation Function

The activation function used is the logistic function [*Rumelhart and McClelland*] with a change of scale to allow the output to be both positive and negative. Thus

$$f(net) = \frac{2}{(1 + e^{-x_i})} - 1$$

$$= (2f_1 - 1) \tag{24}$$

where

$$f_1 = \frac{1}{(1 + e^{-x_i})} \tag{25}$$

and

$$x_i = \sum_j (w_{ij} o_j) + \theta_i \tag{26}$$

with w_{ij} the network weight between the i'th and j'th nodes, θ_i the bias at the i'th node and o_j the output from the j'th node. The derivative of the activation function, required in the error back propagation algorithm is simply

$$f'(net) = 2f_1(1 - f_1) \tag{27}$$

All inputs to the network are also normalized to prevent saturation of the activation functions and the outputs are suitably scaled to give the correct command to the unicycle in Newton metres.

Error Back Propagation

The error back propagation algorithm (the standard delta rule) [*Rumelhart and McClelland*] is used to train the network. Initial off–line training is done using experimental data obtained with the ad hoc friction compensation scheme outlined in *chapter 2*. This allows pruning of the network to a simpler structure for implementing in real time for further on–line training.

Performance of the Neural Network Friction Compensator

The implemented neural network converges quickly when trained on new data. Typically, within the first two to three seconds of on–line training, convergence is reached, although this is still too slow when compared with the growth time constants of the system (on the order of 1/3 seconds). The real time implementation allows only a single error back propagation loop per control sample period as the computaticnal load of the control algorithm combined with the error back propagation algorithm is relatively high.

The network does very well in learning that which it is structured to learn, as is apparent from time histories of training signal and neural network estimate thereof of figure 3.10. Stability of the full closed loop lateral system is, however, not very good and fairly large roll excursions occur. This appears to be not as much the fault of the neural network, as that of the structure of the compensating scheme. As will be seen in the section on MRAC friction compensation, *approximate* cancellation of the friction is not good enough to yield a "stiff" system: much better performance is achieved if the friction is *overpowered* at all times, rather than only some of the time.

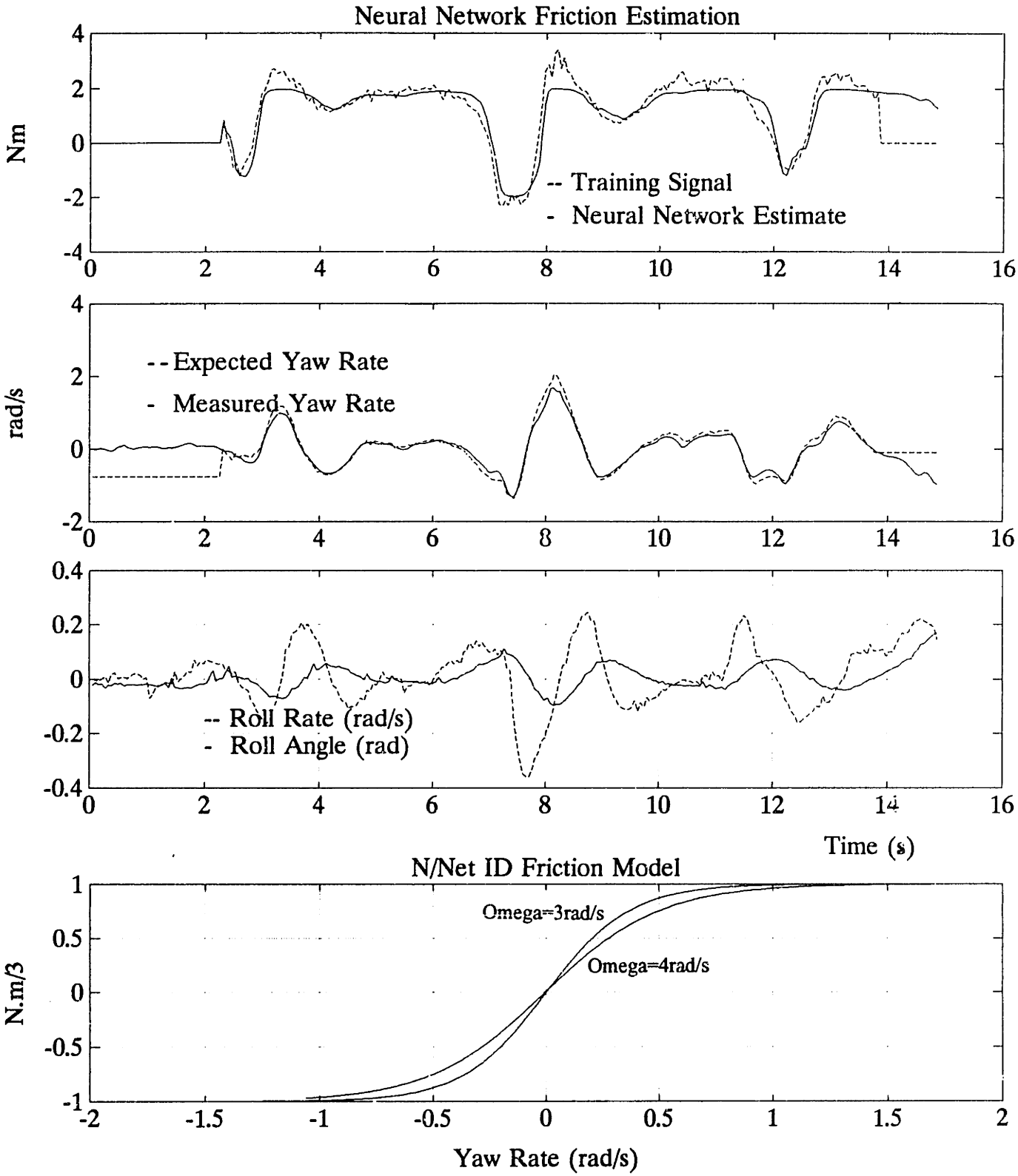

Figure 3.10. Performance of neural network friction compensator. Although the friction parameter estimates converge relatively quickly, the stability margins are significantly reduced, leading to much poorer performance than in the case of the MRAC controllers presented in the sequel.

LYAPUNOV STABILITY BASED MODEL REFERENCE ADAPTIVE CONTROLLER

Introduction

The Model Reference Adaptive Control (MRAC) technique [see e.g. *Landau*] offers a methodology to solving the problem of adaptive control of systems in which uncertainty in the parameters exists. The methodology has the invaluable advantage of being stability based, where the continuous time adaptation laws are determined strictly through consideration of the stability requirements of the system to be controlled.

This being the case, it may appear that the obvious solution to successful control of any parameter dependent system, for example the unicycle robot, is to define a model structure with the parameters unknown and to simply apply the MRAC method to the problem. This is a viewpoint difficult to oppose, since theoretically, precise conditions on parameter update laws and sufficiency of excitation of the probing signals in order to guarantee stability and parameter convergence may be determined in the design process. These may be extended as far as defining requirements to meet a desired form of stability: asymptotic, bounded, exponential, global, local, and more. The successful implementation, however, involves much more than is at first apparent, as is demonstrated in this section.

The performance of humans and other creatures of nature in the execution of a multitude of activities is an excellent lesson in persistence of excitation and careful model identification. It appears that the ability to execute tasks and functions is hugely enhanced by good knowledge of the specific nature and finer details of the

task. Without explicitly writing down a suitable definition of a model for example, the human unicyclist somehow learns an extremely good input–ouput mapping of the dynamics of the unicycle–"human actuator" combination, through persistent, repetitive execution of the various functions involved in riding a unicycle. Even when the model finally becomes well defined and the parameters of the model are well tuned to a specific unicycle, say a short one, the parameters have to be adjusted or re–learnt when changing to riding of a tall unicycle. It seems clear then that a good approach to achieving successful high performance "closed loop" control of any system involves careful and extensive identification of the task and the cause and effect relations (transfer functions) involved, as well as continuous training to optimize the knowledge of the parameters of the system. Indeed, this serves as good motivation for the ideas of persistence of excitation, identification and extensive good modeling techniques.

This digression may be interpreted in many ways, but the one chosen here is to serve as motivation for combining the best characteristics of each of the various control design approaches and careful modeling into a good solution for controlling the unicycle robot. To this end, the structure of the very successful linear controllers (including the gain scheduled controller) is maintained. Having reached the point of facing the nonlinear effects and hence the need to overcome these in a suitable fashion, which does not require retuning of the control parameters for every new friction condition, only this aspect which is uncertain is to be approached in an adaptive setting. It does not make a great deal of sense to adapt on any more parameters than is necessary.

The friction nonlinearity represents unstructured uncertainty to the linear gain scheduled controller. The MRAC technique is applied to compensate for the nonlinear

nature of the unstructured uncertainty by assuming some structure for the nonlinearity and determining suitable parameter estimation laws for successful tracking of the reference model. Figure 3.11 shows the structure of the implemented MRAC friction compensator. Note that in this figure, the friction effect is redrawn as an effective feedback nonlinearity.

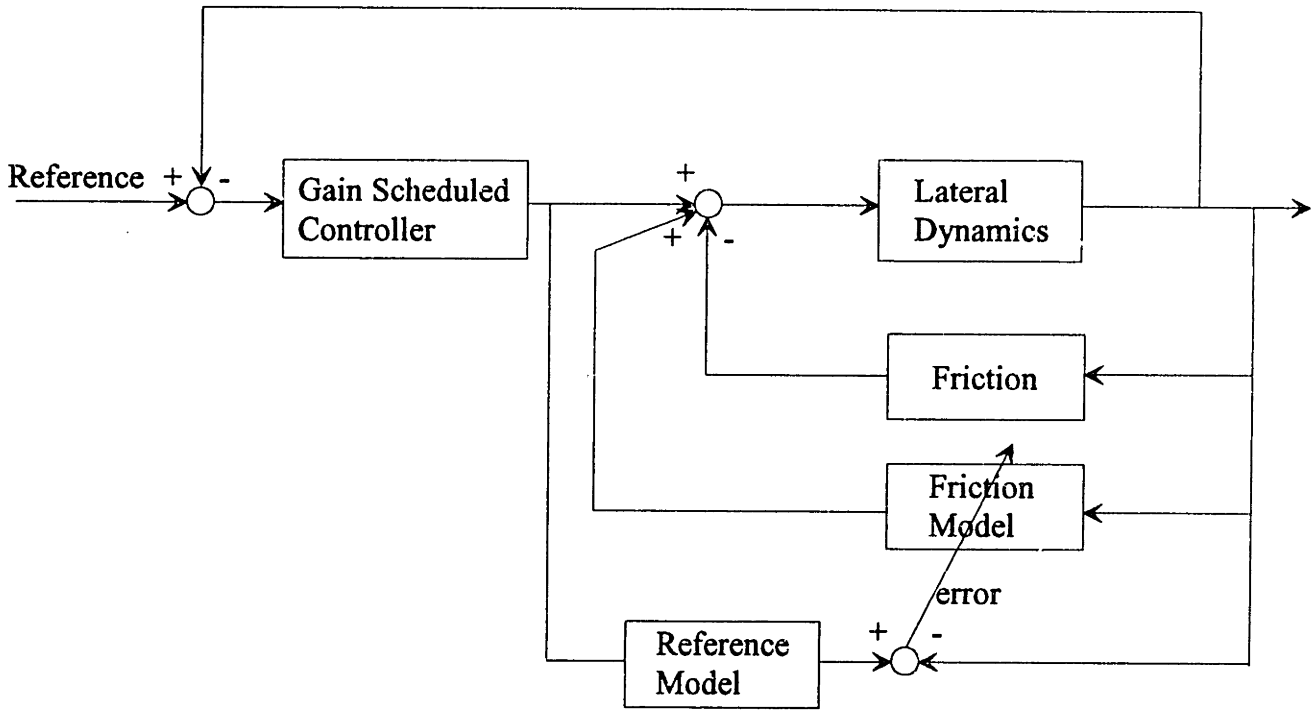

Figure 3.11. MRAC friction compensator structure as applied to unicycle lateral control problem.

Preliminaries

The following standard results from real analysis are useful in proving stability of the MRAC control algorithms to be derived in this section.

Lemma 1. A function $f(\cdot):R_+ \to R$ is uniformly continuous if it's derivative is bounded,

i.e. $\|f'(\cdot)\|_\infty < \infty$.

Proof: Assume $f'(t)$ is bounded. Then, the derivative of $f(t)$ in $\mathbb{R}$ is given by

$$\lim_{t \to t_0} \left\{ \frac{f(t) - f(t_0)}{t - t_0} \right\} = f'(t) \tag{28}$$

if the limit exists. For $C>0$ and $\| f'(\cdot) \|_\infty = \sup_{t \in [t_0,t]} \left\{ |f'(t)| \right\} = C$, by the mean value theorem, $\exists\ \xi \in [t_0,t]$, such that

$$\| f(t) - f(t_0) \| < \| f'(\xi) \|_\infty \| t - t_0 \| = C \| t - t_0 \|$$

Set $\| t - t_0 \| = \delta$ and $C = \epsilon/\delta$, δ and $\epsilon > 0$, ϵ independent of t, then this is analogous to stating that given $\epsilon > 0$, $\exists\ \delta > 0$, such that $\forall \| t - t_0 \| < \delta$,

$$\| f(t) - f(t_0) \| < \epsilon/\delta(\delta) = \epsilon \tag{29}$$

which is the definition of uniform continuity of $f(\cdot)$.

Lemma 2. For a positive definite function $V(e(t))$, if $\dot{V}(e(t)) = -Ke^2$, $K>0$, then $e \in \mathcal{L}_2$.

Proof: Consider $V(e(t))$, for any $t>t_0$. Then, since $V(\cdot)$ is positive definite,

$$V(e(t)) = V(e(t_0)) + \int_{t_0}^{t} (-Ke^2)\, dt > 0 \tag{30}$$

or, since $V(e(t_0))$ is finite,

$$\int_{t_o}^{t} |(Ke^2)|\, dt \qquad < V(e(t_o)) \qquad < \infty \tag{31}$$

which, by definition is equivalent to stating $e \in \mathscr{L}_2$.

Lemma 3. For a function $V(\cdot):R_+ \to R$, if $\dot{V}(\cdot) \in \mathscr{L}_2$ and the time derivative $\ddot{V}(\cdot) \in \mathscr{L}_\infty$, then $\dot{V}(\cdot) \to 0$ as $t \to \infty$.

Proof: A formal proof of this lemma is given in [*Slotine and Lie*,Yale workshop ... May 1987]

Theorem.(Lyapunov). For any positive definite symmetric matrix **Q**, there exists a positive definite symmetric matrix **P**, which for the stable linear system $\dot{\mathbf{x}}=\mathbf{Ax}$, i.e. with $\mathrm{Re}\{\lambda(\mathbf{A})\}<0$, satisfies the matrix Lyapunov equation

$$\mathbf{A'P + PA} \qquad = -\mathbf{Q} \tag{32}$$

Proof: [*Kailath*] Necessity. Show that a suitable solution for **P** is given (for $\mathrm{Re}\{\lambda(\mathbf{A})\}<0$) by

$$\mathbf{P} \quad = \int_0^\infty e^{\mathbf{A'}t} \mathbf{Q} e^{\mathbf{A}t} dt \tag{33}$$

where the integrand exists due to the condition on the eigenvalues of A, that $\mathrm{Re}\{\lambda(\mathbf{A})\}<0$. Substituting equation (33) into (32),

$$
\begin{aligned}
A'P + PA &= \int_0^\infty A' e^{A't} Q e^{At} dt + \int_0^\infty e^{A't} Q e^{At} A \, dt \\
&= \int_0^\infty \frac{d}{dt} (e^{A't} Q e^{At}) \, dt \\
&= \left\{ e^{A't} Q e^{At} \right\}_0^\infty \\
&= -Q
\end{aligned} \tag{34}
$$

Sufficiency. Assume $\exists$ Q, P positive definite symmetric matrices satisfying the Matrix Lyapunov equation. Consider the Lyapunov function for the linear system

$$V = x'Px \tag{35}$$

then

$$
\begin{aligned}
\dot{V} &= x'A'Px + x'PAx \\
&= -x'Qx
\end{aligned} \tag{36}
$$

and stability follows.

Corollary. (La Salle). For the time invariant system $\dot{x}=Ax$, Q may be positive semi–definite if $x'Qx$ is not identically zero along any trajectory of the system. This is in fact an observability requirement for the system output $y=Cx$, where $x'Qx=x'C'Cx$, i.e. $Q=C'C$.

Remark. It is worthy of note that the system may be time varying, $\dot{x}(t)=A(t)x(t)$. As long as *constant* matrices P and Q can be found satisfying the

Lyapunov equation, the stability argument still holds [*Anderson–Bitmead–Johnson et al*].

Unicycle MRAC Friction Compensation Considering only Yaw Dynamics

The assumed friction model is a suitable function which does not have to be smooth or continuous

$$\mathcal{F} = \mathcal{F}(\Omega(t),\dot{\psi}(t)) \tag{37}$$

and the reference model is the yaw equation of motion as in the previous section, given by equation (8). Note that the model is dependent on both wheelspeed and yaw rate, although not necessarily explicitly.

The compensator structure is simply the I/O linearizing control law of equation (12), with the tracking error ($e = \dot{\psi}_p - \dot{\psi}_m$) driving the parameter update algorithm. The reference model of equation (8) may be rewritten

$$\ddot{\psi}_m = (n_t\Gamma_{gs} - f_{\dot{\psi}}\dot{\psi}_m - I_2^w\Omega\dot{\varphi})/I_3 \tag{38}$$

and the (assumed) actual plant dynamics are given by

$$\ddot{\psi}_p = (n_t u_2 - f_{\dot{\psi}}\dot{\psi}_p - I_2^w\Omega\dot{\varphi} - \mathcal{F}(\cdot))/I_3 \tag{39}$$

where the inertia is lumped into one parameter, $I_3 = I_3^f + I_3^w$. Note that the actual plant is driven by a different input, u_2, to that of the model input, Γ_{gs}, where Γ_{gs} is

the command generated by the gain scheduled linear controller and does not take into account the friction effect. These control commands are related as

$$u_2 = \Gamma_{gs} + \hat{\mathcal{F}}(\cdot)/n_t \tag{40}$$

For the error of interest (yaw rate error) $e = \dot{\psi}_p - \dot{\psi}_m$, applying the control law of equation (40), the error dynamics may be written

$$\begin{aligned} \dot{e} &= \ddot{\psi}_p - \ddot{\psi}_m \\ &= ((\hat{\mathcal{F}} - \mathcal{F}) - f_{\dot{\psi}} e)/I_3 \end{aligned} \tag{41}$$

Write the friction in terms of the unknown parameter, ξ_f, as

$$\mathcal{F} = \frac{d\mathcal{F}}{d\xi_f}\xi_f \tag{42}$$

Defining the parameter error $\theta = \xi_f - \hat{\xi}_f$, a Lyapunov function candidate is

$$V = \frac{1}{2}(\gamma e^2 + \theta^2) \tag{43}$$

which, for $\gamma > 0$, is positive definite in the tracking error e and parameter error θ. The derivative $\dot{V} = \frac{d}{dt}V$ yields

$$\begin{aligned} \dot{V} &= \gamma e\dot{e} + \theta\dot{\theta} \\ &= \gamma e(\frac{d\mathcal{F}}{d\xi_f}(\hat{\xi}_f - \xi_f) - f_{\dot{\psi}} e)/I_3 + \theta\dot{\theta} \end{aligned} \tag{44}$$

Setting the parameter update law as

$$\dot{\theta} = (\gamma e \frac{d\mathcal{F}}{d\xi_f})/I_3$$
$$= -\dot{\hat{\xi}}_f \qquad (45)$$

the Lyapunov function derivative with respect to time becomes

$$\dot{V} = -\gamma f_{\dot{\psi}} e^2/I_3 \qquad (46)$$

which is negative definite in the tracking error (e). The tracking error will thus converge asymptotically to zero as $t \to \infty$.

Proof: For any initial nonzero $V_0=V(e(t_0),\theta(t_0))$ (>0, since V pdf), then since $\dot{V}$ is negative definite in the tracking error e ($\dot{V}=0$ only for e identically zero), $V(e(t),\theta(t)) < V_0 \; \forall \; t>t_0$. By lemma 2, then $e \in \mathcal{L}_\infty$, i.e. e is bounded, thus θ is bounded since $V(e(t_0),\theta(t_0))$ is finite and $V(\;(t)\;)<V(\;(t_0)\;)$.

Now,

$$\ddot{V} = -2\gamma f_{\dot{\psi}} e\dot{e}/I_3 = -2\gamma f_{\dot{\psi}} e(\frac{d\mathcal{F}}{d\xi_f}(\dot{\hat{\xi}}_f - \dot{\xi}_f) - f_{\dot{\psi}} e)/I_3)/I_3 \qquad (47)$$

with $\theta=\hat{\mathcal{F}}-\mathcal{F}$ bounded and e bounded, $\ddot{V} \in \mathcal{L}_\infty$, such that by lemma 1, $\dot{V}$ is uniformly continuous and hence by lemma 3 it may be shown that $\dot{V} \longrightarrow 0$ as $t \longrightarrow \infty$, i.e. the output $\dot{\psi}_p(t)$ tracks the reference trajectory $\dot{\psi}_m(t)$.

In order to further guarantee parameter convergence ($\dot{\hat{\xi}}_f \longrightarrow \dot{\xi}_f$), richness conditions on the output $\dot{\psi}$ are needed.[see e.g. *Canudas, Åström and Wittenmark*]

STABILITY OF THE FULL LATERAL CLOSED LOOP SYSTEM

Introduction

In the previous section, the MRAC parameter adaptation algorithm is derived assuming that by considering only the relevant equation of motion the parameter estimation laws are easily determined without impacting the stability of the rest of the system.

In this section, it is shown for the unicycle robot that this is indeed true. Designing the adaptive controller by considering the complete lateral system with gain scheduled lateral controller loops closed, yields exactly the same parameter adaptation laws while maintaining stability of the full closed loop system.

MRAC Design with Full Lateral Model Excluding Turntable Dynamics.

Consider the full lateral model, with state vector $\mathbf{x}=[\dot{\phi}\ \phi\ \dot{\psi}\ \psi\ i_{\psi}]'$. Define the *reference model* as

$$\dot{\mathbf{x}}_m(t) = \mathbf{A}\,\mathbf{x}_m(t) + \mathbf{B}\,\Gamma_{gs}(t) \tag{48}$$

with

$$\Gamma_{gs} = -\mathbf{G}(\Omega(t))(\mathbf{x}_m(t) - \mathbf{x}_{ref}(t)) \tag{49}$$

the gain scheduled linear controller feedback command. The *actual* system is assumed represented by

$$\dot{\mathbf{x}}_p(t) = \mathbf{A}\,\mathbf{x}_p(t) + \mathbf{B}\,(\,\Gamma_p(t) - \mathscr{L}\xi_a(\cdot)) \tag{50}$$

with

$$\Gamma_p(t) = -\mathbf{G}(\Omega(t))(\mathbf{x}_p(t) - \mathbf{x}_{ref}(t)) + \mathscr{L}\hat{\xi}_a(\cdot) \tag{51}$$

Define the error state and derivative with respect to time as

$$\mathbf{e}(t) = \mathbf{x}_p(t) - \mathbf{x}_m(t) \tag{52}$$

$$\dot{\mathbf{e}}(t) = (\mathbf{A} - \mathbf{BG})\mathbf{e}(t) - \mathbf{B}\,\mathscr{L}(\xi_a - \hat{\xi}_a) \tag{53}$$

where, for example, if the assumed tire friction model for the unicycle robot is ($\mathscr{L}$ ξ_a)= $C\mathrm{sgn}(\dot{\psi}) + K\Delta\psi$, then the "friction distribution matrix", $\mathscr{L}$ is of order 1×m, where m is the number of friction parameters (m=2 in the case if a two parameter friction model), thus

$$\mathscr{L} = \begin{bmatrix} \frac{d\mathcal{F}}{d\xi_{f_1}} & \frac{d\mathcal{F}}{d\xi_{f_2}} \end{bmatrix} \tag{54}$$

$$= [\,\mathrm{sgn}(\dot{\psi})\;\; \Delta\psi\,] \tag{55}$$

and the friction parameter vector is of order m×1

$$\xi_a = \begin{bmatrix} C \\ K \end{bmatrix}_{m\times 1} \tag{56}$$

For the Lyapunov function, with $\theta = [\xi_a - \hat{\xi}_a]$

$$V = e(t)'Pe(t) + \theta'\Gamma^{-1}\theta \tag{57}$$

which is a positive definite function (pdf) in e and θ, for P and Γ positive definite matrices. The derivative with respect to time is

$$\begin{aligned}\dot{V} &= \dot{e}'Pe + e'P\dot{e} + \dot{\theta}'\Gamma^{-1}\theta + \theta'\Gamma^{-1}\dot{\theta} \\ &= e'(A-BG)'Pe - e'PB\mathscr{L}(\xi_a - \hat{\xi}_a) + e'P(A-BG)e \\ &\quad -(\xi_a - \hat{\xi}_a)'\mathscr{L}'B'Pe + \dot{\theta}'\Gamma^{-1}\theta + \theta'\Gamma^{-1}\dot{\theta}\end{aligned} \tag{58}$$

Then for an assumed constant wheelspeed such that the lateral gain scheduled system is time invariant (this is approximately true for operation at a commanded wheelspeed setpoint with $\frac{d}{dt}\Omega \approx 0$), since (A–BG) is Hurwitz, $\exists$ a positive definite matrix Q, satisfying the matrix Lyapunov equation

$$(A-BG)'P + P(A-BG) = -Q \tag{59}$$

Selecting the parameter update law as

$$\begin{aligned}\dot{\theta}'\Gamma^{-1} &= e'PB\mathscr{L} \\ &= -\dot{\hat{\xi}}_a'\Gamma^{-1}\end{aligned} \tag{60}$$

or, equivalently

$$\dot{\hat{\xi}}_a = -\Gamma\mathscr{L}'B'Pe \tag{61}$$

the Lyapunov function time derivative becomes

$$\dot{V} = -e'Qe \tag{62}$$

which is negative definite in the tracking error, e. Thus, it is concluded that the tracking error asymptotically converges to zero as $t \rightarrow \infty$. Note that this result is entirely dependent on the strong assumption that the only unknown aspect of the plant is the friction nonlinearity which only explicitly impacts the yaw equation of motion. For P and Γ diagonal, any modeling errors which may cause disparity in the response of the roll dynamics relative to what the reference model expects, cannot propagate into the parameter update laws in order for the adaptive controller to account for these errors as well as the friction effects. This becomes clear in the following section where the adaptation laws are explicitly written out. The bottom line is (not surprisingly!) that in order for this adaptive controller to account for any error, explicit definition of a model for the error cause must be included into the problem formulation.

Proof: The proof follows the same arguments as for the case of MRAC design for the model considering only yaw dynamics.

Parameter Update Laws

For the parameter update law derived above

$$\dot{\xi}_a = -\Gamma \mathscr{L}' B' Pe$$

with

$$\mathbf{e} = \begin{bmatrix} \dot{\phi} \\ \phi \\ \dot{\psi} \\ \psi \\ \dot{i}_{\psi} \end{bmatrix}_{\text{actual}} - \begin{bmatrix} \dot{\phi} \\ \phi \\ \dot{\psi} \\ \psi \\ \dot{i}_{\psi} \end{bmatrix}_{\text{model}} \tag{63}$$

Defining

$$\Gamma = \begin{bmatrix} \Gamma_{11} & 0 \\ 0 & \Gamma_{22} \end{bmatrix} \tag{64}$$

$$\mathbf{P} = \begin{bmatrix} P_{11} & 0 & \cdots & 0 \\ 0 & P_{22} & \cdots & 0 \\ \vdots & & \ddots & \vdots \\ 0 & 0 & \cdots & P_{55} \end{bmatrix} \tag{65}$$

and assuming the tire friction model of [*Papadopoulos*] as

$$\mathcal{F} = K_1 \Delta\psi + K_2 \dot{\psi} \tag{66}$$

such that the friction distribution matrix is

$$\mathcal{L} = [\, \dot{\psi}_p \;\; \Delta\psi_p \,] \tag{67}$$

then, the update law reduces to

$$\dot{\hat{\xi}}_a = \begin{bmatrix} \dot{\hat{K}}_2 \\ \dot{\hat{K}}_1 \end{bmatrix}$$

$$= \begin{bmatrix} -\Gamma_{11}\dot{\psi}_p B_3 P_{33}(\dot{\psi}_p - \dot{\psi}_m) \\ -\Gamma_{22}\Delta\psi B_3 P_{33}(\dot{\psi}_p - \dot{\psi}_m) \end{bmatrix}$$

$$= \begin{bmatrix} -\Gamma_{11} \dfrac{d\hat{\mathcal{F}}_1}{d\hat{K}_2} B_3 P_{33}(\dot{\psi}_p - \dot{\psi}_m) \\ -\Gamma_{22} \dfrac{d\hat{\mathcal{F}}_2}{d\hat{K}_1} B_3 P_{33}(\dot{\psi}_p - \dot{\psi}_m) \end{bmatrix} \tag{68}$$

with

$$\begin{aligned} \hat{\mathcal{F}}_1 &= \hat{K}_2 \dot{\psi}_p \\ \hat{\mathcal{F}}_2 &= \hat{K}_1 \Delta\psi \end{aligned} \tag{69}$$

The parameter update law is thus similar to the one (equation (45)) derived in the previous section (apart from the "gains", Γ_{ii} and P_{ii}), only dependent on errors in the yaw dynamics ($\dot{\psi}_p - \dot{\psi}_m$), and stability of the full closed loop system is maintained with this adaptive control algorithm active.

MRAC DESIGN WITH MODEL INCLUDING YAW AND TURNTABLE DYNAMICS.

For the unicycle robot, the turntable friction is easily measured and does not vary significantly enough to warrant adaptive compensation of this effect too. Instead, a fixed parameter turntable friction compensation term ($\hat{\mathcal{F}}_t$) is added to the control law

$$\Gamma = \Gamma_{gs} + \mathscr{L}\hat{\xi}(\cdot)/n_t + \hat{\mathcal{F}}_t/n_t \tag{70}$$

(n_t is turntable gear ratio)

If, however, this is not the case, i.e. the friction due to the turntable drive train is, for example, more significantly dependent on the turntable position or speed or both, or

other parameters, then an adaptive control strategy for accounting for this variation is given here. In this section, special use of the yaw inertia matrix is made to yield simpler parameter update laws, an application inspired by [*Slotine*].

Consider the yaw dynamics of the unicycle robot with the turntable dynamics appended [*Vos*, S.M.]. The state $\dot{\eta}$ represents turntable angular velocity relative to the frame.

Reference Model

$$(I_3^w + I_3^f)\ddot{\psi}_m + I_2^w \Omega \dot{\phi} = -f_{\dot{\psi}}\dot{\psi}_m + f_{\dot{\eta}}\dot{\eta}_m + n_t \Gamma_{gs} \tag{71a}$$

$$I_3^t(\ddot{\eta}_m + \ddot{\psi}_m) = -f_{\dot{\eta}}\dot{\eta}_m - n_t \Gamma_{gs} - \hat{\mathcal{F}}_f \tag{71b}$$

Assumed Actual Plant

$$(I_3^w + I_3^f)\ddot{\psi}_p + I_2^w \Omega \dot{\phi} = -f_{\dot{\psi}}\dot{\psi}_p + f_{\dot{\eta}}\dot{\eta}_p + n_t \Gamma - \mathcal{F}_f + \mathcal{F}_t \tag{72a}$$

$$I_3^t(\ddot{\eta}_p + \ddot{\psi}_p) = -f_{\dot{\eta}}\dot{\eta}_p - n_t \Gamma - \mathcal{F}_t \tag{72b}$$

with the I/O linearizing control law

$$\Gamma = \Gamma_{gs} + (\hat{\mathcal{F}}_f - \hat{\mathcal{F}}_t)/n_t \tag{73}$$

where the turntable dynamics reference model includes the added torque due to compensation for the friction arising at the tire/surface interface. Equations (71) and (72) may be rewritten as (add $(\cdot)$b to $(\cdot)$a and include the control law of equation (73))

Model

$$(I_3^w + I_3^f + I_3^t)\ddot{\psi}_m + I_3^f\ddot{\eta}_m + I_2^w\Omega\dot{\phi} = -f_{\dot{\psi}}\dot{\psi}_m - \hat{\mathcal{T}}_f \tag{74}$$

$$I_3^t(\ddot{\eta}_m + \ddot{\psi}_m) = -f_{\dot{\eta}}\dot{\eta}_m - n_t\Gamma_{gs} - \hat{\mathcal{F}}_f \tag{75}$$

Plant

$$(I_3^w + I_3^f + I_3^t)\ddot{\psi}_p + I_3^f\ddot{\eta}_p + I_2^w\Omega\dot{\phi} = -f_{\dot{\psi}}\dot{\psi}_p - \mathcal{T}_f \tag{76}$$

$$I_3^t(\ddot{\eta}_p + \ddot{\psi}_p) = -f_{\dot{\eta}}\dot{\eta}_p - n_t\Gamma_{gs} - \hat{\mathcal{F}}_f + \hat{\mathcal{F}}_t - \mathcal{T}_t \tag{77}$$

Define the matrices

$$\mathbf{I} = \begin{bmatrix} (I_3^w+I_3^f+I_3^t) & I_3^t \\ I_3^t & I_3^t \end{bmatrix}$$

$$\mathbf{C} = \begin{bmatrix} f_{\dot{\psi}} & 0 \\ 0 & f_{\dot{\eta}} \end{bmatrix} \qquad \mathbf{K} = \begin{bmatrix} I_2^w\Omega\dot{\phi} \\ 0 \end{bmatrix}$$

$$\boldsymbol{\theta} = \begin{bmatrix} \xi_f - \hat{\xi}_f \\ \xi_t - \hat{\xi}_t \end{bmatrix} \qquad \mathbf{F} = \begin{bmatrix} -\mathcal{T}_f \\ -\mathcal{T}_t \end{bmatrix} \qquad \mathbf{B} = \begin{bmatrix} 0 \\ -n_t \end{bmatrix} \tag{78}$$

and for the assumed friction model parameters (ξ_t and ξ_f)

$$\mathscr{L}\boldsymbol{\theta} = \begin{bmatrix} -\mathcal{T}_f + \hat{\mathcal{T}}_f \\ -\mathcal{T}_t + \hat{\mathcal{T}}_t \end{bmatrix} = \begin{bmatrix} -\dfrac{d\mathcal{T}_f}{d\xi_f} & 0 \\ 0 & -\dfrac{d\mathcal{T}_t}{d\xi_t} \end{bmatrix} \begin{bmatrix} \xi_f - \hat{\xi}_f \\ \xi_t - \hat{\xi}_t \end{bmatrix} \tag{79}$$

For the error defined as

$$\mathbf{e} = \begin{bmatrix} \dot{\psi}_p \\ \dot{\eta}_p \end{bmatrix} - \begin{bmatrix} \dot{\psi}_m \\ \dot{\eta}_m \end{bmatrix} \tag{80}$$

the error dynamics are

$$\dot{\mathbf{e}} = -\mathbf{I}^{-1}\mathbf{C}\mathbf{e} - \mathbf{I}^{-1}\mathscr{L}\boldsymbol{\theta} \tag{81}$$

Noting that, since the (symmetric) inertia matrix has the property that $-\mathbf{I}$ is Hurwitz it is a positive definite matrix, construct the Lyapunov function

$$V = (\mathbf{e}'\mathbf{I}\mathbf{e} + \boldsymbol{\theta}'\boldsymbol{\gamma}^{-1}\boldsymbol{\theta})/2 \tag{82}$$

with

$$\boldsymbol{\gamma} = \begin{bmatrix} \gamma_1 & 0 \\ 0 & \gamma_2 \end{bmatrix} \qquad (\gamma_i \text{ positive}) \tag{83}$$

Determine the Lyapunov function derivative with respect to time, noting that for the damping matrix $\mathbf{C}'=\mathbf{C}$, as

$$\begin{aligned} \dot{V} &= (\dot{\mathbf{e}}'\mathbf{I}\mathbf{e} + \mathbf{e}'\mathbf{I}\dot{\mathbf{e}} + \dot{\boldsymbol{\theta}}'\boldsymbol{\gamma}^{-1}\boldsymbol{\theta} + \boldsymbol{\theta}'\boldsymbol{\gamma}^{-1}\dot{\boldsymbol{\theta}})/2 \\ &= -\mathbf{e}'\mathbf{C}'\mathbf{e} + (-\boldsymbol{\theta}'\mathscr{L}'\mathbf{e} - \mathbf{e}'\mathscr{L}\boldsymbol{\theta} + \dot{\boldsymbol{\theta}}'\boldsymbol{\gamma}^{-1}\boldsymbol{\theta} + \boldsymbol{\theta}'\boldsymbol{\gamma}^{-1}\dot{\boldsymbol{\theta}})/2 \end{aligned} \tag{84}$$

Select the parameter update laws as

$$\dot{\boldsymbol{\theta}}' = \mathbf{e}'\mathscr{L}\boldsymbol{\gamma} \tag{85}$$

or, equivalently, for $\dot{\xi}_f \approx 0$ and $\dot{\xi}_t \approx 0$ since the parameters are assumed either

constant for a given operating condition or do not vary significantly with time

$$\dot{\xi}_f = \gamma_1 \frac{d\mathcal{F}_f}{d\xi_f}(\dot{\psi}_p - \dot{\psi}_m) \tag{86}$$

$$\dot{\xi}_t = \gamma_2 \frac{d\mathcal{F}_t}{d\xi_t}(\dot{\eta}_p - \dot{\eta}_m) \tag{87}$$

yields

$$\dot{V} = -\mathbf{e}'\mathbf{C}\mathbf{e} \tag{88}$$

hence asymptotic stability is guaranteed for the error dynamics, since the Lyapunov function is negative definite in the error **e**.

Proof: As for the previous cases, since V is positive definite and $\dot{V}$ is negative definite in the tracking error, then $V(t)<V(t_o)$, $\forall t \geq t_o$. This implies that $\|\mathbf{e}\|$ is bounded and $\|\boldsymbol{\theta}\|$ is bounded. Then, since $\ddot{V}=\mathbf{e}'\mathbf{C}(\mathbf{I}^{-1}\mathbf{C}\mathbf{e}+\mathbf{I}^{-1}\mathcal{L}\boldsymbol{\theta})+(\mathbf{I}^{-1}\mathbf{C}\mathbf{e}+\mathbf{I}^{-1}\mathcal{L}\boldsymbol{\theta})'\mathbf{C}\mathbf{e}$, this is also bounded, thus by Lemma 1, $\dot{V}$ is uniformly continuous and by Lemma 3, $\dot{V}\to 0$ as $t\to\infty$. Thus the error dynamics are asymptotically stable.

THE EFFECTIVE ERROR DYNAMICS

It is useful in terms of gaining insight to the parameter adjustment effects on the system, to consider the error dynamics. Under the assumptions of the design, the MRAC system typically yields stable error dynamics satisfying the equation

$$\begin{aligned}\dot{e}(t) &= (A - BG)e(t) - B(\mathscr{L}\xi - \mathscr{L}\hat{\xi}) \\ &= (A - BG)e(t) - B\mathscr{L}(\xi + \left\{ \int_{t_0}^{t} \Gamma \mathscr{L}' B' P e \, dt + \hat{\xi}(t_0) \right\}) \qquad (89)\end{aligned}$$

The error dynamics are thus effectively integral error regulation in order to eliminate the tracking errors.

IMPLEMENTATION OF MRAC FRICTION COMPENSATOR

The Reference Model in Implementation

The model reference adaptive control strategy, by it's nature, requires integration of the *reference* model dynamics forward in real time in order to generate a reference trajectory for the controller. In implementation, it is typical for the MRAC system to give good performance for extended periods of time before unexpectedly "blowing up" as instability occurs [e.g. *Rohrs*]. This has been exemplified in the unicycle robot case, since for a system of such unstable natural characteristics, it does not take long for the tracking errors to propagate to too large values and subsequently destabilize the process.

A possible reason for this is that tracking errors may grow due to inaccuracy and biases in both sensors and actuators as well as the plant model. This combined effect of model errors and sensor biases may lead to propagation of the tracking errors different to what is expected by the adaptive update laws, and when the errors become large enough, the parameter adaptation law effectively becomes nonsense, since the parameters estimated by the MRAC parameter update law have no longer any relevance to the problem at hand.

Consider, for example, the parameter update laws derived above applied to a system with some errors (modeling and/or sensor errors). The friction canceling control term is

$$\mathbf{u} = \mathscr{L}\hat{\xi}(\cdot)/n_t \tag{90}$$

which is directly dependent on the estimate $\hat{\xi}$. While it is true that the parameters of the MRAC strategy may not converge to correct values while the errors do converge to zero, this is exactly the undoing of the implemented system. Consider the model and system equation of motion, with the error Δ due to the unknown effect of incorrect modeling or sensor biases (assume full state measurement) and $\mathcal{G}(\cdot)$ and $\hat{\mathcal{G}}(\cdot)$ the friction nonlinearity and estimate, respectively,

$$\underline{\text{Model}}: \quad \dot{\mathbf{x}}_m = \hat{f}(\mathbf{x}_m) + \hat{\mathcal{G}}(\cdot) \tag{91}$$

$$\underline{\text{Plant}}: \quad \dot{\mathbf{x}}_p = f(\mathbf{x}_p) + \mathcal{G}(\cdot) + \Delta \tag{92}$$

Propagating the states through integration yields the propagated error (assuming zero initial conditions)

$$\mathbf{e} = \int_{t_0}^{t} \{f(\mathbf{x}_p) - \hat{f}(\mathbf{x}_m) + \mathcal{G}(\cdot) - \hat{\mathcal{G}}(\cdot) + \Delta\}\, dt \tag{93}$$

The MRAC strategy is designed assuming $f(\cdot)=\hat{f}(\cdot)$, and the parameter update law explicitly takes care of the nonlinearity $\mathcal{G}(\cdot) - \hat{\mathcal{G}}(\cdot)$. No strategy, however, takes care of the error term Δ, which arises in the state error $\mathbf{e}(t)$ in integral form. Applying this to the parameter update law, then yields

$$\dot{\hat{\xi}} = -\gamma \frac{\partial \mathcal{G}}{\partial \xi} e \tag{94}$$

which, when integrated yields

$$\hat{\xi}(t) = \xi_{correct}(t) + \int_{t_0}^{t}\int_{t_0}^{t} K \Delta \, dt \tag{95}$$

where

$\xi_{correct}(t)$ — correct value. Note that this does not imply that the parameter estimate converges to the actual correct value, but simply that the *actual* error (the actual difference between the system response and that predicted by the model, excluding the Δ term) is driven to zero.

$\int_{t_0}^{t}\int_{t_0}^{t} K \Delta \, dt$ — Erroneous additive value which results in the *measured* error decaying to zero, but this is not the *actual* error which the MRAC system was designed to compensate for.

This may further be viewed in the light of e.g. the case where persistence of excitation exists, which, if $\Delta=0$ would result in the correct error decaying to zero by the MRAC control law *and* the parameter estimates converging to the actual values.

In effect, the stability of the system would then depend upon the correct parameter estimate being determined after some time t_s, i.e.

$$\hat{\xi}(t) = \xi_{correct}(t) \qquad \forall\, t > t_s \qquad (96)$$

If, however, $\Delta \neq 0$, then the measured "error" will decay to zero, but the parameter estimates would be incorrect and the system may destabilize. In this case, the estimate becomes that of equation (95) and since the condition for stability (where persistence of excitation exists) is that the term $\mathcal{G}$ is satisfactorily canceled, this is violated and stability is not guaranteed.

Also, the Lyapunov function time derivative with the error Δ included becomes

$$\dot{V} = -e'Qe + \Delta'Pe + e'P\Delta$$

which is not guaranteed negative definite, hence stability of the error dynamics cannot be concluded.

An easy means of solving this problem arises out of the discrete time implementation of the MRAC controller. In the case of the unicycle, the differential equations are integrated forward in time by Euler integration since the sample period is much shorter than any of the system time constants. By integrating the model dynamics forward in time assuming that the tracking error is *zero* at the beginning of each sample period, i.e. assume $\mathbf{x}_{m_k} = \mathbf{x}_{p_k}$ for the k'th sample period, the model error does not propagate and cannot thus cause any difficulty. The resulting tracking errors are effectively only considered to contribute performance disparity (difference between "model" and actual response) due to friction effects over the previous sample period and then reset to zero after the effect has been included in the parameter update law.

The reference model is thus implemented as (ΔT sample period)

$$x_{ref}(k+1) \quad = x_{ref}(k) + \dot{x}_{ref}(k)\Delta T$$

after z samples, reset the propagated reference trajectory

$$x_{ref}(k+z) \quad = x_{measured}(k+z) \tag{97}$$

In the case of the unicycle robot, z=1 yields excellent performance.

It is highly unlikely that the modeling/bias error would change as rapidly as the sample period (if it does, new sensors or modeling techniques should be considered imperative!) so that the net effect is to completely eliminate this type of problem.

For the unicycle example, the yaw rate sensor (which is of critical importance in the MRAC friction cancellation algorithm since this equation of motion is the reference model) has a slowly drifting bias, which easily drives the MRAC system unstable. Figure 3.12 shows the performance in the case of simply propagating the reference model from some initial condition without reset. The case in which the tracking errors are propagated indefinitely yields instability after only 4–5 seconds, whilst the adjusted propagation case ("Error Reset") maintains *good* performance indefinitely.

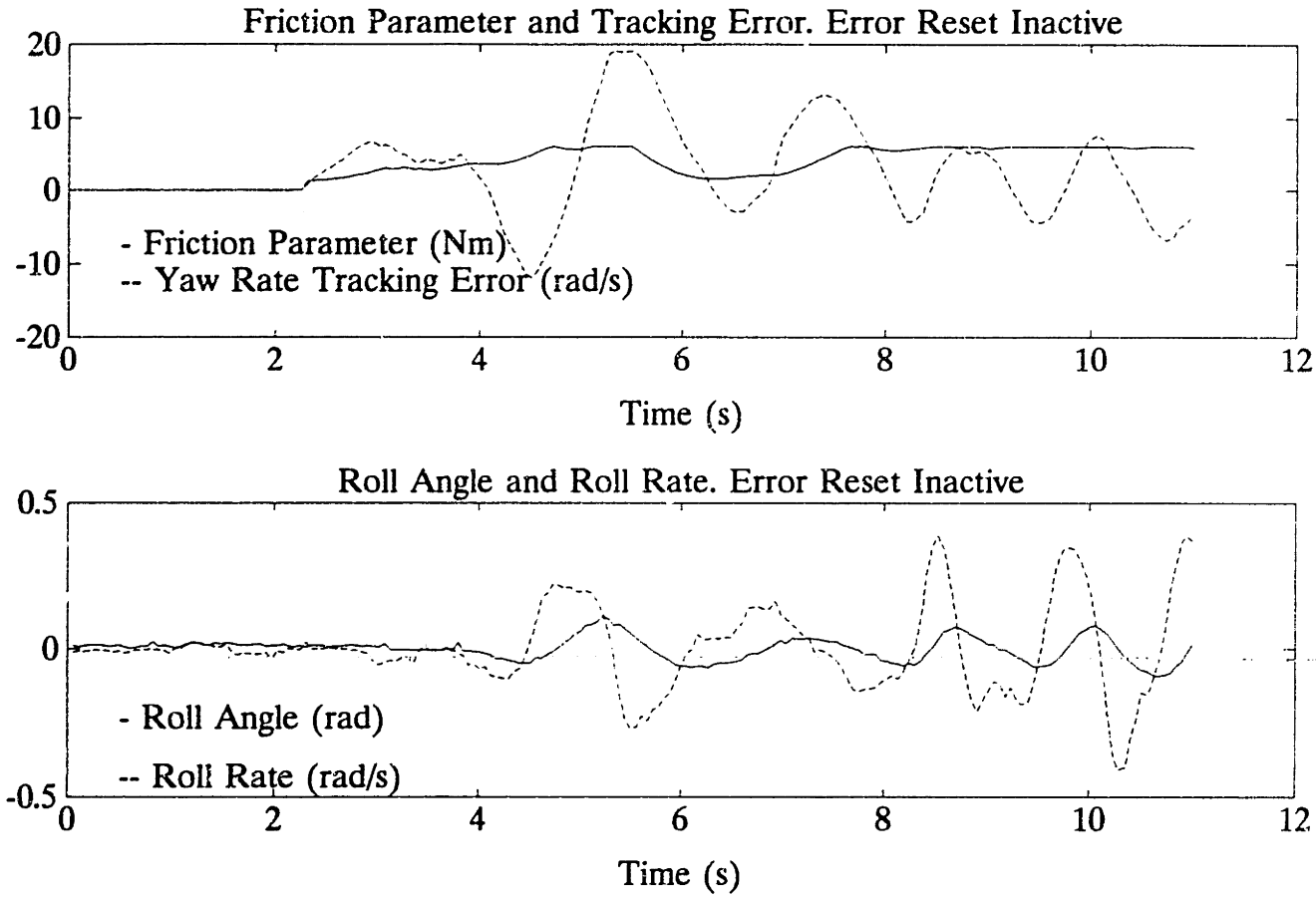

Figure 3.12. Performance using the reference model propagating the tracking error continuously, as opposed to the reference model only propagating the error over a single sample period before resetting. Note instability of continuous error propagating system. In comparison, "Error Reset" system as used in all other figures of this chapter, does not destabilize due to this problem.

Performance of MRAC Compensators

The performance of the adaptive controller assuming various friction models is presented in this section. In all of the cases, the reference model is propagated according to the "Error Reset" strategy discussed above.

Bounding the Friction Model Parameters

For any one of the friction models proposed, the performance of the compensation scheme is rather unsatisfactory, in that large roll errors result when the friction model parameters drift to unrealistic values due to lack of persistence of excitation. Figure 3.13 shows a typical case, where for the control and parameter update laws of equations (40) and (45), instability finally resulted from the friction parameter drifting to the extent that it became negative.

Since the friction models, as included in the equations of motion, are such that the relevant parameter should always be positive in order for the friction effect to reflect opposing of the motion of the moving element, the case of the parameter becoming negative is clearly nonsensical and would easily lead to destabilizing the system.

In fact, it may be shown that the parameters may be negative for short periods of time whilst still maintaining stability. Consider the friction model in the yaw equation of motion, equation (8)

$$-\mathcal{F}(\dot{\psi},\Omega) + n_t\Gamma = f_{\dot{\psi}}\dot{\psi} + I_2^w\Omega\dot{\varphi} + (I_3^f + I_3^w)\ddot{\psi}$$
$$\mathcal{F} = c\,\mathrm{sgn}(\dot{\psi}) \qquad (98)$$

with $c=c(\Omega)$. For the error $e=\dot{\psi}_p-\dot{\psi}_m$, (subscript m refers to reference model and p refers to plant), the error dynamics are

$$\dot{e} = (-f_{\dot{\psi}}e + (\hat{c}-c)\,\mathrm{sgn}(\dot{\psi}))/I_{3_s} \qquad (99)$$

For the Lyapunov function V (P positive definite) of the full equations of motion,

with $\mathbf{x}(t)=[\dot{\phi}\ \phi\ \dot{\psi}]'$

$$\dot{\mathbf{x}}(t) \quad = \quad (A-BG)\mathbf{x}(t) \tag{100}$$

$$V \quad = \mathbf{x}'P\mathbf{x} + (c-\hat{c})^2 \tag{101}$$

then, since the (LTI) system (excluding the friction nonlinearity) is feedback stabilized through $\Gamma_{gs}=-G\mathbf{x}$, $\exists$ Q (pd), such that

$$A'P + PA = -Q \tag{102}$$

and the time derivative of V

$$\dot{V} \quad = -\mathbf{x}'Q\mathbf{x} + 2\,(c-\hat{c})\,|\dot{\psi}|\,\{\frac{\gamma}{I_{3_t}}(1-\frac{\dot{\psi}_{ref}}{|\dot{\psi}|}\,\mathrm{sgn}(\dot{\psi})) - b_3P_{33}\} \tag{103}$$

where $B'=[0\ 0\ b_3]$ and it is assumed that P is diagonal. For stability, it is required that the function $\dot{V}$ is negative definite, thus

$$\hat{c} > c - \frac{\mathbf{x}'Q\ \mathbf{x}}{2|\dot{\psi}_p|\{\frac{\gamma}{I_{3_t}}(1\ -\ \frac{\dot{\psi}_{ref}}{|\dot{\psi}_p|}\ \mathrm{sgn}(\dot{\psi}_p))\ -\ b_3P_{33}\}} \tag{104}$$

When suitable compensation occurs (good friction cancellation), then the reference and actual yaw rates are approximately equal, and in the case of the roll angles and rates negligibly small, then

$$\hat{c} > c + \frac{\mathbf{x}'Q\mathbf{x}}{2b_3P_{33}}\frac{1}{|\dot{\psi}_p|} \quad = c + \frac{Q_{33}|\dot{\psi}_p|}{2\,b_3P_{33}} \tag{105}$$

i.e. the compensating estimate *overpowers* the destabilizing actual friction. For the case where the actual yaw rate is different to the model (reference) yaw rate, which may easily occur in the case of the unicycle, since the mean operating condition is $\dot{\psi}_p \approx 0$, get (set $\dot{\psi}_{ref} = -\epsilon\dot{\psi}_p$)

$$\hat{c} > c - \frac{Q_{33}|\dot{\psi}_p|I_{3t}}{2\gamma(1+\epsilon)} \tag{106}$$

Clearly, the parameter estimate may sometimes be less than the actual value, for example where over–correction of the friction effect has occurred. This cannot continue as such for long, since the stability of the system relies on the friction effect being overpowered. Certainly, the friction parameter should never need to be negative as this would indicate that the friction effect is to aid the yaw rate motion, not oppose it. In order to prevent drifting and other errors in the parameter update law from impacting the system too dramatically, the friction parameters are bounded to always be positive, then stability is always guaranteed even though the friction cancellation may sometimes be over compensating. With this strategy, the implemented adaptive system has exhibited excellent stability; whereas instability easily occurs if this is not done.

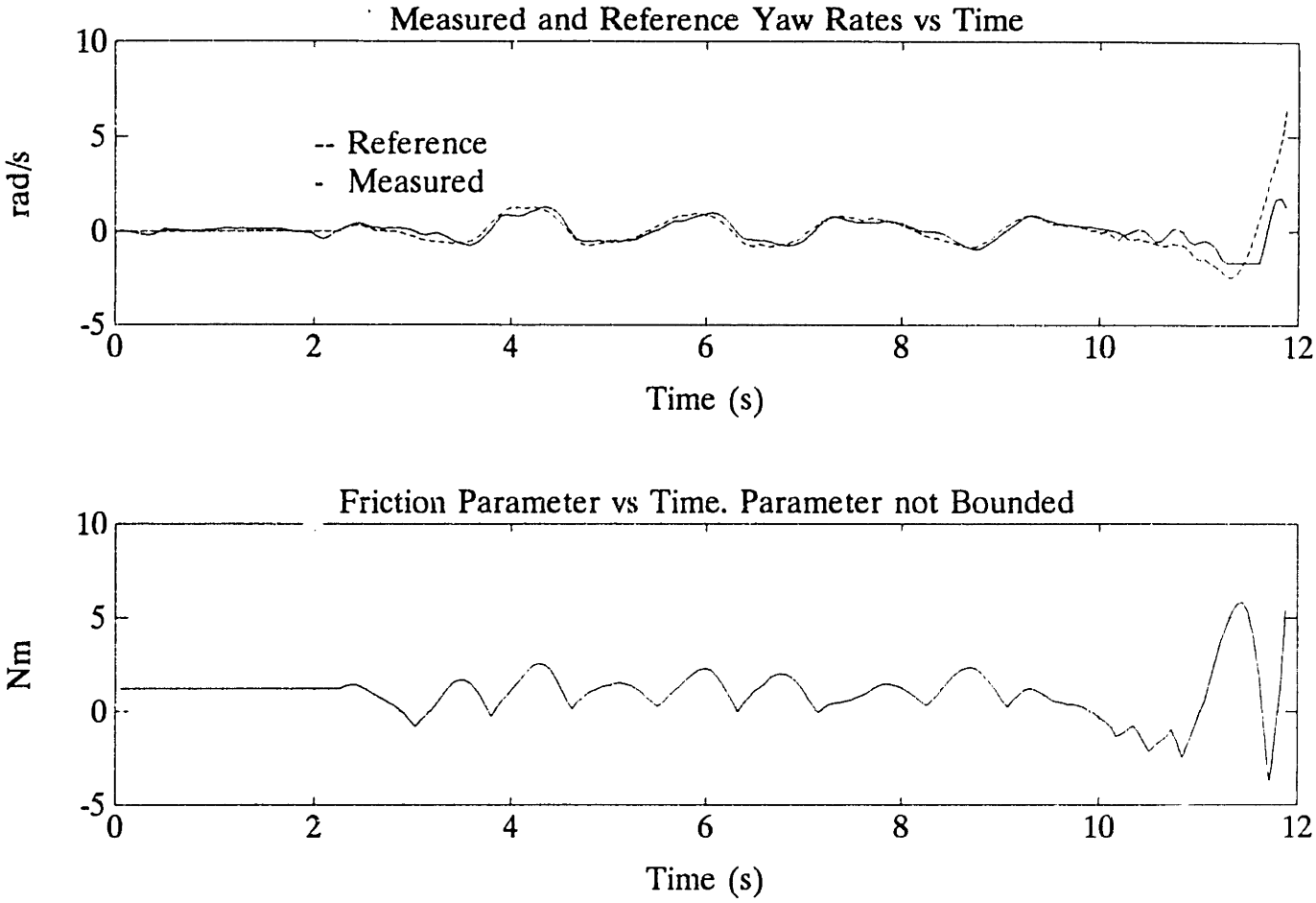

Figure 3.13. MRAC friction compensation with friction parameter allowed to drift as far as becoming negative. The parameter being negative effectively implies the incorrect notion that the friction effect is to *assist* the motion of the unicycle instead of opposing it. If recovery to a positive value for the estimate is timely, stability is maintained; but if this is not the case, the system quickly destabilizes as occurs in the data presented, at time t≈12 seconds.

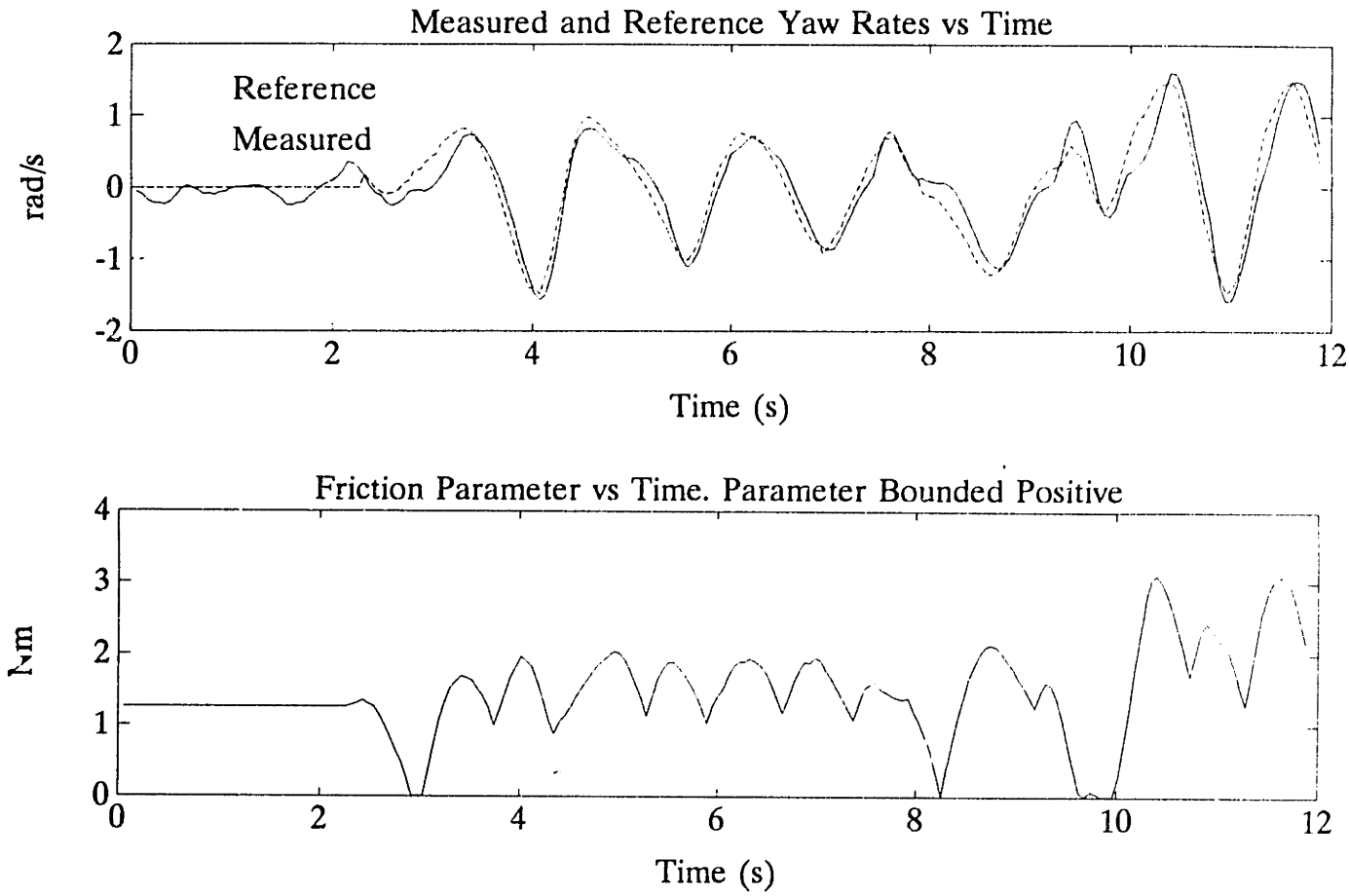

Figure 3.14. Same controller as in figure 3.13 with the bound on the friction parameter $\hat{c}>0$ $\forall t>t_0$ enforced. Note good performance and stability. Without this bound, system may sometimes destabilize due to parameter drift.

Is Friction Compensation Enough?

With the parameters bounded to be within physically meaningful ranges, the parameter estimates tend to converge nicely to steady values for a given operating condition. The performance, however, still leaves much to be desired, as the system simply does not exhibit the "stiffness" that is necessary for robust operation of the

unicycle robot.

Figure 3.15 shows performance of the MRAC system active with the friction model assumed 1) the simple Coulomb model $\hat{\mathcal{F}}=\hat{c}\text{sgn}(\dot{\psi})$ and 2) the model of [*Papadopoulos*] $\hat{\mathcal{F}}=K_1\Delta\psi + K_2\dot{\psi}$. Each of these models results in the respective parameters converging to values which are physically reasonable, and the two strategies yield almost equally poor stiffness of the system in roll.

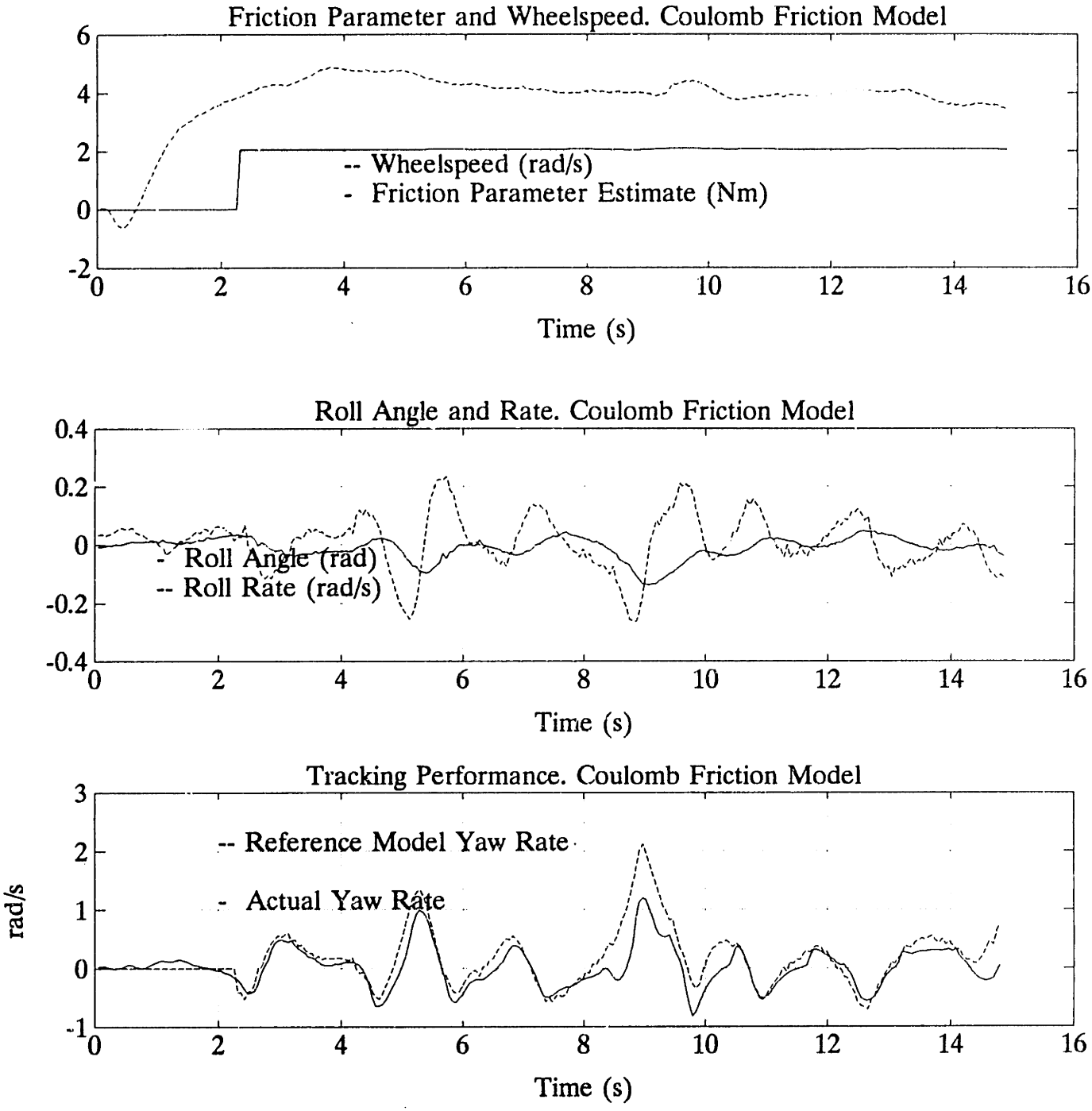

Figure 3.15a. MRAC friction compensation using the Coulomb friction model of equation (107). Note good parameter convergence, but relatively poor roll rate and angle regulation.

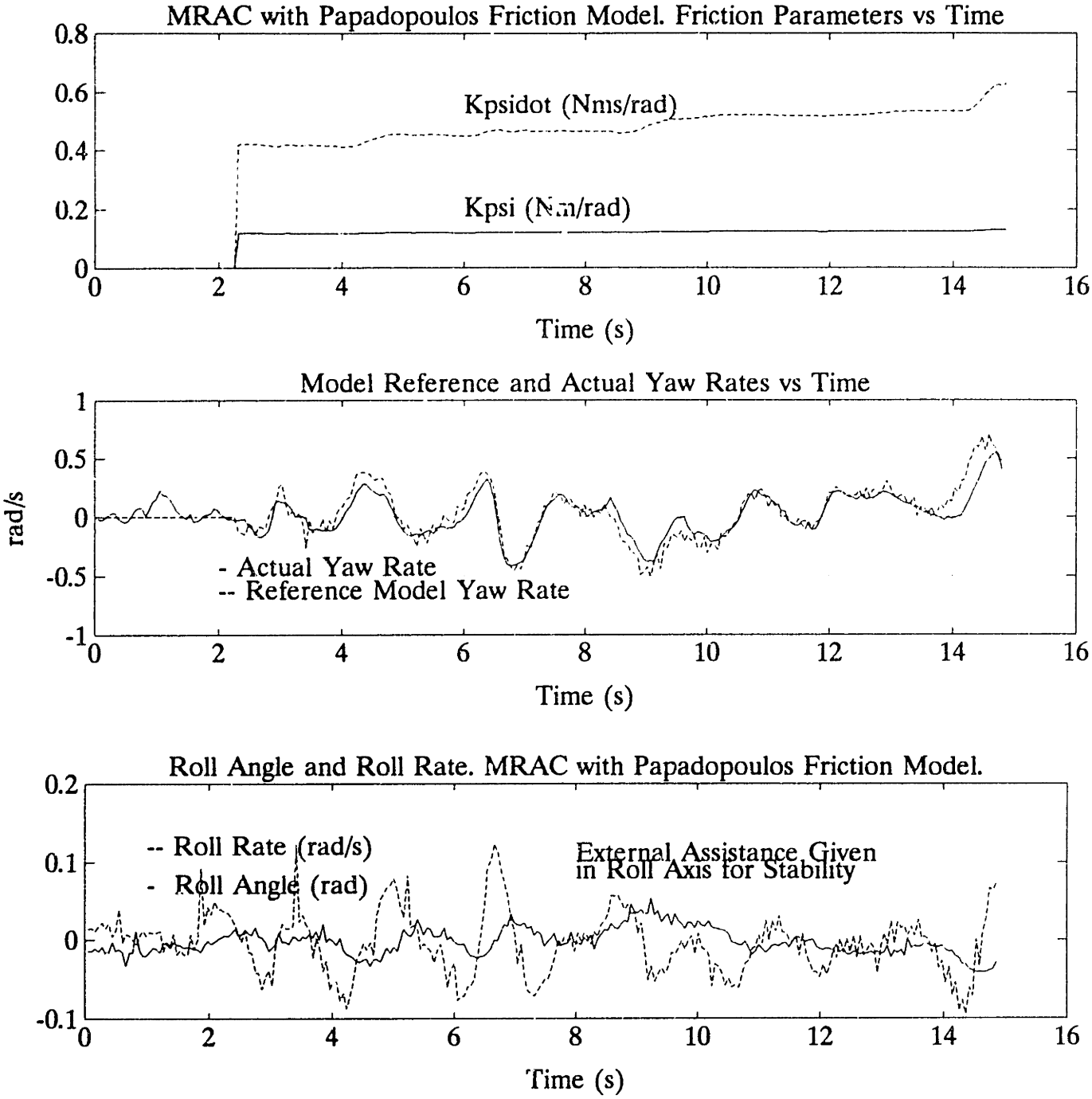

Figure 3.15b. Same as in figure 3.15a, with the friction model due to [*Papadopoulos*] implemented. Again, good parameter estimate convergence to stable values is obtained, but poor roll angle and rate regulation apparent.

The first question which comes to mind is why do both models yield virtually the

same tracking performance with each model's parameters converging to steady values for a steady state operating condition? The answer is simply that since the yaw controller is always operating about the nominal value of $\dot{\psi}$=0, the yaw angle change is extremely small, thus the effect of the term $K_1\Delta\psi$ in the second model is negligible. The two models are then

Coulomb Model :
$$\hat{\mathcal{F}} = \hat{c}\ \mathrm{sgn}(\dot{\psi}) \tag{107}$$

Papadopoulos :
$$\hat{\mathcal{F}} = K_1\Delta\psi + K_2\dot{\psi} \approx K_2\dot{\psi} \tag{108}$$

then, for small values of yaw rate, the two models are essentially the same, i.e.

$$\hat{c}\ \mathrm{sgn}(\dot{\psi}) \approx K_2\dot{\psi} \tag{109}$$

For this reason, backed up by experimental performance, the model used as the "best" for the friction problem on the unicycle robot is the simple Coulomb friction model, although if extensive long slew maneuvers are carried out, the model due to [*Papadopoulos*] is better suited.

Use of Dither Signal to Overpower Friction Effects in Yaw about the Origin

Consider the MRAC system using the (favored) Coulomb friction model. The relevant equations are

Friction Model:

$$\hat{\mathcal{F}} = \hat{c}\ \mathrm{sgn}(\dot{\psi}) \tag{110}$$

Reference Model of equation (8) (subscript p refers to plant):

$$\mathcal{F}(\dot{\psi}_p,\Omega) + n_t\Gamma = f_{\dot{\psi}}\dot{\psi}_p + I_2^w\Omega\dot{\varphi} + (I_3^f + I_3^w)\ddot{\psi}_p \tag{111}$$

Parameter Update Law of equation (45), setting $I_{3_t}=(I_3^f + I_3^w)$

$$\dot{\hat{c}} = -\frac{\gamma e}{I_{3_t}}\,\mathrm{sgn}(\dot{\psi}_p) = -\dot{\theta} \tag{112}$$

For the Lyapunov function used in determining equation (112)

$$V = \frac{1}{2}(\gamma e^2 + \theta^2) \tag{113}$$

Apply the control law

$$\Gamma = \Gamma_{gs} + \frac{\hat{c}}{n_t}(a\ \mathrm{sgn}(\dot{\psi}) - \beta\ \mathrm{sgn}(e)) \tag{114}$$

instead of the standard I/O linearizing law of equation (40), which yields the time derivative of the Lyapunov function *more* negative definite, i.e.

$$\dot{V} = -\gamma(f_{\dot{\psi}}/I_{3_t})e^2 - \frac{\gamma\hat{c}}{I_{3_t}}\beta\, e\,(\frac{(a-1)}{\beta}\,\mathrm{sgn}(\dot{\psi}) + \mathrm{sgn}(e)) \tag{115}$$

This is negative definite for the relation

$$1 - \beta \leq \alpha \leq 1 + \beta \tag{116}$$

Various values were tested in experiment, and the best performance is achieved for

$$\beta = 1 \qquad \text{and} \qquad \alpha = 0 \tag{117}$$

This implies that the system is in effect an *adaptive switching controller*, the amplitude of the switching control law being adaptively determined for minimizing of the tracking error. [*Slotine*] has used similar switching control laws to great success, where the amplitude of the switching term is a constant value determined to satisfy negative definite $\dot{V}$.

Implementing this control law *dramatically* improves the system performance in a stability robustness sense, as well as improved tracking performance. Figure 3.16 shows performance using the adaptive switching (dither) control law.

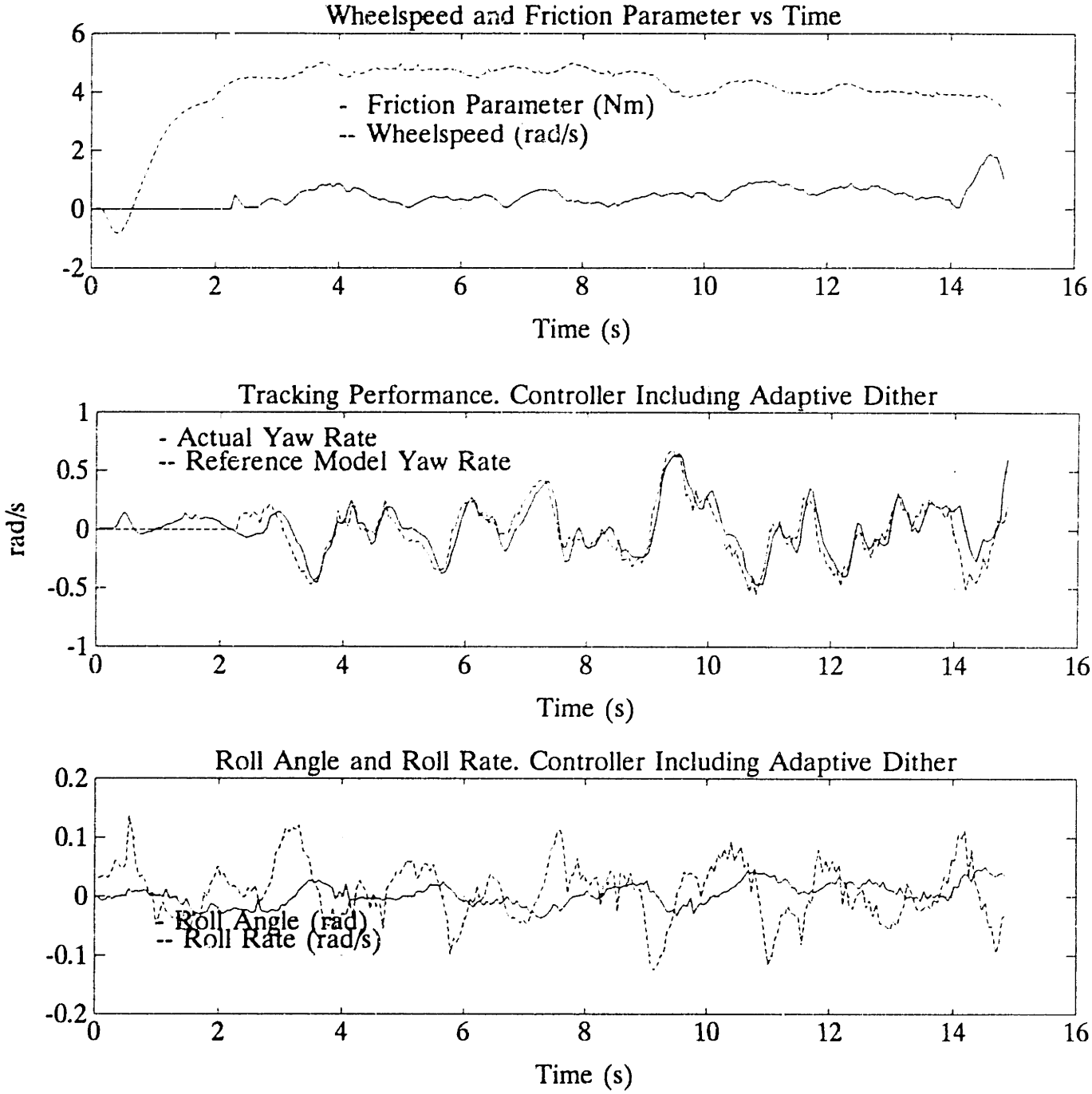

Figure 3.16. The same system as in figure 3.15a, but with the dither signal of the adaptive switching control law (equation (114)) applied. The system stiffness is much improved, although not as apparent in the time histories shown here, as in real life experimental observation.

Fast Changes in Parameters

In the MRAC design procedure, the Lyapunov function time derivative is forced to be negative definite by judicious choice of the parameter update laws. Usually, the parameter update laws then assume that the parameters do not vary rapidly (i.e. $\frac{\partial(\text{parameter})}{\partial t} \approx 0$) in order to practically be able to implement the strategy. More specifically, the actual parameter rate of change, or value, is not known (if it were known, the need for adaptive parameter estimation would be redundant) such that only by assuming this to be negligible, is it implementable.

The parameter update law is usually of the form

$$\dot{\theta} = \gamma e \frac{\partial(\text{function})}{\partial(\text{unknown parameter})} \tag{118}$$

and the parameter error

$$\begin{aligned} \theta &= (\text{parameter vector}) - (\text{estimate of parameter vector}) \\ &= \xi - \hat{\xi} \end{aligned} \tag{119}$$

Now, what if $\dot{\xi} \neq 0$? If it is assumed that at least some knowledge of the parameter exists, then the parameter and the parameter estimate may be rewritten

$$\xi = \xi_{\text{nominal}} + \Delta\xi \qquad \text{(actual)} \tag{120}$$

$$\hat{\xi} = \hat{\xi}_{\text{nominal}} + \Delta\hat{\xi} \qquad \text{(estimate)} \tag{121}$$

where $\hat{\xi}_{\text{nominal}}$ is the estimated nominal value of the parameter, $\|\hat{\xi}\| >> \|\Delta\hat{\xi}\|$ and likewise for the actual parameter ξ. The parameter error is now approximated by

$$\begin{aligned} \theta &= \xi - \hat{\xi} \\ &= \xi_{\text{nominal}} - \hat{\xi}_{\text{nominal}} + \Delta\xi - \Delta\hat{\xi} \\ &\approx \Delta\xi - \Delta\hat{\xi} \end{aligned} \tag{122}$$

The time derivative of the parameter error is then, assuming that the actual parameter *error* is constant (not always true, but a better assumption than assuming the *parameter* is constant as is done in determining the parameter update law of equation (112))

$$\dot{\theta} = -\frac{\partial(\Delta\hat{\xi})}{\partial t} \tag{123}$$

The simple implication of this is that the parameter has some "guidance" in $\hat{\xi}_{\text{nominal}}$ when changing to a new operating condition, such that the range over which the estimate has to change is much reduced and may even be constant if the parameter function versus operating condition is closely approximated by $\hat{\xi}_{\text{nominal}}$.

Performance of the system for fast changes in operating condition is much improved for this change in the parameter update procedure. In the unicycle example, the approximate nature of the parameter as a function of wheelspeed is determined by operating the adaptive controller over a range of wheelspeeds and curve fitting through the experimentally obtained parameter estimate data. Figure 3.17 illustrates the data points (i.e. MRAC parameter estimates) for operating over the full range of wheelspeeds. As predicted by [*Papadopoulos*], the friction parameter (refer to the relation resulting in equation (109)) depends on the inverse of wheelspeed. The nominal model assumed is thus

$$\hat{\xi}_{\text{nominal}}(\Omega) = 5.5/\Omega \text{ (Nm)} \quad \forall\, \Omega \neq 0 \tag{124}$$

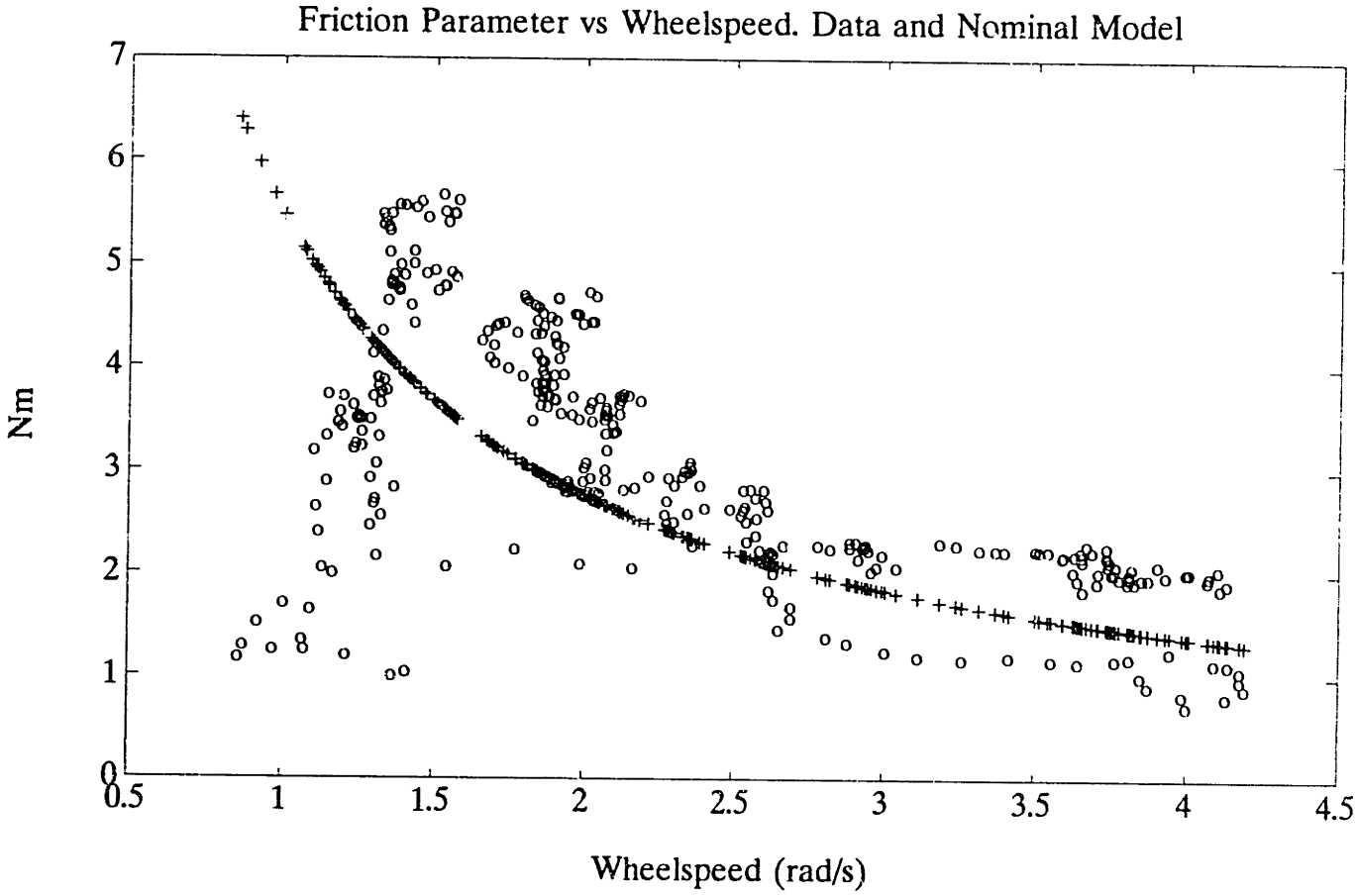

Figure 3.17. Friction parameter determined by operating the MRAC system using update law of equation (112) over large range of wheelspeeds. The curve fit given by equation (124) describes the nominal parameter estimate required in equation (121).

The system performance in this case is shown together with the case of the original parameter estimation law of equation (112) which often resulted in instability, in figure 3.18.

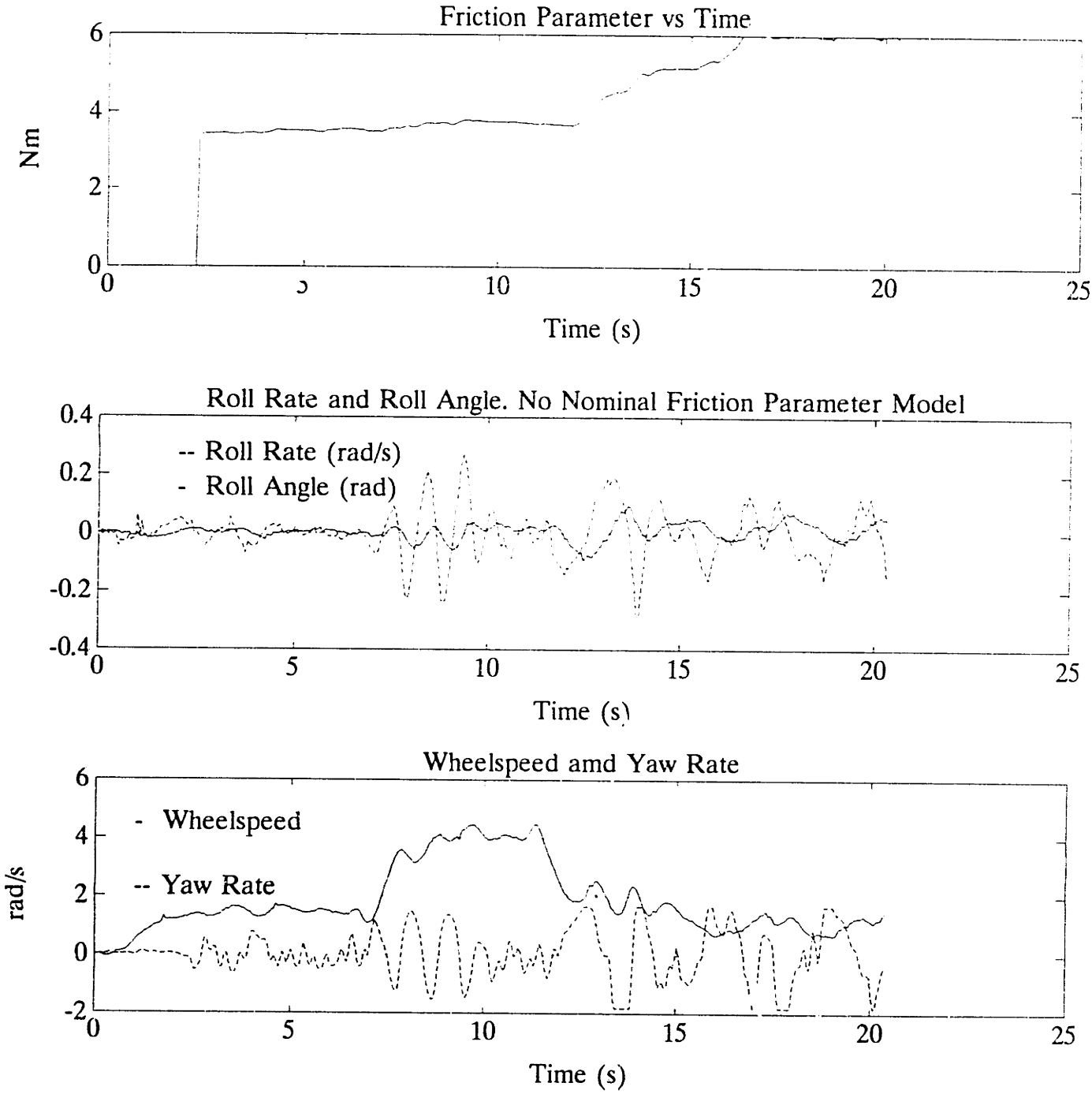

Figure 3.18a. System performance using the original parameter estimation law of equation (112) for fast variation of operating condition. Note system tendency toward instability due to the large parameter estimate change required over a relatively short time period.

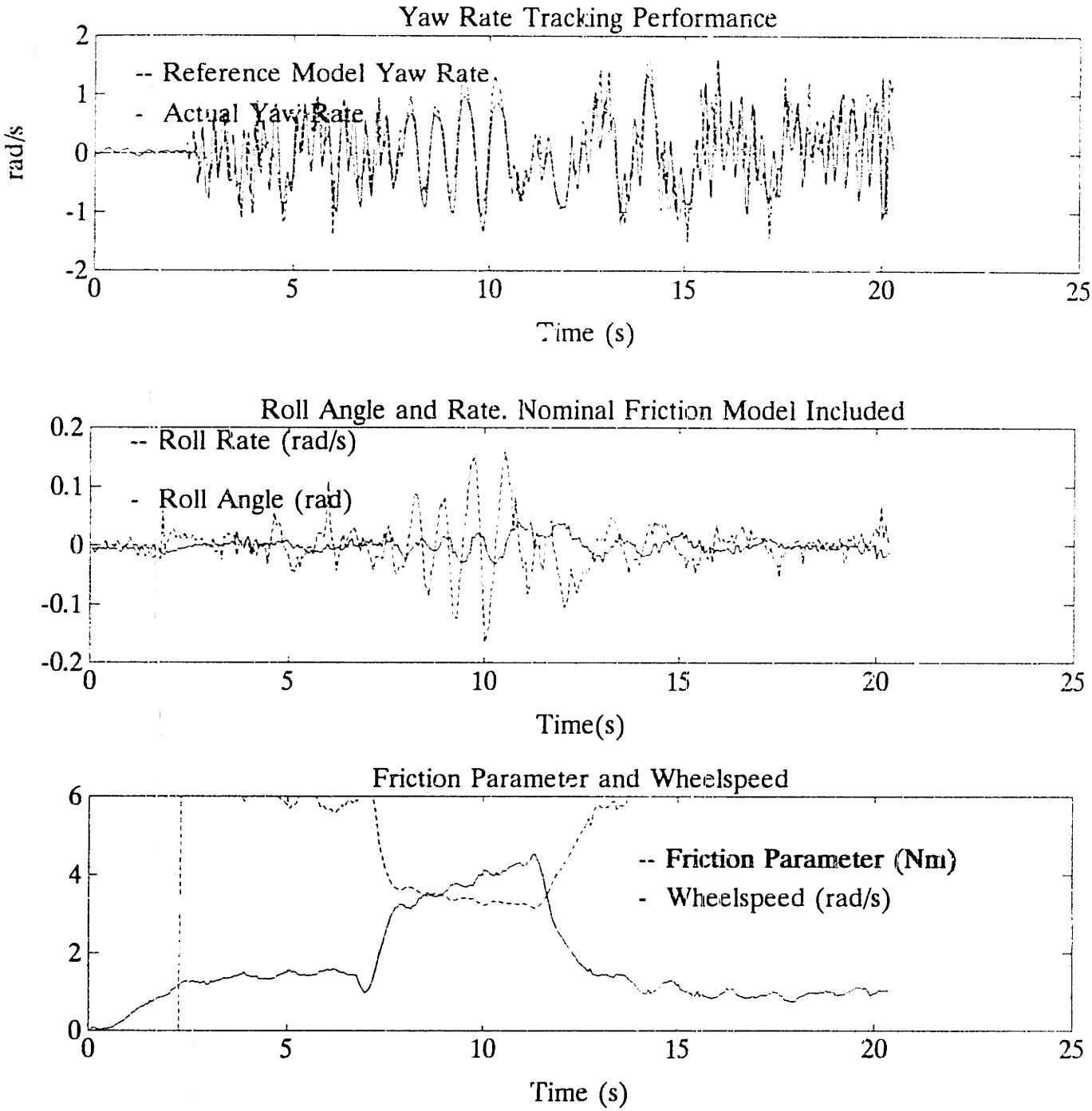

Figure 3.18b. Same as figure 3.18a, but using the parameter update law of equation (123), where a much reduced range of change of $\Delta\hat{\xi}$ needs to be achieved in a short time, than for the case of figure 3.18a and stability properties are much improved.

CONCLUSION

In this chapter, many practical issues involved in achieving good performance of adaptive friction compensation strategies are discussed. Both neural network and MRAC compensation schemes are derived and implemented on the yaw friction problem of the unicycle robot.

The neural network implementation exhibited relatively good performance in learning the parameter it was structured to learn. From the point of view of roll performance of the unicycle, however, this friction compensation strategy resulted in the system stability being only marginal. This is not surprising, as the structure of the network concentrated on learning the yaw friction model at the tire/surface interface. Since the method is ad hoc in the sense that no stability issues are considered in determining the control law and parameter update law, it is not clear how to adjust these strategies in order to improve matters. Although these techniques offer interesting means of determining input–output relations of systems, the classical control and estimation methods offer a more structured approach to achieving good closed loop performance. Combining the ability of such methods to learn complex input–output relations with stability based control techniques may yet prove a feasible control strategy for parameter uncertain systems, but the experience of this (limited) study using the neural network as a nonparametric map tends to indicate that a great deal more development from a stability point of view needs to be done in this area.

The MRAC friction compensation system is equally poorly behaved if *directly* implemented as derived from the Lyapunov stability based synthesis procedure. It is demonstrated here , however, that excellent performance may be obtained if certain

implementation issues are borne in mind.

Bounding of the adaptation parameters to within physically feasible limits is a very obvious and simple solution to preventing parameter drift which may easily destabilize the system. Even though it may be shown that the parameter value being grossly incorrect is tolerable for stability, this may not be acceptable in reality. In the case of the unicycle friction compensation scheme, allowing the friction estimate to be so incorrect as to be "assisting" the system performance, is clearly nonsensical and easily leads to instability. Simply bounding the parameters to always be of the correct sign already makes a vast improvement.

A not atypical problem arising in MRAC adaptive control systems, is that of the sudden "blow up's" which occur after extensive periods of good performance. It is shown here that one cause for this is the integrating up (over time) of system model and sensor errors, which manifest in the parameter estimation update algorithm. Since the system strives to drive the tracking error to zero as best it can, this may lead to grossly inaccurate parameter estimates which can easily destabilize the system. This is clearly demonstrated in the case of the unicycle, where instability occurs after only a few seconds of operation. By resetting the discrete time implementation of the reference model trajectory generator at each integration step (may be extended to every z'th integration step, where z is smaller than the number of integrations required to integrate such modeling or sensor bias errors into significant values), this problem is completely alleviated. This is achieved by setting the reference trajectory state equal to the measured value at the present sample instant, in order to predict the next sample trajectory estimate for use in the error driven parameter update law, thus effectively eliminating any sensor biases and minimizing the effect of incorrect models. Performance of the unicycle is

demonstrated to be indefinitely stable with this strategy, whilst instability occurs very quickly if not used.

Use of "dither" signals which ensure greater "negative definiteness" of the relevant Lyapunov function derivative, is made to improve the stability of the MRAC friction compensation algorithms. The best amplitude of the dither signal is estimated continuously in real time, using the same parameter estimation laws of the original design, resulting in a form of *adaptive switching control* strategy. The stiffness of the system is dramatically improved by this change.

Finally, for fast changes in operating condition, it is necessary to add more structure to the parameter update algorithm in order to maintain stability. By employing knowledge of the nominal parameter characteristics as a function of operating condition and adapting on only the uncertain aspects, stability is maintained for much faster operating condition changes. In the unicycle example, fast changes from zero to maximum wheelspeed often destabilizes the MRAC procedure, since the parameters cannot adapt quickly enough. By assuming only crude knowledge of the nominal parameter value as a function of wheelspeed and adapting only the parameter *error* instead of the full parameter value, performance and stability are well maintained.

CHAPTER 4. GAIN SCHEDULED CONTROLLER DESIGN

INTRODUCTION

For many years, the approach to control of linear *parameter* varying systems has been to design linear controllers at a number of design points corresponding to operating conditions distributed across the operating envelope, and to define some scheduling technique according to which the gains are adjusted as a function of operating condition. This approach, while often yielding extremely satisfactory performance for many systems, has also been known to fail in certain cases; one possible reason being that the design strategy is rather ad hoc and it is not clear how the feedback gains should be scheduled.

Although abundant in practical applications, gain scheduling has not been formally addressed in the literature, with the work of [*Shamma*] the only notable effort at a systematic, albeit rather conservative, analysis of this technique. This work [*Shamma*] formalizes the rules of thumb which control system designers apply in the gain scheduling problem, namely: 1) that as long as the scheduling parameter is varied slowly enough (e.g. at least one decade slower than the closed loop dynamics), and the effective "frozen" systems at each parameter value are stable, then the system is stable, and 2) that the scheduling technique should capture the parameter dependence: for example, since the unicycle dynamics are proportional to wheelspeed, the gain scheduling should reflect dependence on the inverse of wheelspeed.

[*Rugh*] gives an overview of the typical approach used in this design methodology, sketching the framework of linearization about discrete operating points (i.e. fixed

parameter values) and fitting scheduling strategies through the controller parameters

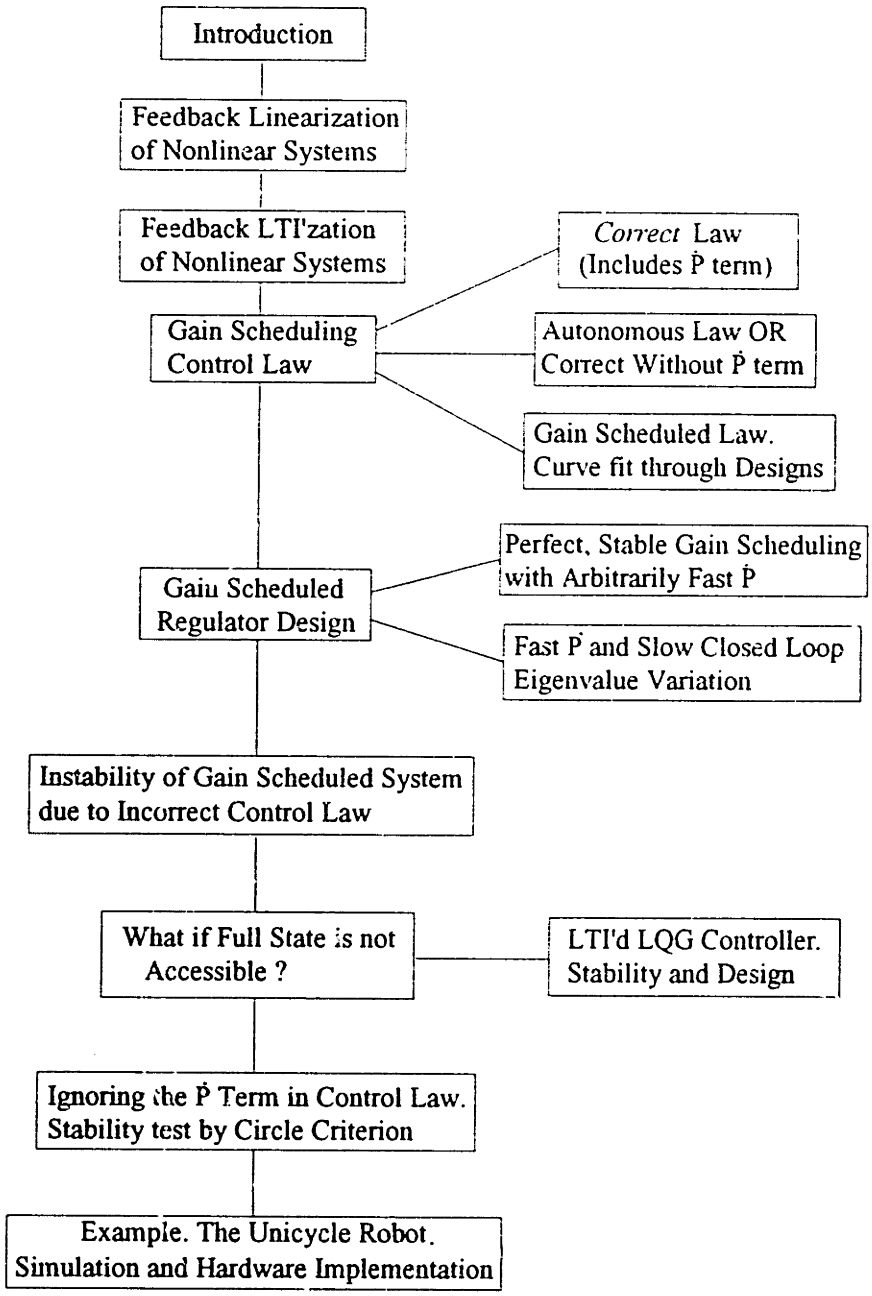

Figure 4.1. Chapter Roadmap.

determined at each design point. This work does not succeed in the attempt to formalize the methodology nor does it address the arising stability issues.

Since the problem is fundamentally a non Linear Time Invariant (i.e. *not* an LTI issue) issue, it is approached from a nonlinear point of view in this chapter. For the case of the system to be controlled being nonlinear and parameter dependent, and satisfying specific feedback LTI'ability conditions, it is shown that the scheduling parameter need ***not*** be restricted to slow variation; indeed, for perfect knowledge of the system, stability is guaranteed for *arbitrary* fast variation of the scheduling parameters.

For the feedback linearizable system, a diffeomorphism (smooth and invertible state transformation) exists which allows the nonlinear system to be viewed in a tangent space which is Linear Time Invariant for fixed parameter values. If the system is in addition feedback LTI'able, then the transformed system is LTI, regardless of the parameter values or the rate of change of the parameters. For full state accessibility (necessary for the transformation too), it is then possible to assign desired closed loop behavior to the transformed system by any favored LTI control design strategy, which, when transformed back to the real system, yields the same closed loop dynamics regardless of the operating condition (parameter value) or rate of change of parameters. The feedback LTI'ing control law combined with the diffeomorphism, define exactly the correct scheduling laws which must be adhered to in order to deduce stability of the full gain scheduled system, regardless of rate of change and/or instantaneous value of scheduling parameters.

In this approach, care needs to be taken that a practicable design is achieved. Since the procedure yields a strategy which is analogous to pole/zero cancellation in the

linear control world, caution needs to prevail such that the resulting design does not attempt to "invert the plant" in a "high bandwidth" sense: i.e. the z–space design should result in the actual system closed loop dynamics being reasonable. "Reasonable" is used with the implication that attempting to cancel system natural dynamics and replace these with much higher performance dynamics will invariably lead to difficulty (if not instability) in application.

Maintaining invariant closed loop behavior regardless of the values of the scheduling parameters, may not always be desirable. An aircraft would typically not be able to perform similarly at high speed, low angle of attack and at low speed, high altitude conditions. For this reason, it is of great use to have knowledge of the stability characteristics of the gain scheduling designs for closed loop dynamics which *vary* with operating condition. In this case, "slow" variation of the *closed loop dynamics* (scheduling parameters are still allowed to change as fast as is possible for the system) as a function of parameter variation is allowable, whilst still maintaining the stability and robustness character of the fixed point designs. The above discussion has involved the possibility of arbitrarily fast parameter variation and has introduced the idea that an equivalently fast control gain variation can still lead to LTI closed loop dynamics.

The reality of physical systems is that parameters are typically only able to vary at certain limited rates: it is not possible, for example, to change the dynamic pressure of the flight condition of an aircraft instantaneously. This is fundamentally limited by the aircraft's (limited) ability to change speed and altitude. Given then the maximum achievable rate of change of the scheduling parameters, the *closed loop dynamics* may be allowed to vary slowly with the scheduling parameters. Since the parameter then also varies slowly with time, the closed loop system departs from being true LTI, in a

quantifiably limited way.

It is, however, important to stress that the formal results presented here do not require slow variation of the scheduling parameters as prescribed by previous analyses.[*Shamma, Rugh, etc*]

Full state accessibility is a requirement for the system to be feedback linearizable (more specifically, input state linearizable) and subsequently feedback LTI'd for design of the gain scheduled controller. For obvious reasons, this is not always possible and it is necessary to be able to design a gain scheduled control system which uses a reduced set of measurements. To this end, it is certainly possible to design a Kalman Filter in the transformed LTI space in order to continuously obtain optimal estimates of the full state vector for use in an LQG controller setting. In implementation, the estimator runs in transformed state space with the physical system state estimate determined by transformation via the diffeomorphism. This completely defines a fully gain scheduled LQG controller, with no requirement on full state accessibility, which allows fast parameter variation (as in the full state feedback case) and which is guaranteed stable.

FEEDBACK LINEARIZATION OF NONLINEAR SYSTEMS

Introduction

The transformation of a nonlinear system into a set of coordinates which yield the transformed system LTI for fixed parameter values, is of particular interest to the gain scheduling problem. The original work on such transformations is due to [*Krener*] and [*Brockett*] in the seventies, with the eighties heralding a flurry of work

[*Isidori, Su, Hunt–Su–Meyer* and others] resulting in explicit conditions being shown under which exact linearization through transformation and feedback is possible. The works of [*Isidori* and *Van der Schaft*] are excellent expository texts covering the development to the present state of the art. None of these works, however, make the connection with the traditional gain scheduling problem.

A vast number of systems to be controlled arise in the nonlinear affine form below, with m inputs, p outputs and q parameters

$$\dot{\mathbf{x}}(t) = f(\mathbf{x}(t),\mathbf{P}) + \sum_{i=1}^{m} g_i(\mathbf{x}(t),\mathbf{P})u_i(t) \qquad (1)$$

$$y_i(t) = h_i(\mathbf{x}(t)) \qquad 1 \le i \le p \qquad (2)$$

with f,g and h smooth vector fields in an open neighborhood of the origin in $\mathbf{R}^n$, $\mathbf{x}\in\mathbf{R}^n$, $\mathbf{P}\in\mathbf{R}^q$ and

$$f(\mathbf{x}(t),\mathbf{P}) = \begin{bmatrix} f_1(\mathbf{x}(t),\mathbf{P}) \\ f_2(\mathbf{x}(t),\mathbf{P}) \\ \vdots \\ f_n(\mathbf{x}(t),\mathbf{P}) \end{bmatrix} \qquad (3)$$

$$g_i(\mathbf{x}(t),\mathbf{P}) = \begin{bmatrix} g_{i_1}(\mathbf{x}(t),\mathbf{P}) \\ g_{i_2}(\mathbf{x}(t),\mathbf{P}) \\ \vdots \\ g_{i_n}(\mathbf{x}(t),\mathbf{P}) \end{bmatrix} \qquad (4)$$

The following assumes that the parameters are fixed at some value $\mathbf{P}_{nom}$. The system functions are thus no longer dependent on $\mathbf{P}$, which is dropped from the relevant expressions.

Elements of Differential Geometry

The analysis to follow relies on extensive use of Lie derivatives along vector fields and real valued functions, some basic elements of which are presented below.

The **Lie derivative** of some *real valued function* $\lambda(\mathbf{x})$ along the function f, or equivalently, the projection of this function gradient $(\nabla\lambda(\mathbf{x}))$ along the function f is written as

$$\mathcal{L}_f\lambda(\mathbf{x}) = \sum_{i=1}^{n} \frac{\partial\ \lambda(\mathbf{x})}{\partial\ x_i} f_i(\mathbf{x}) \tag{5}$$

which may be recursively applied, thus

$$\mathcal{L}_f^k\lambda(\mathbf{x}) = \frac{\partial\ (\mathcal{L}_f^{k-1}\lambda(\mathbf{x}))}{\partial\ \mathbf{x}} f(\mathbf{x})$$

$$= \sum_{i=1}^{n} \frac{\partial\ (\mathcal{L}_f^{k-1}\lambda(\mathbf{x}))}{\partial\ x_i} f_i(\mathbf{x}) \tag{6}$$

The **Lie bracket**: derivative of one *vector field* along another vector field, the vector fields defined on an open set in $\mathbf{R}^n$, is defined

$$[f(\mathbf{x}),g(\mathbf{x})] = \frac{\partial\ g(\mathbf{x})}{\partial\ \mathbf{x}} f(\mathbf{x}) - \frac{\partial\ f(\mathbf{x})}{\partial\ \mathbf{x}} g(\mathbf{x}) \tag{7}$$

where $\frac{\partial\ g(\mathbf{x})}{\partial\ \mathbf{x}}$ and $\frac{\partial\ f(\mathbf{x})}{\partial\ \mathbf{x}}$ are the Jacobian matrices of g and f respectively

$$\frac{\partial\, g(\mathbf{x})}{\partial\, \mathbf{x}} = \begin{bmatrix} \frac{\partial g_1}{\partial x_1} & \frac{\partial g_1}{\partial x_2} & \cdots & \frac{\partial g_1}{\partial x_n} \\ \frac{\partial g_2}{\partial x_1} & \frac{\partial g_2}{\partial x_2} & \cdots & \frac{\partial g_2}{\partial x_n} \\ \vdots & \vdots & \ddots & \vdots \\ \frac{\partial g_n}{\partial x_1} & \frac{\partial g_n}{\partial x_2} & \cdots & \frac{\partial g_n}{\partial x_n} \end{bmatrix} \tag{8}$$

$$\frac{\partial\, f(\mathbf{x})}{\partial\, \mathbf{x}} = \begin{bmatrix} \frac{\partial f_1}{\partial x_1} & \frac{\partial f_1}{\partial x_2} & \cdots & \frac{\partial f_1}{\partial x_n} \\ \frac{\partial f_2}{\partial x_1} & \frac{\partial f_2}{\partial x_2} & \cdots & \frac{\partial f_2}{\partial x_n} \\ \vdots & \vdots & \ddots & \vdots \\ \frac{\partial f_n}{\partial x_1} & \frac{\partial f_n}{\partial x_2} & \cdots & \frac{\partial f_n}{\partial x_n} \end{bmatrix} \tag{9}$$

The Lie bracket may be applied recursively, as in the case of the Lie derivative, and is written for ease of notation as

$$ad_f^k\, g(\mathbf{x}) = [f(\mathbf{x}), ad_f^{k-1} g(\mathbf{x})] \qquad \forall\ k \geq 1 \tag{10}$$

with

$$ad_f^0\, g(\mathbf{x}) = g(\mathbf{x})$$

Transformation of Coordinates

For the nonlinear transformation of the coordinates of a nonlinear system to those of a linear system, the transformation is written

$$\mathbf{z} = \Phi(\mathbf{x}, P)$$

$$= \begin{bmatrix} \phi_1(\mathbf{x},\mathbf{P}) \\ \phi_2(\mathbf{x},\mathbf{P}) \\ \vdots \\ \phi_n(\mathbf{x},\mathbf{P}) \end{bmatrix} \tag{11}$$

The transformation is a ***global diffeomorphism*** if the following conditions hold

1) $\Phi(\mathbf{x},\mathbf{P})$ is invertible, i.e. $\mathbf{z} = \Phi^{-1}(\mathbf{x},\mathbf{P})$ $\forall\ \mathbf{x}\in\mathbf{R}^n$
2) Both the forward map $\Phi(\mathbf{x},\mathbf{P})$ and inverse map $\Phi^{-1}(\mathbf{x},\mathbf{P})$ are smooth mappings and thus have continuous partial derivatives of any order, $\forall\ \mathbf{x}\in\mathbf{R}^n$.

The transformation is a ***local diffeomorphism*** if it is a diffeomorphism in a neighborhood of some point (typically the equilibrium point of the system to be controlled) in $\mathbf{R}^n$.

Lemma: For $\Phi(\mathbf{x})$ smooth in a subset $\Omega\in\mathbf{R}^n$, the Jacobian $\nabla\Phi$ is nonsingular at a point $x_0\in\Omega$ if and only if $\Phi(\mathbf{x})$ defines a local diffeomorphism in Ω.

Proof: [*Isidori, Nijmeijer & van der Schaft*]

Involutivity

A distribution of vector fields $[a_1(\mathbf{x})\ a_2(\mathbf{x})\ a_3(\mathbf{x})\ \cdots\ a_n(\mathbf{x})]$ is said to be ***Involutive*** if the Lie bracket of any two of the constituent vector fields of the distribution is contained in the distribution. Thus

$$[a_i(\mathbf{x}),a_j(\mathbf{x})] \in [a_1(\mathbf{x})\ a_2(\mathbf{x})\ a_3(\mathbf{x})\ \cdots\ a_n(\mathbf{x})] \quad \text{for any } i,j \le n \tag{12}$$

this is equivalent to writing [*Isidori,Su*], for scalar fields $c_{ijk}(\mathbf{x})$

$$[a_i(\mathbf{x}),a_j(\mathbf{x})] \;=\; \sum_{k=1}^{n} c_{ijk}(\mathbf{x})a_k(\mathbf{x}) \tag{13}$$

Involutivity may be tested for by evaluating the rank of the following matrices. If

$$\text{rank}[a_1(\mathbf{x})\ a_2(\mathbf{x})\ \cdots\ a_n(\mathbf{x})\ [a_i(\mathbf{x}),a_j(\mathbf{x})]] = \text{rank}[a_1(\mathbf{x})\ a_2(\mathbf{x})\ \cdots\ a_n(\mathbf{x})]$$

$$\text{for any integer } 0<i,j\leq n \text{ and any } \mathbf{x} \tag{14}$$

then the distribution is involutive. This implies that the space spanned by the vector fields contains the Lie bracket of any two of the constituent vector fields and thus the constituent vector fields are linearly independent.

Integrability

A distribution of vector fields $[a_1(\mathbf{x})\ a_2(\mathbf{x})\ a_3(\mathbf{x})\ \cdots\ a_m(\mathbf{x})]$ is said to be ***completely integrable*** if the vector fields $a_i(\mathbf{x})$ are linearly independent, and for every point there exists an m–dimensional submanifold $M \in \mathbf{R}^n$ such that the distribution spans the tangent space of M.

Equivalently [*Isidori*], the distribution $[a_1(\mathbf{x})\ a_2(\mathbf{x})\ a_3(\mathbf{x})\ \cdots\ a_m(\mathbf{x})]$ on $\mathbf{R}^n$ is said to be *completely integrable* if and only if $\exists$ (n–m) scalar functions $\lambda_i(\mathbf{x}):\mathbf{R}^n\rightarrow\mathbf{R}$, which satisfy

$$\mathcal{L}_{a_i}\lambda_j = 0 \qquad \forall\ 1 \leq i \leq m \text{ and } 1 \leq j \leq n-m \tag{15}$$

The previous definitions and results are succinctly stated in the theorem due to Frobenius.

Frobenius' Theorem: A set of linearly independent vector fields (constituting a nonsingular distribution) is completely integrable if and only if it is involutive.

Proof: see [*Isidori*].

Remark: The notion of complete integrability allows use of the scalar functions $\lambda_i: \mathbf{R}^n \rightarrow \mathbf{R}$ which satisfy $\mathcal{L}_{f_i}\lambda_j = 0 \; \forall \; 1 \leq i \leq m$ and $1 \leq j \leq n-m$, to define a coordinate transformation into the tangent space at any point on the system manifold (which contains the system functions f_i and g). Thus, at a point $(\mathbf{x}^*)$ of concern, integrability ensures that there exists a transformation of coordinates such that the time evolution of the system in a neighborhood of the point on the system manifold is captured by time evolution of the *transformed* LTI system. Figure 4.2 illustrates the manifold and tangent space for a 2nd order system.

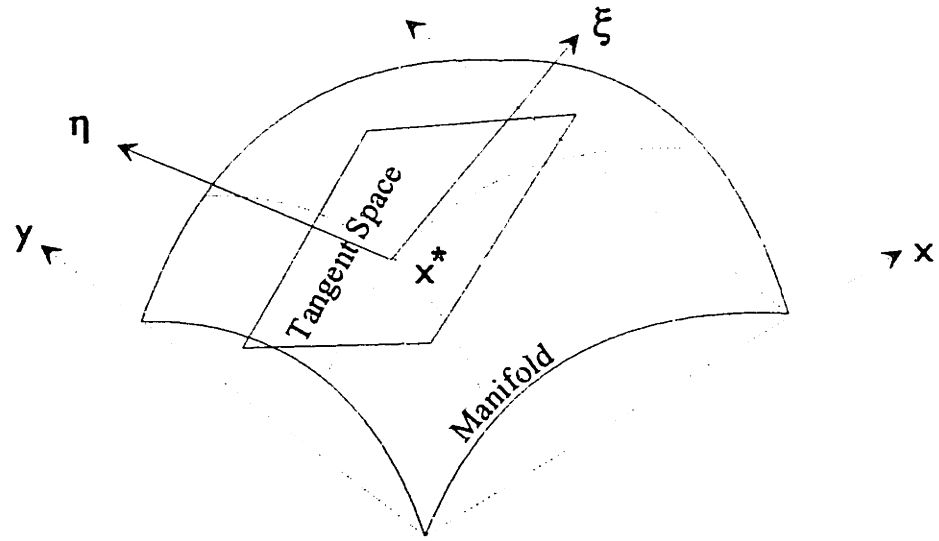

Figure 4.2. System manifold and tangent space at $\mathbf{x}^\star$. The coordinate transformation transforms from x–y space on the manifold to ξ–η coordinates in tangent space

The above results now allow statement of the *full state* Exact Linearization problem.

Theorem: *Full State Exact Feedback Linearization.* The single input system

$$\dot{\mathbf{x}}(t) \quad = \quad f(\mathbf{x},\mathbf{P}) + g(\mathbf{x},\mathbf{P})u \qquad\qquad \mathbf{x} \in \mathbf{R}^n \qquad\qquad (16)$$

is Exactly Feedback Linearizable in the neighborhood of some point $\mathbf{x}^\star$ and for a fixed value of $\mathbf{P}_{nom}$, if and only if the conditions (writing $f(\mathbf{x})$ for $f(\mathbf{x},\mathbf{P}_{nom})$ and likewise for $g(\cdot)$)

1) *Controllability*: the matrix $[g(\mathbf{x}^\star)\ \mathrm{ad}_f g(\mathbf{x}^\star)\ \mathrm{ad}_f^2 g(\mathbf{x}^\star)\ \cdots\ \mathrm{ad}_f^{n-1} g(\mathbf{x}^\star)]$ has rank n, i.e. rank equal to the dimension of the system.
2) *Involutivity*: the distribution $[g(\mathbf{x}^\star)\ \mathrm{ad}_f g(\mathbf{x}^\star)\ \mathrm{ad}_f^2 g(\mathbf{x}^\star)\ \cdots\ \mathrm{ad}_f^{n-2} g(\mathbf{x}^\star)]$ is

involutive in a neighborhood of $x^{\star}$.

are satisfied, where we have denoted $f(\mathbf{x},\mathbf{P}_{nom})$ by $f(\mathbf{x})$ etc. The transformation is determined from the function $\lambda(\mathbf{x})$ satisfying the integrability conditions, thus

$$\mathbf{z} \quad = \Phi(\mathbf{x}) \quad = [\lambda(\mathbf{x}) \; \mathcal{L}_f\lambda(\mathbf{x}) \cdots \mathcal{L}_f^{n-1}\lambda(\mathbf{x})]' \tag{17}$$

The transformation which satisfies (17) is determined by evaluating

$$\mathcal{L}_g\lambda(\mathbf{x}) = \mathcal{L}_{\mathrm{ad}_f g}\lambda(\mathbf{x}) = \cdots = \mathcal{L}_{\mathrm{ad}_f^{n-2}g}\lambda(\mathbf{x}) = 0 \tag{18}$$

and the nontriviality condition

$$\mathcal{L}_{\mathrm{ad}_f^{n-1}g}\lambda(\mathbf{x}) \neq 0 \tag{19}$$

preventing the trivial solution $\lambda(\mathbf{x}) = 0$.

Note that the function $\lambda(\mathbf{x})$ may be viewed as a redefined output function such that the relative degree of the system is n, i.e. relative degree equal to the order of the system.

The linearizing control law is determined from the transformation by considering the derivative with respect to time of the n'th transformation matrix row, thus

$$\begin{aligned} \dot{z}_n \; = \dot{T}_n \; &= \frac{\partial T_n}{\partial \mathbf{x}}\dot{\mathbf{x}} \\ &= \mathcal{L}_{\dot{\mathbf{x}}} T_n \end{aligned}$$

$$= \mathcal{L}_{\dot{\mathbf{x}}} \mathcal{L}_f^{n-1}\lambda(\mathbf{x}) \tag{20}$$

but, the system dynamics satisfy $\dot{\mathbf{x}} = f(\mathbf{x}) + g(\mathbf{x})\mathrm{u}$, then

$$\begin{aligned} \dot{z}_n &= \mathcal{L}_f^n \lambda(\mathbf{x}) + (\mathcal{L}_g \mathcal{L}_f^{n-1}\lambda(\mathbf{x}))\mathrm{u} \\ &= \nu \end{aligned} \tag{21}$$

yielding the linearizing control law

$$\mathrm{u} = \alpha(\mathbf{x}) + \beta(\mathbf{x})\nu \tag{22}$$

with

$$\alpha(\mathbf{x}) = \frac{-\mathcal{L}_f^n \lambda(\mathbf{x})}{\mathcal{L}_g \mathcal{L}_f^{n-1}\lambda(\mathbf{x})} \quad \text{and} \quad \beta(\mathbf{x}) = \frac{1}{\mathcal{L}_g \mathcal{L}_f^{n-1}\lambda(\mathbf{x})} \tag{23}$$

Proof: see e.g. [*Isidori, Van der Schaft, Hunt–Su–Meyer*]

Note: This strategy assumes a fixed value for the parameters $\mathrm{P}_{\mathrm{nom}}$, implicit in the transformation (17) where the time derivative $\frac{\mathrm{dP}}{\mathrm{dt}} = 0$.

Remark 1) For the case of the LTI system, the nonlinear "controllability" matrix $[g(\mathbf{x}^\star) \quad \mathrm{ad}_f g(\mathbf{x}^\star) \quad \mathrm{ad}_f^2 g(\mathbf{x}^\star) \quad \cdots \quad \mathrm{ad}_f^{n-1} g(\mathbf{x}^\star)]$, yields exactly the controllability matrix for LTI systems. Consider the LTI system $\dot{\mathbf{x}} = \mathrm{A}\mathbf{x} + \mathrm{B}\mathrm{u}$. Then

$$g(\mathbf{x}^\star) = \mathrm{B}$$

$$
\begin{aligned}
\mathrm{ad}_f g(\mathbf{x}^*) &= -\frac{\partial f}{\partial \mathbf{x}} \mathrm{B} = -\mathrm{AB} \\
\mathrm{ad}_f^2 g(\mathbf{x}^*) &= -\frac{\partial f}{\partial \mathbf{x}} \mathrm{ad}_f g(\mathbf{x}^*) = \mathrm{A}^2\mathrm{B} \\
&\vdots \\
\mathrm{ad}_f^{n-1} g(\mathbf{x}^*) &= (-1)^{n-1}\mathrm{A}^{n-1}\mathrm{B}
\end{aligned} \tag{24}
$$

The nonlinear "controllability" test evaluates the rank of the matrix, which becomes exactly the test

$$\mathrm{rank}[\mathrm{B}|\mathrm{AB}|\mathrm{A}^2\mathrm{B}|\cdots|\mathrm{A}^{n-1}\mathrm{B}] \tag{25}$$

which is the controllability matrix for the LTI system.

Remark 2) The Multi–Input–Multi–Output case yields similar results for the coordinate transformation and feedback linearizing control law. See e.g. [*Hunt–Su–Meyer*].

Remark 3) The transformation matrix $\Phi(\cdot)$ captures the essence of the nonlinearity and parameter dependence of the original system. For the linear parameter dependent systems of special concern in the gain scheduling problem, this transformation is usually linear, but parameter dependent.

FEEDBACK LTI'ZATION

The previous section discussed the procedure for feedback linearization of a nonlinear parameter dependent system of the form of equations (1,2). It is of interest to further

extend this to the case of obtaining an LTI system through transformation and suitable feedback control, without requiring that the parameters are constant or without restriction on the variation of the parameters other than knowledge of the nature of the variation.

Consider the Feedback Linearizing control law derivation of equation (20).

$$\begin{aligned} \dot{z}_n = \dot{T}_n &= \frac{\partial T_n}{\partial \mathbf{x}} \dot{\mathbf{x}} + \sum_{i=1}^{q} \frac{\partial T_n}{\partial P_i} \dot{P}_i \\ &= \mathcal{L}_{\dot{\mathbf{x}}} T_n + \sum_{i=1}^{q} \frac{\partial T_n}{\partial P_i} \dot{P}_i \\ &= \mathcal{L}_{\dot{\mathbf{x}}} \mathcal{L}_f^{n-1} \lambda(\mathbf{x}) + \sum_{i=1}^{q} \frac{\partial T_n}{\partial P_i} \dot{P}_i \end{aligned} \tag{26}$$

The feedback LTI'ing control law is then

$$u = \alpha(\mathbf{x},P) + \beta(\mathbf{x},P) \{ \nu - \sum_{i=1}^{q} \frac{\partial T_n}{\partial P_i} \dot{P}_i \} \tag{27}$$

where $\alpha(\mathbf{x},P)$ and $\beta(\mathbf{x},P)$ are

$$\alpha(\mathbf{x},P) = \frac{-\mathcal{L}_f^n \lambda(\mathbf{x},P)}{\mathcal{L}_g \mathcal{L}_f^{n-1} \lambda(\mathbf{x},P)} \quad \text{and} \quad \beta(\mathbf{x},P) = \frac{1}{\mathcal{L}_g \mathcal{L}_f^{n-1} \lambda(\mathbf{x},P)}$$

THE GAIN SCHEDULING CONTROL LAW

Applying the Feedback LTI'zation described above to the affine nonlinear system

$$\dot{\mathbf{x}}(t) = f(\mathbf{x},\mathbf{P}) + g(\mathbf{x},\mathbf{P})u \qquad \mathbf{x} \in \mathbf{R}^n,\ \mathbf{P} \in \mathbf{R}^q \tag{28}$$

where the full state is assumed available for measurement, the transformed system is then in the LTI form

$$\dot{\mathbf{z}} = A_z z(t) + B_z \nu \tag{29}$$

where the feedback LTI'ing control law is written

$$u = \alpha(\mathbf{x},\mathbf{P}) + \beta(\mathbf{x},\mathbf{P}) \{ \nu - \sum_{i=1}^{q} \frac{\partial T_n}{\partial P_i} \dot{P}_i \} \tag{30}$$

If $\dot{P}_i=0$ and the diffeomorphism is linear in the state ($\mathbf{z}=\Phi\mathbf{x}$ and $\mathbf{x}=\Phi^{-1}\mathbf{z}$) , then this control law can be written as an equivalent time invariant feedback law which is linear in gains which are parameter dependent, i.e. $u=-G(P)x$, which defines exactly the correct *autonomous gain scheduling* control law which will guarantee stability regardless of the value of the parameters. If the parameters are varied at some rate ($\dot{P}$ nonzero), it will not be possible to write the control as an autonomous law since the feedback gains will contain the time varying components due to the last term $\sum_{i=1}^{q} \frac{\partial T_n}{\partial P_i} \dot{P}_i$. In this case, the control law constitutes the *linear gain scheduling* control law, which is linear for Φ linear in $\mathbf{x}$, but time varying. In the sequel, the term "*correct*" gain scheduling control law will refer to the *linear gain scheduling* law which may include time dependence. Conditions under which the correct law may be replaced (while still maintaining stability) by the autonomous law will also be discussed. Note

that the linearity of the control law in system space depends on the diffeomorphism being linear in the state variables, which for the linear parameter dependent system of concern in this work, is true. In the sequel, thus, assume the diffeomorphism to be linear in the state variables, and parameter dependent.

The transformed LTI system matrices appear in the form

$$A_z = \begin{bmatrix} 0 & 1 & \cdots & 0 \\ 0 & 0 & 1 & \vdots \\ \vdots & & \ddots & \vdots \\ \vdots & & & 1 \\ 0 & 0 & \cdots & 0 \end{bmatrix} \qquad B_z = \begin{bmatrix} 0 \\ 0 \\ \vdots \\ \vdots \\ 1 \end{bmatrix} \tag{31}$$

and the transformation $\mathbf{z}(t) = \Phi(\mathbf{x}(t))$ is smooth and invertible, i.e. $\mathbf{x}(t) = \Phi^{-1}(\Phi(\mathbf{x}(t)))$ $= \Phi^{-1}(\mathbf{z}(t))$

The second term in (26) may also be determined directly from the transformed system as follows.

Consider the linear parameter dependent diffeomorphism applied to the linear parameter dependent single input system

$$\dot{\mathbf{x}} = A_x(P)\mathbf{x} + B_x(P)u \tag{32}$$

then

$$\mathbf{z} = \Phi(\mathbf{x},P)\mathbf{x} \tag{33}$$

and

$$\dot{z} = \Phi(x,P)\dot{x} + \{\sum_{i=1}^{q} \frac{\partial \Phi(x,P)}{\partial P_i} \dot{P}_i\}$$

$$= \Phi(x,P)A_x(P)\Phi^{-1}(x,P)\, z + \Phi(x,P)B_x(P)u + \{\sum_{i=1}^{q} \frac{\partial \Phi(x,P)}{\partial P_i} \dot{P}_i\} \quad (34)$$

then, selecting the control law (writing B_x for $B_x(P)$)

$$u = \alpha(x,P) + \beta(x,P)\nu - (B_x'B_x)^{-1}B_x'\Phi^{-1}(x,P)\sum_{i=1}^{q} \frac{\partial T_n}{\partial P_i} \dot{P}_i \quad (35)$$

yields the system of equation (31), thus, the control law of (35) and (30) are equivalent.

Gain Scheduled Regulator Design

Assume that some suitable (e.g. LQR or pole–placement) LTI control design methodology is now applied to yield desired (asymptotically stable) closed loop dynamics of the system in z–space. The feedback law is of the form

$$\nu = -K_z z(t) \quad (36)$$

yielding closed loop dynamics

$$\dot{z}(t) = \begin{bmatrix} 0 & 1 & \cdots & 0 \\ 0 & 0 & 1 & \vdots \\ \vdots & & \ddots & \vdots \\ \vdots & & & 1 \\ -K_0 & -K_1 & \cdots & -K_{n-1} \end{bmatrix} z(t) = A_{z_{cl}} z(t) \quad (37)$$

with eigenvalues satisfying

$$\text{Real}\{\ \lambda_i[A_{z_{cl}}]\ \} < 0 \tag{38}$$

i.e. strictly stable.

Definition: An equilibrium point $\mathbf{z}^\star$ of a system is said to be stable if, given $\epsilon>0$, $\exists$ $\delta>0$ such that $\forall\ \mathbf{z}(t_0)\epsilon B_\delta(\mathbf{z}^\star) \Rightarrow \mathbf{z}(t)\epsilon B_\epsilon(\mathbf{z}^\star)\ \forall\ t\geq t_0$, where the notation $B_\delta(\mathbf{z}^\star)$ and $B_\epsilon(\mathbf{z}^\star)$ refer to balls of radii δ and ϵ respectively, centered at $\mathbf{z}^\star$. Thus, rewriting, the equilibrium point $\mathbf{z}^\star$ is stable if

$$\forall\ \|\ \mathbf{z}(t_0) - \mathbf{z}^\star\ \| < \delta \Rightarrow \|\ \mathbf{z}(t) - \mathbf{z}^\star\ \| < \epsilon \quad \forall\ t\geq t_0 \tag{39}$$

Note: The definition may equally well have been given for asymptotic stability, exponential stability etc.

For the regulator feedback control law stabilizing the system of equation (31) in $\mathbf{z}$–space, the definition is thus valid with the equilibrium point being the origin, $\mathbf{z}^\star=\underline{0}$.

Theorem: Consider an affine *parameter dependent* system of the form equation (28), which is feedback LTI'able and which thus yields an equivalent transformed LTI system. Assume the Diffeomorphism is linear in the state ($\mathbf{z}=\Phi(\mathbf{P})\mathbf{x}$) . If the transformed system (in $\mathbf{z}$–space) is stabilized in some sense by feedback in transformed space, then it is stabilized in the same sense in system space, regardless of the system parameter values or the rate of change of the parameter.

Proof: The transformed system is of the form (equation(37))

$$\dot{z}(t) = \begin{bmatrix} 0 & 1 & \cdots & 0 \\ 0 & 0 & 1 & \vdots \\ \vdots & & \ddots & \vdots \\ \vdots & & \ddots & 1 \\ -K_0 & -K_1 & \cdots & -K_{n-1} \end{bmatrix} z(t) = A_{z_{cl}} z(t) \qquad (40)$$

and since K_i are selected for stability of the closed loop system (equilibrium point at the origin, $z^{\star}=0$, corresponding to system space equilibrium point $x^{\star}=0$), then

$$\text{Real}\{ \lambda_i[A_{z_{cl}}] \} < 0$$

In the sense of the stability definition given above, then given $\epsilon > 0$, $\exists\ \delta > 0$ such that

$$\forall \| z(t_0) - z^{\star} \| < \delta \implies \| z(t) - z^{\star} \| < \epsilon \quad \forall\ t \geq t_0 \qquad (41)$$

Now, since the system is feedback linearizable, there exists a diffeomorphism $\Phi(\cdot)$ which by definition is smooth and invertible such that

$$z(\cdot) = \Phi(x(\cdot)) \quad \Leftrightarrow \quad x(\cdot) = \Phi^{-1}(z(\cdot)) \qquad (42)$$

Then, in a neighborhood (Ω) of the equilibrium point, the Jacobian $\nabla\Phi$ is nonsingular, such that for

$$\|\underline{J}\| \triangleq \inf_{x \in \Omega} \|\nabla\Phi(x)\| \qquad (43)$$

then

$$\| \underline{J}(\mathbf{x} - \mathbf{x}^{\star}) \| \leq \| \Phi(\mathbf{x}) - \Phi(\mathbf{x}^{\star}) \| \quad \forall\, \mathbf{x} \in \Omega \tag{44}$$

Rewrite equation (41), then $\forall \mathbf{x} \in \Omega$

$$\forall \| \underline{J}(\mathbf{x}(t_0) - \mathbf{x}^{\star}) \| \leq \| \Phi(\mathbf{x}(t_0)) - \Phi(\mathbf{x}^{\star}) \| < \delta$$
$$\Longrightarrow \| \underline{J}(\mathbf{x}(t) - \mathbf{x}^{\star}) \| \leq \| \Phi(\mathbf{x}(t)) - \Phi(\mathbf{x}^{\star}) \| < \epsilon \quad \forall\, t \geq t_0$$

multiply by $\|\underline{J}\|^{-1}$ both sides, then given $\epsilon > 0$, $\exists\ \delta > 0$, such that

$$\forall \quad \| \mathbf{x}(t_0) - \mathbf{x}^{\star} \| < \|\underline{J}\|^{-1}(\delta) = \delta'$$
$$\Longrightarrow \| \mathbf{x}(t) - \mathbf{x}^{\star} \| < \|\underline{J}\|^{-1}(\epsilon) = \epsilon' \quad \forall\, t \geq t_0 \tag{45}$$

thus the equilibrium point in system space ($\mathbf{x}^{\star}$) is stable in the same sense as that of the transformed system.

Remark: Depending on whether the diffeomorphism is local or global, the stability of the equilibrium point is local or global, since δ' and ϵ' are dependent on the parameter value via the diffeomorphism. The fact that these vary with the parameters is easily overcome by taking the supremum over all possible parameter values, i.e. for the set $\mathcal{P}$ defined as the set of feasible parameters

$$\delta' = \sup_{P_i \in \mathcal{P}} \{\|\underline{J}\|^{-1}\}\ \delta \quad \text{and} \quad \epsilon' = \sup_{P_i \in \mathcal{P}} \{\|\underline{J}\|^{-1}\}\ \epsilon \tag{46}$$

where the diffeomorphism is dependent on the parameter values.

Perfect, Stable Gain Scheduling with *Arbitrarily* Fast Variation of Parameters

For the transformed state feedback control law

$$\nu = -\mathbf{K}_z\mathbf{z}(t) \tag{47}$$

with $\mathbf{K}_z=[K_0\ K_1 \cdots K_{n-1}]$, a constant feedback gain matrix, the closed loop dynamics are LTI and stable, regardless of parameter values. If. in addition, the system is feedback LTI'd, then the transformed system with the stabilizing control law (47) is LTI and stable regardless of both parameter values and *rate of change* of parameters. By virtue of the smoothness and invertibility of the diffeomorphism $\Phi(\mathbf{x},\mathbf{P})$, the transformation from system space to transformed space is one–to–one and onto. The closed loop dynamics in system space ($\mathbf{x}$–space) are thus also LTI and have exactly the closed loop eigenvalues of the system in $\mathbf{z}$–space.

The diffeomorphism combined with the feedback LTI'ing control law then defines the *correct* gain scheduling law to be used if LTI closed loop dynamics are desired for the system while guaranteeing stability, *regardless of the rate of variation* of the system parameters or the *values* of the parameters. The added requirement on the feedback LTI'ing control law allows this result. As will be seen in the sequel, the extra term $-\beta(\mathbf{x},\mathbf{P})\sum_{i=1}^{q}\frac{\partial T_n}{\partial P_i}\dot{P}_i$ is not always necessary, thus allowing arbitrary parameter variation under certain conditions whilst maintaining stability, with only the feedback linearizing (*not* feedback LTI'ing) law applied.

The gain scheduling control law in system space for the actual system, is then written as

$$\begin{aligned} u &= \alpha(\mathbf{x},\mathbf{P}) + \beta(\mathbf{x},\mathbf{P}) \{ \nu - \sum_{i=1}^{q} \frac{\partial T_n}{\partial P_i} \dot{P}_i \} \\ &= \alpha(\mathbf{x},\mathbf{P}) - \beta(\mathbf{x},\mathbf{P}) \{ \mathbf{K}_z \mathbf{z}(t) + \sum_{i=1}^{q} \frac{\partial T_n}{\partial P_i} \dot{P}_i \} \\ &= \alpha(\mathbf{x},\mathbf{P}) - \beta(\mathbf{x},\mathbf{P}) \{ \mathbf{K}_z \Phi(\mathbf{x}(t)) + \sum_{i=1}^{q} \frac{\partial T_n}{\partial P_i} \dot{P}_i \} \end{aligned} \tag{48}$$

where $\Phi(\cdot)$ is the parameter dependent diffeomorphism. Note that the feedback linearizing control law, including the diffeomorphism, captures exactly the required scheduling law for guaranteed closed loop stability.

Remark 1) The feedback linearization procedure assumes full state accessibility and perfect knowledge of the plant. These assumptions are not always satisfied, but do not generally present a problem since suitable robust control design techniques can tolerate uncertainty in the plant and, as will be discussed in the sequel, estimation of the full state vector in a Linear Quadratic Regulator (LQG) setting will yield the same results for the gain scheduling control law with stability guarantees. Model Reference Adaptive Control (MRAC) techniques can also be used to assist in maintaining performance robustness if the plant parameters are not accurately known. [*Kokotovic*] then uses the Extended Matching Condition (EMC) to ensure a parameter independent diffeomorphism and a transformed system with parameters occurring linearly for a structure well suited to parameter adaptive control.

Remark 2) For the exact feedback linearized system where perfect knowledge of the system and parameters is assumed, the degree to which stability over the entire range of parameter values of the scheduled system is achieved, is dependent on how well the actual feedback law implemented mimics the *correct* law defined by equation (48). Clearly, if the range of parameter variations about some operating point is known, within which the control law approximates the *correct* gain scheduling law arbitrarily closely, the system will be stable, regardless of the rate of variation of the parameters within the known range. Given that the $\dot{P}$ term is included in the control law, a test for stability is then how well does the gain scheduling implemented control law mimic the correct law in the region of interest.

Fast Parameter Variations and _Slow_ Closed Loop Eigenstructure Variation

In this section, it is shown that for the case of the desired closed loop dynamics *not* LTI, stability may still be guaranteed for maximal (as fast as is achievable by the system) parameter variation rates if the *closed loop dynamics* (eigenvalues) are "slowly" varying with parameter values. Note that this is an entirely different issue to enforcing slow variation of the parameters: indeed, without belaboring the point, the parameters are allowed to vary as fast as is possible.

Definition. A function f(x) is Lipschitz continuous if it is continuous and there exists a constant $K_l > 0$, such that

$$\| f(x) - f(x^*) \| \leq K_l \| x - x^* \| \quad \forall \text{ feasible } x, x^* \tag{49}$$

Theorem. Locally Lipschitz continuous transformed space feedback gains. If the transformed space feedback gains evaluated at the nominal parameter value, $\mathbf{K}_z(\hat{\mathrm{P}})$, of the LTI system (LTI due to feedback linearization) satisfy a local Lipschitz continuity condition arbitrarily closely, then the gain scheduled system is stable for any feasible parameter value and for any feasible rate of change of the parameters. The Lipschitz constant is

$$K_l < \frac{\epsilon}{\| (\hat{\mathbf{P}}_{ref} - \hat{\mathbf{P}}(0))[1 - e^{-\tau_1/\tau_p}] \|}$$

For $\tau_{max} = \sup_{i=1,\cdots,n}\{\tau_i\}$ for n closed loop modes, select

$\tau_1 = \infty$ (strictly correct), or

$\tau_1 = 3\tau_{max}$ (96% settling time), or

$\tau_1 = 5\tau_{max}$ (99% settling time).

Proof: Consider the feedback LTI'd system of the previous section. The (regulator) system is stable if the control law satisfies the correct scheduling procedure captured in the expression for the control

$$u = \alpha(\mathbf{x},\mathbf{P}) - \beta(\mathbf{x},\mathbf{P}) \{ \mathbf{K}_z \Phi(\mathbf{x}(t)) + \sum_{i=1}^{q} \frac{\partial T_n}{\partial P_i} \dot{P}_i \} \qquad (50)$$

Define the feasible set of parameters as $\mathcal{P}$, i.e. any feasible parameter value $\mathbf{P}$ is contained in $\mathcal{P}$. ($\mathbf{P}$ may be a vector if the system depends on more than one parameter)

For the parameter variation bounded by a first order system of the form

$$\dot{\hat{\mathbf{P}}}(t) = \frac{-1}{\tau_p}\hat{\mathbf{P}}(t) + \frac{1}{\tau_p}\hat{\mathbf{P}}_{ref} \tag{51}$$

where $\hat{\mathbf{P}}_{ref}$ is the maximum expected parameter change and

$$\tau_p = \inf_{\mathbf{P}\in\mathcal{P}} \{\tau_{p_i}\} \tag{52}$$

i.e. τ_p represents the shortest equivalent time constant bound on the variation of parameters in the feasible set; thus, any parameter change from $\mathbf{P}(t)$ to $\mathbf{P}(t+\delta t)$ occurs slower than this bound.

The gain scheduled control law is now implemented in the form

$$u = \alpha(\mathbf{x},\mathbf{P}) - \beta(\mathbf{x},\mathbf{P})\left\{ \mathbf{K}_z(\hat{\mathbf{P}})\,\Phi(\mathbf{x}(t)) + \sum_{i=1}^{q} \frac{\partial \mathbf{T}_n}{\partial \mathbf{P}_i}\dot{\mathbf{P}}_i \right\} \tag{53}$$

where $\hat{\mathbf{P}}$ is the equivalent first order filtered version of $\mathbf{P}$, i.e. via equation (51).

Since $\mathbf{K}_z(\hat{\mathbf{P}})$ is assumed Lipschitz continuous, then there exists a Lipschitz constant $K_l>0$, such that $\forall\ \hat{\mathbf{P}}, \mathbf{P}^\star \in \mathcal{P}$ (feasible $\mathbf{P}$)

$$\| \mathbf{K}_z(\hat{\mathbf{P}}) - \mathbf{K}_z(\mathbf{P}^\star) \| \le K_l \| \hat{\mathbf{P}} - \mathbf{P}^\star \| \tag{54}$$

or

$$\| \Delta \mathbf{K}_z \| \leq K_l \| \Delta \hat{\mathbf{P}} \| \tag{55}$$

Now, the evolution of $\hat{\mathbf{P}}(t)$ is exactly known as bounded by (setting $t_0=0$)

$$\hat{\mathbf{P}}(t) - \hat{\mathbf{P}}(0) = \int_0^{\tau_1} e^{\left\{\frac{-(t-\tau)}{\tau_p}\right\}} \frac{1}{\tau_p} (\hat{\mathbf{P}}_{ref} - \hat{\mathbf{P}}(0)) d\tau$$

$$= (\hat{\mathbf{P}}_{ref} - \hat{\mathbf{P}}(0))[1 - e^{-\tau_1/\tau_p}] \tag{56}$$

Then the gain variations may be written as a function of $\hat{\mathbf{P}}$ variations as [Note: This could as easily be written for each individual gain, yielding a similar result where the Lipschitz constant is tested for each gain, not the more conservative approach given here of simply bounding all gain margins by the smallest gain margin]

$$\begin{aligned} \| \mathbf{K}_z(\hat{\mathbf{P}}(t)) - \mathbf{K}_z(\hat{\mathbf{P}}(0)) \| &\leq K_l \| \hat{\mathbf{P}}(t) - \hat{\mathbf{P}}(0) \| \\ &\leq K_l \| (\hat{\mathbf{P}}_{ref} - \hat{\mathbf{P}}(0))[1 - e^{-\tau_1/\tau_p}] \| \end{aligned} \tag{57}$$

The variation of $\mathbf{K}_z(\hat{\mathbf{P}})$ is of concern here, and only over periods of time on the order of the closed loop time constants, τ_1. In order for the gain scheduled control law to effectively see the *correct* control law, the Lipschitz constant must be selected as

$$K_l < \frac{\epsilon}{\| (\hat{\mathbf{P}}_{ref} - \hat{\mathbf{P}}(0))[1 - e^{-\tau_1/\tau_p}] \|} \tag{58}$$

then

$$\| \mathbf{K}_z(\hat{\mathbf{P}}(\tau_{max})) - \mathbf{K}_z(\hat{\mathbf{P}}(0)) \| \leq \epsilon \tag{59}$$

Select ϵ as the ***smallest gain margin*** (using the ***Circle Criterion*** discussed below) of any one of the feedback gains K_i at the present parameter value, arbitrarily in time, but bounded in magnitude,

$$\epsilon = \inf_{\substack{\delta K_i \\ i=0,\cdots,n-1}} \{ \nu = -[K_0+\delta K_0 \cdots K_i+\delta K_i \cdots K_{n-1}+\delta K_{n-1}] \mid \mathbf{z}^{\star} \text{ stable equ. pt} \} \tag{60}$$

The transformed ($\mathbf{z}$–space) space gains are thus safely within gain margin ranges as seen by the gain scheduled controller over time periods τ_1. Note that the actual gains in system space ($\mathbf{x}=\Phi^{-1}(\mathbf{z})$) are not at all necessarily constant over this time period.

The Lipschitz constant may be written, for $\Delta\hat{\mathbf{P}}_{max}$ the largest expected parameter change from the present value

$$K_l \leq \frac{\epsilon}{\|\Delta\hat{\mathbf{P}}_{max}\|[1-e^{-\tau_1/\tau_p}]} \tag{61}$$

Note: Strictly speaking, the definition of stability involves the notion of evaluating the system for all time after the initial time. This implies that the parameter change should be allowed to evolve fully to its new value before evaluating the Lipschitz constant. The strict stability constraint is then that the Lipschitz constant be selected as (set $\tau_1=\infty$)

$$K_l \leq \frac{\epsilon}{\|\Delta\hat{\mathbf{P}}_{max}\|[1-e^{-\infty/\tau_p}]} = \frac{\epsilon}{\|\Delta\hat{\mathbf{P}}_{max}\|} \tag{62}$$

Equation (61), however, gives a rule of thumb which in most practical cases will be suitable for evaluating the stability of the gain scheduled system. Define the slowest closed loop time constant as given by τ_{max}, where $\tau_{max} = \sup_{i=1,\cdots,n}\{\tau_i\}$ for n closed loop modes. Then, $\tau_1 = 3\tau_{max}$ for the initial condition settled to within 5%, $\tau_1 = 5\tau_{max}$ for settling to within 1%, or $\tau_1 = \tau_{max}$ (63% point) may be used for a less conservative estimate.

Selecting ϵ using the Circle Criterion

In order to guarantee that the system is stable for arbitrary time variation of the parameter within a bounded range, the Circle Criterion [see e.g. *Vidyasagar, Lefschetz, Narendra and Taylor*] stated here without proof, may be used.

For systems (SISO) of the form of figure 4.3, consisting of a Linear Time Invariant system in the forward path, and a time varying nonlinearity in the feedback loop, which may be written as

$$\begin{aligned} \dot{\mathbf{x}}(t) &= A\mathbf{x}(t) + Be(t) \\ y(t) &= C\mathbf{x}(t) + De(t) \\ e(t) &= -\phi(t,y(t)) \\ g(s) &= C[sI - A]^{-1}B + D \end{aligned} \tag{63}$$

with $A \in \mathbf{R}^{nxn}$, $B \in \mathbf{R}^n$, $\mathbf{x}(t) \in \mathbf{R}^n$, $C \in \mathbf{R}^n$and e(t), y(t), D all scalars. The system must also be such that [A,C] is observable, [A,B] is controllable and the function ϕ satisfies

$$\phi(t,0) = 0 \qquad \forall t \geq 0 \tag{64a}$$

$\phi(t,y)$ lies in the sector $[\alpha,\beta]$, i.e. $\alpha y^2 < y\phi(t,y) < \beta y^2 \ \forall t \geq 0, \forall y \in \mathbf{R}$ (64b)

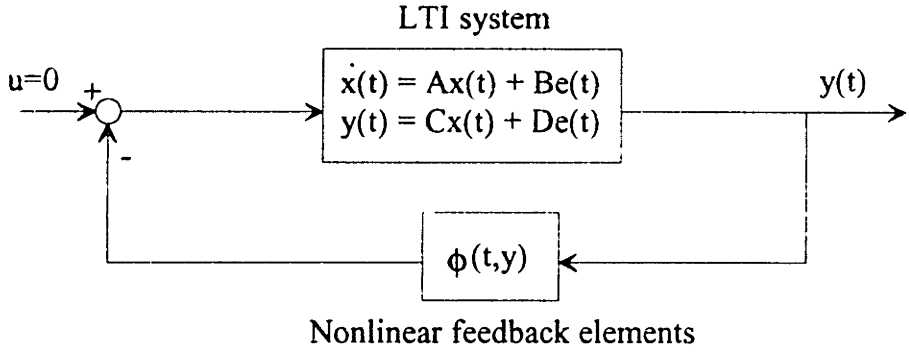

Figure 4.3. System structure for application of Circle Criterion.

Circle Criterion. Assume the system of (63), with A having no eigenvalues on the imaginary axis and with ν eigenvalues having positive real parts. If ϕ lies in the sector $[\alpha,\beta]$, i.e. $\alpha y^2 \leq y\phi(t,y) \leq \beta y^2 \ \forall y \in \mathbf{R}$ and $\forall t \geq 0$, then a sufficient condition for stability is one of

1) If $0<\alpha<\beta$, the Nyquist plot of $g(j\omega)$ does not enter the disk $D(\alpha,\beta)$ and encircles it ν times in the counterclockwise direction.

2) If $0=\alpha<\beta$, the Nyquist plot of $g(j\omega)$ lies in the half plane $\{s:\mathrm{Re}(s)>=-1/\beta\}$.

3) If $\alpha<0<\beta$, the Nyquist plot $g(j\omega)$ lies in the interior of the disk $D(\alpha,\beta)$.

4) If $\alpha<\beta<0$, replace g with $-g$, α with $-\beta$ and β with $-\alpha$ and apply (1).

Note: For application to the gain scheduling controller design problem, where the closed loop dynamics are to vary as a function of parameter value, the system equations should be written in the form

$$\dot{z}(t) = \begin{bmatrix} 0 & 1 & \cdots & 0 \\ 0 & 0 & 1 & \vdots \\ \vdots & & \ddots & \vdots \\ \vdots & & & 1 \\ -K_0 & -K_1 & \cdots & -K_{n-1} \end{bmatrix} z(t) = A_{z_{cl}} z(t) \qquad (65)$$

Since it is desired to determine the allowable (whilst maintaining stability) variation of the feedback gains K_i as arbitrary functions of time, define a fictitious output function which allows the system to be viewed in the correct framework for application of the circle criterion. As the closed loop dynamics are to vary with the parameter, the effective feedback control law appears as

$$u = -K_z z(t) = -[K_0+\delta K_0 \cdots K_i+\delta K_i \cdots K_{n-1}+\delta K_{n-1}]z(t) \qquad (66)$$

with K_i the nominal gains associated with the present parameter value ($\hat{P}(t)$) and δK_i the change over the time period τ_{max}. Note that $\delta K_i=\delta K_i(t)$ (time varying). Writing the effective gain variation as scaled versions of one of the δK_i's, e.g. defining

$$\delta K_0(t)=\delta K_0, \qquad \delta K_1(t)=\frac{K_1}{K_0}\delta K_0 \qquad \cdots \qquad \delta K_{n-1}=\frac{K_{n-1}}{K_0}\delta K_0 \qquad (67)$$

and the time varying nonlinearity

$$e(t) = -\phi(t,y(t)) \qquad = -\delta K_0\, y(t) \tag{68}$$

the output function is selected as

$$y(t) = [1 \ \frac{K_1}{K_0} \ \frac{K_2}{K_0} \ \cdots \ \frac{K_{n-1}}{K_0}]\, z(t) = C\, z(t) \tag{69}$$

yielding a restructured system in the correct form. Now, the Circle Criterion may be directly applied to determine limits on δK_0 and, hence, all the feedback gain perturbations which will guarantee stability for arbitrary time histories of these perturbations within the determined bounds, for the specific ratio of gain variation in equation (69). If the actual **z**–space gains are of the same ratio for all P, then this test is strictly correct. Otherwize, the test gives good ballpark estimates.

The value for ϵ is then selected as

$$\epsilon = \inf_{i=0,\cdots,n-1} \{ \delta K_i \} \tag{70}$$

The unicycle example at the end of this chapter illustrates the procedure.

Remark 1) Clearly, if arbitrarily fast parameter variations are achievable (i.e. τ_p is very small relative to τ_{max}), then since the closed loop dynamics are not necessarily able to be of arbitrarily small time constants (i.e. τ_{max} may be $>> \tau_p \Rightarrow [1-e^{-\tau_{max}/\tau_p}] \approx 1$), K_l is small if ΔP_{max} is large, hence the *transformed* state gains must be effectively constant. Note that this

implies that the *correct* gain scheduling law of equation (48), must then be applied to accommodate the fast parameter variation. If, on the contrary, the maximum achievable parameter rate of change is slow ($\tau_p >> \tau_{max}$), then $[1-e^{-\tau_{max}/\tau_p}]$ is small, so K_l may be large and the gains $\mathbf{K}_z(\mathbf{P})$ may vary significantly with $\mathbf{P}$, since the effective gain seen by the controller will be $\Delta\mathbf{K}_z \approx \epsilon$ i.e. $\mathbf{K}_z$ within gain margin limits, and the control is, hence, effectively the *correct* gain scheduled control law locally about the present operating parameter value.

Remark 2) Note that the gain scheduled control law $u = \alpha(\mathbf{x},\mathbf{P}) - \beta(\mathbf{x},\mathbf{P}) \{ \mathbf{K}_z(\hat{\mathbf{P}})\Phi(\mathbf{x}(t)) + \sum_{i=1}^{q} \frac{\partial T_n}{\partial P_i} \dot{P}_i \}$ achieves the required correct control law in a local sense. For a given parameter value, the gains $\mathbf{K}_z$ (including the perturbation values δK_i) are within bounds which guarantee stability (Circle Criterion). For changes in $\mathbf{P}$ which may arise due to high frequency disturbances or unmodeled effects, which are then of reduced amplitude (typically, the small amplitude higher frequency parameter variations which occur due to disturbances), the control law is exactly the correct one for these fast local parameter perturbations about the more slowly changing nominal parameter value $\hat{\mathbf{P}}$.

Remark 3) The "slowly" varying transformed state gains $\mathbf{K}_z(\hat{\mathbf{P}})$, which vary in a continuous fashion, imply that the closed loop dynamics vary "slowly" with parameter changes. As in the case of the *correct* gain scheduling law being applied across the entire parameter range with constant closed loop dynamics, the condition previously stated by [*Shamma*] and others, i.e. that the parameters should vary slowly for stability, is not

necessary *if* the control law includes the parameter rate of change term as in the feedback LTI'ing control law of equation (48). Even for the case of slowly varying *closed loop dynamics*, the parameters may be varied as fast as the system is capable of, whilst still maintaining closed loop stability.

Remark 4) The Lipschitz constant may be evaluated for each individual gain according to the expression $K_{l_i} \leq \frac{\epsilon_i}{\|\Delta \hat{P}_{max}\|\left[1-e^{-\tau_{max}/\tau_{P_i}}\right]}$ (for i'th gain), where ϵ_i is selected as $\delta K_i = \frac{K_i}{K_0}\delta K_0$ from the Circle Criterion condition, yielding a less conservative range of acceptable gain variations with parameter change (i.e. the gradient $\frac{\partial K_{z_i}}{\partial \|P\|}$ is determined for each gain as opposed to assuming this as the smallest value over all the gains)

Remark 5) The Circle Criterion may further be used to evaluate whether or not the $\dot{P}$ terms may be ignored in the control law, as will be discussed later. It may be that $\dot{P}$ cannot be measured accurately, in which case knowledge of whether the $\dot{P}$ term may be ignored in the control law is important.

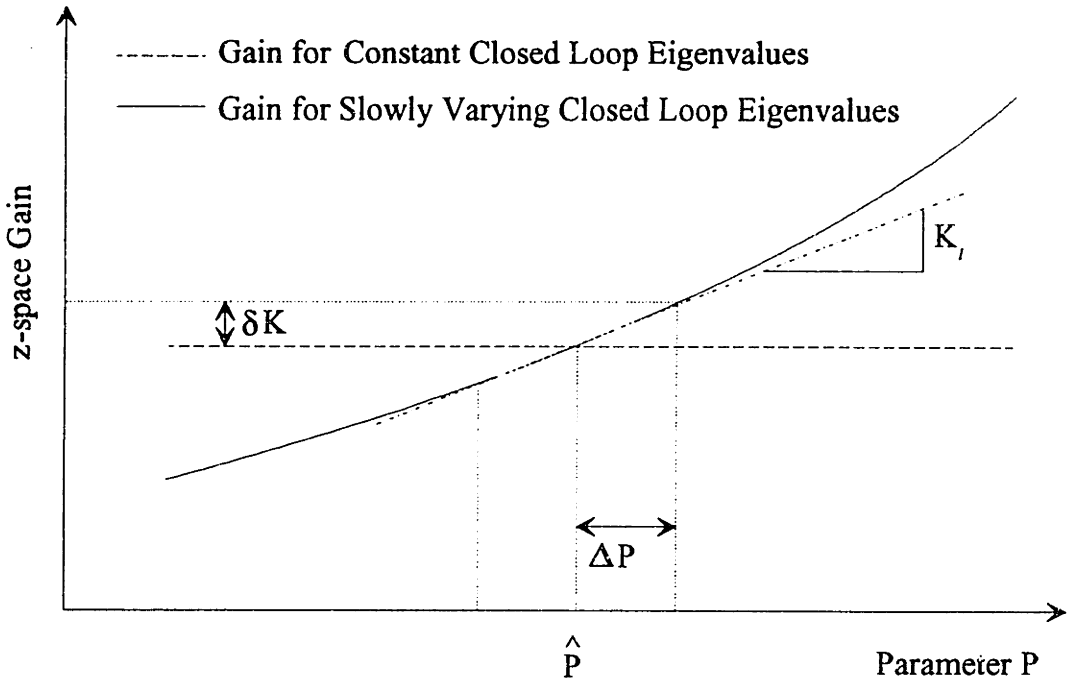

Figure 4.4. Gains vs scheduling parameters for the stability proof. For very fast parameter variation, the correct control law due to the feedback LTI'zation and the diffeomorphism must be implemented for closed loop stability. Reducing the rate of change of parameters, relaxes this requirement to the extent that, for slow parameter variations, the transformed state feedback gains may vary significantly (but Lipschitz continuously) such that in effect the closed loop dynamics may vary significantly with parameter values, while maintaining closed loop stability.

Design Procedure. Full State Accessibility.

1) Check that system is Feedback Linearizable.

   a) *Controllability*: the matrix $[g(\mathbf{x}^\star)\ \mathrm{ad}_f g(\mathbf{x}^\star)\ \mathrm{ad}_f^2 g(\mathbf{x}^\star)\ \cdots\ \mathrm{ad}_f^{n-1} g(\mathbf{x}^\star)]$ has rank n, i.e. rank equal to the dimension of the system.

   b) *Involutivity*: $[g(\mathbf{x}^\star)\ \mathrm{ad}_f g(\mathbf{x}^\star)\ \mathrm{ad}_f^2 g(\mathbf{x}^\star)\ \cdots\ \mathrm{ad}_f^{n-2} g(\mathbf{x}^\star)]$ involutive, which may be tested for by the rank test.

2) Define the diffeomorphism $\Phi(\mathbf{x})$ of equation (17) and transform the system to

the equivalent LTI form in **z**–space.

3) Determine the feedback LTI'ing control law of equation (48).

4) Determine expected parameter variation range and upper bound on parameter variation time constants to define a bound of the form of equation (51).

5) Design full state feedback law in transformed space (**z**–space) assigning closed loop eigenvalues at each desired parameter design point such that the Lipschitz condition of the gain $\mathbf{K}_z$ variation is satisfied for the expected parameter variations determined in (4) above. In order to ensure that the system behaves suitably, it is useful to design the controller in *system* space and then use the closed loop eigenvalues thus obtained as desired values for pole placement design in *transformed* **z**–space. This allows the designer to achieve a design which satisfies specifications written for the system in terms of real (system space) performance criteria.

6) Transform the control law to system space. This defines the correct control law at each design parameter value.

7) Curve fit through design points if the closed loop dynamics do not vary too much as a function of parameter value, OR simply implement the control law using equations (51) and (53). Note that if the Lipschitz condition is satisfied, then the curve fit through suitably closely spaced design points will yield control gains close to the *correct* scheduling law locally, thus guaranteeing stability.

Instability Due to Incorrect Feedback Control Law

One of the problems in gain scheduling applications has been that instability sometimes occurs, even though the eigenvalues of the frozen time systems have negative real parts [*Aggarwal, Wu, unicycle example: see fig 4.14a*]. This is easily explained in the light of the work presented here.

Figure 4.5 shows the typical case. Two parameter values are selected as design points and then in classical scheduling fashion, some form of curve fitting of the gains determines the values to be used at intermediate parameter values. If the transformed state control gains do not satisfy the Lipschitz condition derived above and/or the system space control law does not include the parameter rate of change dependent term, then stability cannot be guaranteed for any rate of change of the parameters other than extremely slow (relative to system time constants where $\dot{P} \approx 0$). Indeed, it is possible that the regression function mapping the gain scheduling gains between design parameter values does not pass through gain values which are stabilizing, although this is fairly unlikely if design points are suitably closely spaced.

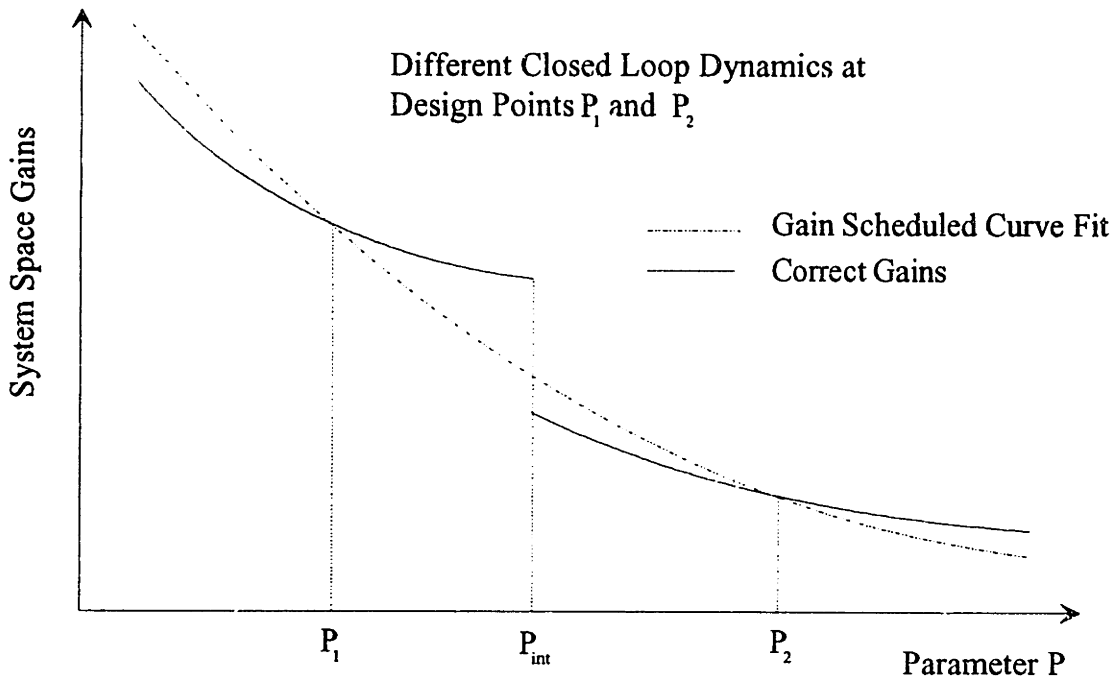

Figure 4.5. Gain scheduling between discrete design parameter values. Consider the gain scheduled control law where the gains are determined by curve fitting through two discrete designs (of different closed loop dynamics) at parameter values P_1 and P_2. If the gains in transformed space do not satisfy the Lipschitz condition and/or the $\dot{P}$ term is neglected in the control law, stability is not guaranteed for arbitrary rates of change of the parameters. Assuming the $\dot{P}$ term is included in the control law, then if the Lipschitz condition is not met, the two *correct* gain scheduling curves drawn through each point will not meet at a common point for the intermediate parameter value, and in fact at all but the design points, an incorrect gain scheduling law will be active, losing stability guarantees.

What if Full State is Not Accessible?

The previous results assume the full state vector is available for measurement in

order to apply the transformation and determine the gain scheduled control law. This is, however, not always the case. It may be argued that the solution to this problem is to design and build/obtain the necessary sensors to in fact obtain the full state vector for measurement, but another alternative is necessary for cases where this is not a viable option.

The obvious solution is to make use of an observer to obtain estimates of the state vector which can then be used in the full state feedback control law determined in the gain scheduled design. One such solution is proposed by [*Cro Granito–Valavani–Hedrick*] where use of an extended Kalman Filter or any other nondivergent filter is made to this end. In this work, the authors make use of such an estimator to obtain the full state estimate for use in a nonlinear servo design technique based on Input–Output linearization. The results obtained depend strongly on obtaining good estimates of the full state vector.

Another possibility, and the one to be further explored here, is to design a Kalman filter for the transformed (even though the full state is not measured, it is possible to write down the transformation for use in defining the **z**–space observer) LTI equivalent system which is of suitable closed loop dynamics as to obtain good estimates of the state. By then implementing the Kalman Filter in **z**–space, driven by actual (physical) system measurements, it is possible to generate the transformed space (z–space) state estimate, which is then easily transformed via the diffeomorphism to system space for use in the gain scheduled regulator feedback law. In transformed space, it is perfectly feasible, by use of the separation principle, to design the regulator and filter separately. Proving stability of the transformed state LQG system follows the same arguments discussed previously for the regulator.

LQG Controller in Framework of Feedback LTI'zation

Consider the standard LQG control system structure of figure 4.6a applied to the transformed feedback LTI'd system in z–space. The separation principle allows separate design of the regulator and Kalman Filter, where the Kalman Filter is designed to be of closed loop bandwidth approximately 3 or 4 times faster than the regulator closed loop dynamics. This ensures that the estimates obtained are good. Ideally, the settling time of a filter is 3 time constants, so the residues should be arbitrarily small for suitable use of the filter state as a full state estimate for the regulator.

Theorem. LTI'd LQG controller stability. For a feedback LTI'able system with only a reduced set of states available for measurement, a single transformed space LQG controller may be designed for *stable* control of the closed loop system over the entire operating envelope. The observer is implemented in transformed coordinates driven by system measurements, while the regulator is implemented in system coordinates.

Proof: For the feedback LTI'able system of equation (31), (with feedback LTI'ing control law of equation (30)), the diffeomorphism may be written as

$$\mathbf{z} = \Phi(\mathbf{x})$$

(Note that this transformation is not implementable, since it requires a transformation of the full state, which is not available due to the reduced set states in the measurements)

Consider the system measurement rewritten in terms of the transformed

state vector

$$\begin{aligned} \mathbf{y}(t) &= \mathbf{C_x x}(t) \\ &= \mathbf{C_x \Phi^{-1}(z}(t)) \end{aligned} \tag{71}$$

Assumption 1: Since, for a parameter dependant system, the diffeomorphism is also parameter dependent, the measurement matrix $\mathbf{C_x \Phi^{-1}(z}(t))$ is a function of the parameter value. Assume that by redefining the measurement matrix with the same states measured, but simply scaling all parameter dependent terms, the output matrix is parameter independent. Thus, define $\mathbf{C}'_x$ such that $\mathbf{C}'_x \mathbf{\Phi^{-1}(z}(t))$ is independent of P.

For the z–space system with process white noise $\xi(t)$ and sensor white noise $\theta(t)$ and $\mathcal{L}=B_z$

$$\dot{\mathbf{z}} = A_z\mathbf{z} + B_z\nu + \mathcal{L}\xi(t)$$
$$\mathbf{y} = \mathbf{C}'_x\mathbf{\Phi^{-1}(z}(t)) + \theta(t)$$

the Kalman filter is to be designed such that the error dynamics are of the form ($\tilde{\mathbf{z}} = \mathbf{z} - \hat{\mathbf{z}}$, for $\hat{\mathbf{z}}$ the estimate of $\mathbf{z}$ and $\mathbf{z}=\mathbf{\Phi}(\mathbf{x})$, $\hat{\mathbf{z}}=\mathbf{\Phi}(\hat{\mathbf{x}})$)

$$\begin{aligned} \dot{\tilde{\mathbf{z}}} &= A_z\tilde{\mathbf{z}} - H_zC'_x(\mathbf{\Phi^{-1}(z}) - \mathbf{\Phi^{-1}}(\hat{\mathbf{z}})) \\ &= A_z\tilde{\mathbf{z}} - H_zC'_x(\mathbf{x} - \hat{\mathbf{x}}) \end{aligned}$$

Assumption 2: Assume there exists a neighborhood of the equilibrium

point x^*, $\Omega \in R^n$, where the Taylor series expansion of the diffeomorphism

$$z - z^* = \nabla\Phi\Big|_{x^*}(x - x^*) + \frac{\nabla^2\Phi}{2}\Big|_{x^*}(x - x^*)^2 + \cdots + \frac{\nabla^n\Phi}{n!}\Big|_{x^*}(x - x^*)^n$$

is approximated arbitrarily closely by the linear expression

$$z - z^* \approx \nabla\Phi\Big|_{x^*}(x - x^*) \qquad \forall\, x \in \Omega$$

where the Jacobian $\nabla\Phi\Big|_{x^*}$ exists and is nonsingular, since $\Phi(\cdot)$ is a diffeomorphism. Note that if the diffeomorphism is linear in z, this expression is *exact.*

Then,

$$\begin{aligned}\dot{\tilde{z}} &= A_z\tilde{z} - H_zC_x'(\nabla\Phi\Big|_{x^*})^{-1}(z - \hat{z}) \\ &= A_z\tilde{z} - H_zC_z(z - \hat{z})\end{aligned}$$

with $C_z = C_x'(\nabla\Phi\Big|_{x^*})^{-1}$, LTI and independent of P.

Select H_z such that the error dynamics are asymptotically stable (solve filter algebraic Riccati equation), i.e.

$$\text{Real}\{\lambda_i(A_z - H_zC_z)\} < 0 \quad i=1,2,\cdots,n$$

Now, the separation principle applied to design of an LQG controller in

z–space (filter gains H_z, regulator gains K_z), yields the closed loop system (see figure 4.6a)

$$\frac{d}{dt}\begin{bmatrix}\hat{z}\\ z\end{bmatrix} = \begin{bmatrix}A_z - H_zC_z - B_zK_z & H_zC_z\\ -B_zK_z & A_z\end{bmatrix}\begin{bmatrix}\hat{z}\\ z\end{bmatrix} + \begin{bmatrix}H_z\\ 0\end{bmatrix}(y - y_{ref}) \qquad (72)$$

which is strictly stable by design, in fact the eigenvalues are exactly the filter and regulator eigenvalues. Now, it may be easily shown that since the full system in z–space is stable, the full closed loop system in x–space is likewise. The proof follows exactly the arguments of the case for only regulator feedback in z–space, by defining the (invertible, since the diffeomorphism $\Phi(\cdot)$ is invertible) transformation matrix (Jacobian) such that, for $x_{aug} = \begin{bmatrix}\hat{x}\\ x\end{bmatrix}$ and $z_{aug} = \begin{bmatrix}\hat{z}\\ z\end{bmatrix}$, for $x, \hat{x} \in \Omega$,

$$\begin{bmatrix}\hat{z}\\ z\end{bmatrix} = \begin{bmatrix}\nabla\Phi & 0\\ 0 & \nabla\Phi\end{bmatrix}\Big|_{x^*}\begin{bmatrix}\hat{x}\\ x\end{bmatrix} \quad \text{or} \quad z_{aug} = T\,x_{aug} \text{ and } x_{aug} = T^{-1}z_{aug}$$

Then, by definition of stability of the system in z–space, given $\epsilon>0$, $\exists$ $\delta>0$, such that

$$\forall \| z_{aug}(t_0) - z_{aug}^* \| < \delta \implies \| z_{aug}(t) - z_{aug}^* \| < \epsilon \quad \forall\, t \geq t_0$$

Apply the transformation to yield

$$\forall \| T\,x_{aug}(t_0) - T\,x_{aug}^*) \| < \delta \implies \| T\,x_{aug}(t) - T\,x_{aug}^* \| < \epsilon \quad \forall\, t \geq t_0$$

Then, in a neighborhood (Ω) of the equilibrium point, the Jacobian T is

nonsingular, such that for

$$\|\underline{J}\| \triangleq \inf_{\mathbf{x},\hat{\mathbf{x}} \in \Omega} \left\| \begin{bmatrix} \nabla\Phi & 0 \\ 0 & \nabla\Phi \end{bmatrix} \right\|$$

then

$$\| \underline{J}(\mathbf{x}_{aug} - \mathbf{x}^{\star}_{aug}) \| \leq \| \mathbf{T}\, \mathbf{x}_{aug} - \mathbf{T}\, \mathbf{x}^{\star}_{aug} \| \quad \forall\, \mathbf{x},\, \hat{\mathbf{x}}_{aug} \in \Omega$$

Now, $\forall\, \mathbf{x},\, \hat{\mathbf{x}} \in \Omega$

$$\forall \| \underline{J}(\mathbf{x}_{aug}(t_0) - \mathbf{x}^{\star}_{aug}) \| \leq \| \mathbf{T}\, \mathbf{x}_{aug}(t_0) - \mathbf{T}\, \mathbf{x}^{\star}_{aug} \| < \delta$$
$$\Rightarrow \| \underline{J}(\mathbf{x}_{aug}(t) - \mathbf{x}^{\star}_{aug}) \| \leq \| \mathbf{T}\, \mathbf{x}_{aug}(t) - \mathbf{T}\, \mathbf{x}^{\star}_{aug} \| < \epsilon \quad \forall\, t \geq t_0$$

multiply by $\|\underline{J}\|^{-1}$ both sides. Then, $\forall\, \mathbf{x},\, \hat{\mathbf{x}}_{aug} \in \Omega$, given $\epsilon > 0$, $\exists\, \delta > 0$, such that

$$\forall \quad \| \mathbf{x}_{aug}(t_0) - \mathbf{x}^{\star}_{aug} \| < \|\underline{J}\|^{-1}(\delta) = \delta'$$
$$\Rightarrow \| \mathbf{x}_{aug}(t) - \mathbf{x}^{\star}_{aug} \| < \|\underline{J}\|^{-1}(\epsilon) = \epsilon' \quad \forall\, t \geq t_0$$

thus the equilibrium point, $\begin{bmatrix} \hat{\mathbf{x}} \\ \mathbf{x} \end{bmatrix} = \begin{bmatrix} \mathbf{0} \\ \mathbf{0} \end{bmatrix}$ in system space, is stable in the same sense as that of the transformed system, if assumptions 1 and 2 hold.

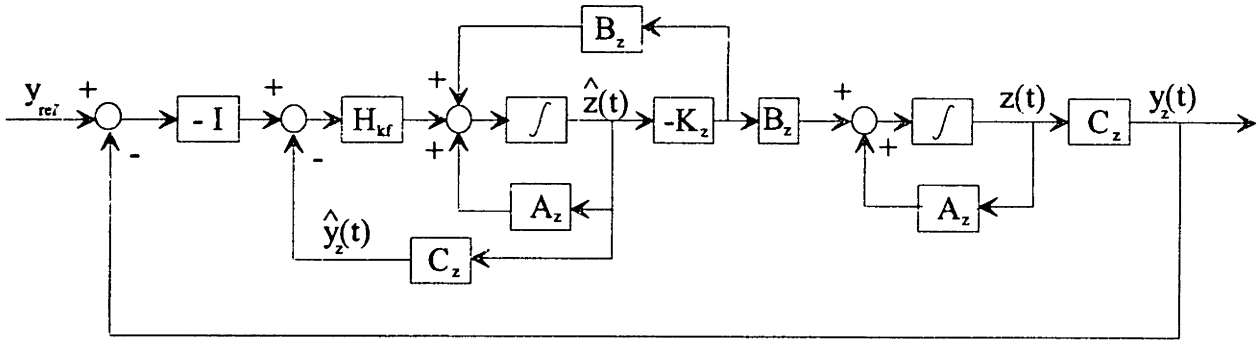

Figure 4.6a. LQG controller structure in transformed space. Assuming the system with full state accessibility is feedback LTI'able, the regulator is designed in **z**–space. This assumption, however needs good state estimates $\hat{\mathbf{x}}(t)$, which may be obtained through suitable filter design. The Kalman filter is designed in **z**–space, by use of the separation principle, and implemented in **z**–space. The **x**–space state estimates are then obtained by transformation via the smooth diffeomorphism to system space for implementing the regulator part of the control law.

The implementation of the LTI' LQG controller is in the form given in figure 4.6b. Note that the (LTI) state estimator runs in transformed coordinates with the diffeomorphism yielding the correct transformation to system coordinates $\hat{\mathbf{x}}$ for use in the *correct* gain scheduled control law.

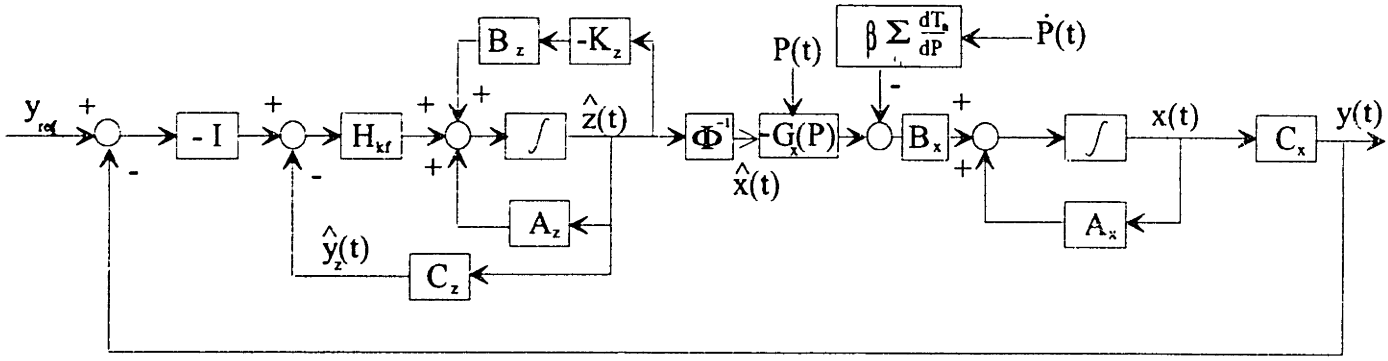

Figure 4.6b. LTI'd LQG structure implemented. The observer runs in transformed space, driven by the actual system measurements and yielding physical system state estimates by transformation of the transformed space estimate via the diffeomorphism.

The **z**–space estimator is of the structure

$$\dot{\hat{\mathbf{z}}}(t) = (A_z - \mathbf{H}_z C_z - B_z \mathbf{K}_z)\hat{\mathbf{z}}(t) + \mathbf{H}_z(\mathbf{y}_z(t) - \mathbf{y}_{z_{ref}}(t)) \qquad (73)$$

where $\mathbf{y}_{z_{ref}}=\mathbf{0}$ for the regulator. Note that $\mathbf{y}_z(t)=\mathbf{y}_x(t)$ in equation (73), so that the **z**–space estimator is driven directly by physical system measurements (scaled as necessary to yield measurements independent of the parameter values). The **z**–space state estimate is then transformed to system space via the diffeomorphism

$$\hat{\mathbf{x}}(t) = \Phi^{-1}(\hat{\mathbf{z}}(t)) \qquad (74)$$

with the system space regulator control law

$$u = a(\hat{x},P) - \beta(\hat{x},P)\left\{ K_z(\hat{P})\,\phi(\hat{x}(t)) + \sum_{i=1}^{q} \frac{\partial T_n}{\partial P_i}\dot{P}_i \right\} \qquad (75)$$

Design Procedure

The design procedure for the case of output feedback follows that of the full state case, with the added step of designing the Kalman Filter in transformed space and then transforming to system space to yield an implementable controller.

Add, thus, the step:

5(a) Define the scaled output matrix such that the measurements in z–space are independent of the parameter P and LTI. Design a Kalman Filter for state estimation in z–space, with the time constants at least 3 to 4 times faster than the corresponding regulator time constants. Implement as shown in figure 4.6b, with the estimator running in transformed coordinates and the diffeomorphism used to transform the z–space estimate into system space for implementing of the regulator control law in system space.

THE IMPACT OF THE PARAMETER TIME DEPENDENCE

Consider the control law of equation (30)

$$u = a(x,P) + \beta(x,P)\left\{ \nu - \sum_{i=1}^{q} \frac{\partial T_n}{\partial P_i}\dot{P}_i \right\}$$

The effect of the parameter rate of change dependent term $\dot{P}_i$ in the control law is to cancel exactly such a term which arises in the last row of the transformed coordinates system. The added term *may be ignored* if the effective contribution is sufficiently smaller than the individual gain margins of the relevant feedback gain K_{z_i}, where $\nu=-\mathbf{K}_z\mathbf{z}=-[K_{z_0}\ K_{z_1}\ \cdots\ K_{z_i}\ \cdots\ K_{z_{n-1}}]\mathbf{z}$. For example, if the gain margin (evaluated using the Circle Criterion) for individually changing K_{z_1} is δK_{z_1} and the parameter rate of change term is of the form $A_z\dot{P}z_1$, then as long as the coefficient $A_z\dot{P}<\delta K_{z_1}$, then this element of the control law may be ignored.

More formally, for the case of a single parameter upon which the system is dependent, consider the n'th row of the state space model of the transformed (via diffeomorphism and ***feedback linearizing*** control law, i.e. without canceling the $\dot{P}$ term as in the feedback LTI'ing control law) system, with $\nu=-\mathbf{K}_z\mathbf{z}$

$$\dot{z}_n = \frac{\partial \Phi(\mathbf{x},P)}{\partial P}\dot{P} - \mathbf{K}_z\mathbf{z} \tag{76}$$

The system may then easily be written in the correct form for use of the Circle Criterion as

$$\dot{\mathbf{z}}(t) = \begin{bmatrix} 0 & 1 & \cdots & 0 \\ 0 & 0 & 1 & \vdots \\ \vdots & & \ddots & \vdots \\ \vdots & & \ddots & 1 \\ -K_0 & -K_1 & \cdots & -K_{n-1} \end{bmatrix} \mathbf{z}(t) + \begin{bmatrix} 0 \\ 0 \\ \vdots \\ \vdots \\ 1 \end{bmatrix} e(t) \tag{77}$$

with the output

$$y(t) = \frac{-\partial \Phi(\mathbf{x},P)}{\partial P} = C\,\mathbf{z}(t) \tag{78}$$

and the nonlinear feedback term

$$e(t) \quad = -\dot{P}\, y(t) \tag{79}$$

In this form, the Circle Criterion directly yields bounds on the parameter rate of change $\dot{P}$ for stability, thus allowing evaluation of whether the (known) $\dot{P}_i$ term may be ignored in the feedback LTI'ing control law whilst still maintaining stability.

The mechanisms by which this term may be ignored are the following.

1) **"Slow" Parameter variation**. In this case, where the parameters vary slowly when compared to the system closed loop bandwidth, then $\dot{P} \approx 0$ on the time scales of the closed loop system time constants and the term may be ignored. The scheduling control law is then the *autonomous gain scheduled* law

$$u \quad = \alpha(x,P) + \beta(x,P)\, \nu \tag{80}$$

This is exactly the case typically cited for the gain scheduling problem.

2) **"Small"** $\beta(x,P) \sum_{i=1}^{q} \frac{\partial T_n}{\partial P_i} \dot{P}_i$ ~~δ^{-1}~~ (δK_j evaluate by Circle Criterion). If this term satisfies the Circle Criterion bounds, i.e. is "small" relative to the other feedback terms, i.e.

$$\sup_{t \in [t_o,t]} \{ \| \beta(x,P) \sum_{i=1}^{q} \frac{\partial T_n}{\partial P_i} \dot{P}_i \| \} < \inf_{j=1 \cdots n} \{ \| \delta K_j \| \} \tag{81}$$

then the effect is equivalent to that of (1) small feedback gain variations which may be viewed as insignificant in a gain margin sense, or (2) small amplitude noise in the measurements of the state vector, both of which should not pose any stability problem.

3) **"Fast", *Infrequent* Parameter changes.** If the parameter changes to a new value, with equivalent parameter change time constant (τ_p) much shorter than the closed loop system time constants, i.e.

$$\tau_p << \tau_{max} \tag{82}$$

with these time constants as defined in equation (52, 58), and remains at the new value for time periods much longer than τ_{max} (i.e. the changes occur "infrequently"), then the system will maintain the stability properties of the feedback LTI'd system with the *autonomous gain scheduled* control law. This kind of parameter change is equivalent to an instantaneous change, after which the system remains at the new parameter value and is LTI even under only feedback linearizing control (the $\dot{P}$ term is zero in the feedback LTI'ing law).

EXAMPLE: THE AUTONOMOUS UNICYCLE ROBOT

The gain scheduling technique is applied to the autonomous unicycle robot and has been successfully implemented and demonstrated on the actual physical system. This section evaluates the existing gain scheduled controller in the light of the preceding results, in order to gain insight regarding the stability of the closed loop system.

Unicycle Parameter Dependent Lateral Dynamics.

The state space model, which is dependent on wheelspeed as derived in [*Vos, S.M.*] is given below. For the state vector, with the terms roll and yaw of similar meaning to common aerospace use,

$$\mathbf{x}(t) = \begin{bmatrix} \text{Roll Rate} \\ \text{Roll Angle} \\ \text{Yaw Rate} \end{bmatrix} = \begin{bmatrix} \dot{\phi}(t) \\ \phi(t) \\ \dot{\psi}(t) \end{bmatrix} \tag{84}$$

then

$$\dot{\mathbf{x}}(t) = \begin{bmatrix} 0 & \frac{k_1 g}{m_{11}} & \frac{k_2 \Omega(t)}{m_{11}} \\ 1 & 0 & 0 \\ \frac{-I_2^W \Omega(t)}{m_{22}} & 0 & \frac{-f_{\dot{\psi}}}{m_{22}} \end{bmatrix} \mathbf{x}(t) + \begin{bmatrix} 0 \\ 0 \\ \frac{n_t}{m_{22}} \end{bmatrix} \Gamma \tag{85}$$

with

$\frac{k_1 g}{m_{11}}$ gravity rolling moment due to roll angle away from vertical

$\frac{k_2 \Omega(t)}{m_{11}}$ gyroscopic coupling from yaw to roll

$\frac{I_2^W \Omega(t)}{m_{22}}$ gyroscopic coupling from roll to yaw

$\frac{f_{\dot{\psi}}}{m_{22}}$ viscous yaw damping due to tire/surface interaction

$\frac{n_t}{m_{22}}$ torque actuator (reaction mass) gearing

Feedback LTI'zation of Unicycle Lateral Dynamics

In order to obtain a feedback LTI'd description of the lateral dynamics, the *controllability* and *involutivity* conditions must be satisfied. To this end, the following Lie brackets are evaluated about the [*unstable*] equilibrium point of $\mathbf{x}(t=0)=\mathbf{0}$.

$$\mathrm{ad}_f g = \frac{\partial g(\mathbf{x})}{\partial \mathbf{x}} f(\mathbf{x}) - \frac{\partial f(\mathbf{x})}{\partial \mathbf{x}} g(\mathbf{x})$$

$$= \begin{bmatrix} \frac{-k_2 \Omega(t) n_t}{m_{11} m_{22}} \\ 0 \\ \frac{f_{\dot{\psi}} n_t}{m_{22} m_{22}} \end{bmatrix} \tag{86}$$

$$\mathrm{ad}_f^2 g = \begin{bmatrix} -\frac{k_2 \Omega(t) n_t}{m_{11} m_{22} m_{22}} f_{\dot{\psi}} \\ \frac{k_2 \Omega(t) n_t}{m_{22} m_{11}} \\ -\frac{I_2^w \Omega^2(t) k_2 n_t}{m_{11} m_{22} m_{22}} + \frac{n_t}{m_{22}^3} f_{\dot{\psi}}^2 \end{bmatrix} \tag{87}$$

Controllability

The test for controllability involves evaluation of the rank of the matrix

$$[g \mid \mathrm{ad}_f g \mid \mathrm{ad}_f^2 g]$$

$$\begin{bmatrix} 0 & -\frac{k_2 \Omega(t) n_t}{m_{11} m_{22}} & -\frac{k_2 \Omega(t) n_t}{m_{11} m_{22} m_{22}} f_{\dot{\psi}} \\ 0 & 0 & \frac{k_2 \Omega(t) n_t}{m_{22} m_{11}} \\ \frac{n_t}{m_{22}} & \frac{f_{\dot{\psi}} n_t}{m_{22} m_{22}} & -\frac{I_2^w \Omega^2(t) k_2 n_t}{m_{11} m_{22} m_{22}} + \frac{n_t}{m_{22}^3} f_{\dot{\psi}}^2 \end{bmatrix} \tag{88}$$

The rank of this matrix is easily checked to be three if $\Omega \neq 0$, which is the order of the system (n=3), thus satisfying the controllability condition as long as the wheel speed is nonzero. Notice that for this Linear Time Varying system, this is exactly the linear system ($\dot{x}$=Ax+Bu) controllability test, i.e. evaluation of the rank of the matrix [B ¦ AB ¦ A^2B].

Involutivity

In order for the system to be *integrable*, i.e. a transformation into a set of coordinates yielding a linear system exists, it must be involutive. This is tested for by evaluating

$$\text{rank}([g \mid \text{ad}_f g]) = \text{rank}([g \mid \text{ad}_f g \mid [g, \text{ad}_f g]])$$

where $[g, \text{ad}_f g]$ is the Lie bracket evaluated as

$$[g, \text{ad}_f g] = \frac{\partial \, \text{ad}_f g}{\partial \mathbf{x}} g - \frac{\partial g}{\partial \mathbf{x}} \text{ad}_f g$$

$$= \begin{bmatrix} 0 \\ 0 \\ 0 \end{bmatrix} \tag{89}$$

Clearly, this Lie bracket cannot affect the rank of the matrix $[g \mid \text{ad}_f g \mid [g, \text{ad}_f g]]$, hence deduce that the system is involutive and hence integrable.

Diffeomorphism

Since the system is both controllable and integrable $\forall$ $\Omega \neq 0$, then there exists a smooth, invertible diffeomorphism via which the coordinate system may be

transformed such that the system is representable in the form of equation (31).

This is determined by evaluating equations (17) and (18)

$$\mathcal{L}_g\lambda(\mathbf{x}) = \left[\frac{\partial\lambda(\mathbf{x})}{\partial\dot{\phi}} \quad \frac{\partial\lambda(\mathbf{x})}{\partial\phi} \quad \frac{\partial\lambda(\mathbf{x})}{\partial\dot{\psi}}\right]\begin{bmatrix} g_1(\mathbf{x}) \\ g_2(\mathbf{x}) \\ g_3(\mathbf{x}) \end{bmatrix}$$

$$= \frac{\partial\lambda(\mathbf{x})}{\partial\dot{\psi}}\frac{n_t}{m_{22}} = 0 \tag{90}$$

and

$$\mathcal{L}_{ad_f g}\lambda(\mathbf{x}) = \left[\frac{\partial\lambda(\mathbf{x})}{\partial\dot{\phi}} \quad \frac{\partial\lambda(\mathbf{x})}{\partial\phi} \quad \frac{\partial\lambda(\mathbf{x})}{\partial\dot{\psi}}\right]\begin{bmatrix} \frac{-k_2\Omega(t)n_t}{m_{11}m_{22}} \\ 0 \\ \frac{f_{\dot{\psi}}n_t}{m_{22}m_{22}} \end{bmatrix}$$

$$= \frac{\partial\lambda(\mathbf{x})}{\partial\dot{\phi}}\frac{-k_2\Omega(t)n_t}{m_{11}m_{22}} + \frac{\partial\lambda(\mathbf{x})}{\partial\dot{\psi}}\frac{f_{\dot{\psi}}n_t}{m_{22}m_{22}}$$

$$= 0 \tag{91}$$

These conditions are more simply expressed as

$$\frac{\partial\lambda(\mathbf{x})}{\partial\dot{\phi}} = \frac{\partial\lambda(\mathbf{x})}{\partial\dot{\psi}} = 0 \tag{92}$$

which is satisfied by setting $\lambda=\phi$. The transformation is then determined as follows.

$$\mathcal{L}_f\lambda(\mathbf{x}) = \left[\frac{\partial\lambda(\mathbf{x})}{\partial\dot{\phi}} \quad \frac{\partial\lambda(\mathbf{x})}{\partial\phi} \quad \frac{\partial\lambda(\mathbf{x})}{\partial\dot{\psi}}\right]\begin{bmatrix} f_1(\mathbf{x}) \\ f_2(\mathbf{x}) \\ f_3(\mathbf{x}) \end{bmatrix}$$

$$= \dot{\phi} \tag{93}$$

and

$$\mathcal{L}_f\mathcal{L}_f\lambda(\mathbf{x}) = \left[\frac{\partial\mathcal{L}_f\lambda(\mathbf{x})}{\partial\dot{\phi}} \quad \frac{\partial\mathcal{L}_f\lambda(\mathbf{x})}{\partial\phi} \quad \frac{\partial\mathcal{L}_f\lambda(\mathbf{x})}{\partial\dot{\psi}}\right]\begin{bmatrix} f_1(\mathbf{x}) \\ f_2(\mathbf{x}) \\ f_3(\mathbf{x}) \end{bmatrix}$$

$$= \frac{k_1 g}{m_{11}}\phi + \frac{k_2\Omega(t)}{m_{11}}\dot{\psi} \tag{94}$$

finally, get the diffeomorphism, which is smooth and invertible as long as $\Omega\neq 0$,

$$\dot{\mathbf{z}} = \begin{bmatrix} 0 & 1 & 0 \\ 1 & 0 & 0 \\ 0 & \frac{k_1 g}{m_{11}} & \frac{k_2\Omega}{m_{11}} \end{bmatrix}\mathbf{z} \qquad \forall\,\Omega\neq 0 \tag{95}$$

Note that the diffeomorphism maps the roll angle and roll rate states directly to equivalent $\mathbf{z}$–space states, z_1 and z_2 respectively, with the implication that time response of these states are exactly those of the system states ϕ and $\dot{\phi}$. In addition, the third row of the diffeomorphism is exactly the roll equation of motion, $z_3=\ddot{\phi}=\cdots$.

The feedback LTI'ing control law may now be determined as given by equation (48). (Note that the third row, T_3, is the only diffeomorphism term which includes the parameter Ω)

$$u = \alpha(\mathbf{x},\mathbf{P}) - \beta(\mathbf{x},\mathbf{P})\left\{\mathbf{K}_z\dot{\mathbf{z}} + \frac{\partial T_3}{\partial\Omega}\dot{\Omega}\right\}$$

with

$$\alpha(\mathbf{x},\mathbf{P}) = \frac{-\mathcal{L}_f^3 \lambda(\mathbf{x},\mathbf{P})}{\mathcal{L}_g \mathcal{L}_f^2 \lambda(\mathbf{x},\mathbf{P})} \quad \text{and} \quad \beta(\mathbf{x},\mathbf{P}) = \frac{1}{\mathcal{L}_g \mathcal{L}_f^2 \lambda(\mathbf{x},\mathbf{P})}$$

The necessary terms are evaluated as

$$\mathcal{L}_g \mathcal{L}_f^2 \lambda(\mathbf{x},\mathbf{P}) = \frac{k_2 \Omega \; n_t}{m_{11} m_{22}} \tag{96}$$

$$\mathcal{L}_f^3 \lambda(\mathbf{x},\mathbf{P}) = \frac{k_1 g}{m_{11}} \dot{\phi} - \frac{k_2 \Omega}{m_{11} m_{22}} (I_2 \Omega \dot{\phi} + f_{\dot{\psi}} \dot{\psi}) \tag{97}$$

$$\frac{\partial T_3}{\partial \Omega} = \frac{k_2}{m_{11}} \tag{98}$$

then, the *correct* feedback LTI'ing control law may be written as

$$u = \frac{m_{22}}{n_t} \{ (\frac{-k_1 g}{k_2 \Omega} + \frac{I_2 \Omega}{m_{22}}) \dot{\phi} + \frac{f_{\dot{\psi}}}{m_{22}} \dot{\psi} - \frac{\dot{\Omega}}{\Omega} \dot{\psi} + \frac{m_{11}}{k_2 \Omega} \nu \} \tag{99}$$

Note that the feedback linearizing control law of equation (22) ignores the extra term $\frac{m_{22} \dot{\Omega}}{n_t \Omega} \dot{\psi}$ which is necessary to obtain the feedback LTI'd system, independent of parameter value or rate of change.

LTI Control Design in Transformed Coordinates (Same Eigenvalues for all Speeds)

The diffeomorphism of equation (95) assumes full state accessibility. If this is the case, then full state feedback in transformed coordinates is the obvious control

strategy for the feedback LTI'd system. The result of the feedback LTI'd control law implemented together with the regulator design in z–space, is a system which exhibits the same *z–space* closed loop behavior regardless of the parameter value or rate of change thereof. For the diffeomorphism in this case mapping directly from z_1 and z_2 to ϕ and $\dot{\phi}$ respectively, this implies the same closed loop behavior of roll angle and roll rate for all values of wheelspeed and rate of change of wheelspeed.

For a control law of the form $\nu = -\mathbf{K}_z\mathbf{z} = -[\mathrm{K}_0\ \mathrm{K}_1\ \mathrm{K}_2]\mathbf{z}$, the closed loop z–space system is of the form (assuming regulator control)

$$\dot{\mathbf{z}}(\mathrm{t}) = \begin{bmatrix} 0 & 1 & 0 \\ 0 & 0 & 1 \\ -\mathrm{K}_0 & -\mathrm{K}_1 & -\mathrm{K}_2 \end{bmatrix} \mathbf{z}(\mathrm{t})$$

with $\mathbf{K}_z$ chosen to yield the desired closed loop eigenvalues. Clearly, it would not be prudent to arbitrarily assign the closed loop dynamics as the physical system has limitations on achievable performance. Rather, it makes sense to initially design at some nominal operating condition in *system* space (x–coordinates) such that the system meets design specifications. Since the eigenvalues are invariant under the diffeomorphism and feedback LTI'ing control law, these may then be used as desired eigenvalues for a pole–placement solution to determining the z–space gains $\mathbf{K}_z$.

Assigning numerical values to the unicycle equations of motion

$$\begin{aligned} \mathrm{k}_1 g &= 429.96 \\ \mathrm{k}_2 \Omega &= 10.944\Omega \\ -\mathrm{I}_2^{\mathrm{w}} \Omega &= -0.0893\Omega \\ -\mathrm{f}_{\dot{\psi}} &= -0.0245 \end{aligned}$$

$$m_{11} = 48.264$$

$$m_{22} = 0.1898$$

$$n_t = 25$$

then the open loop dynamics are given by

$$\dot{\mathbf{x}}(t) = \begin{bmatrix} 0 & 8.9085 & 0.22674\Omega \\ 1 & 0 & 0 \\ -0.4705\Omega & 0 & -0.12908 \end{bmatrix} \mathbf{x}(t) + \begin{bmatrix} 0 \\ 0 \\ 131.72 \end{bmatrix} \Gamma \qquad (100)$$

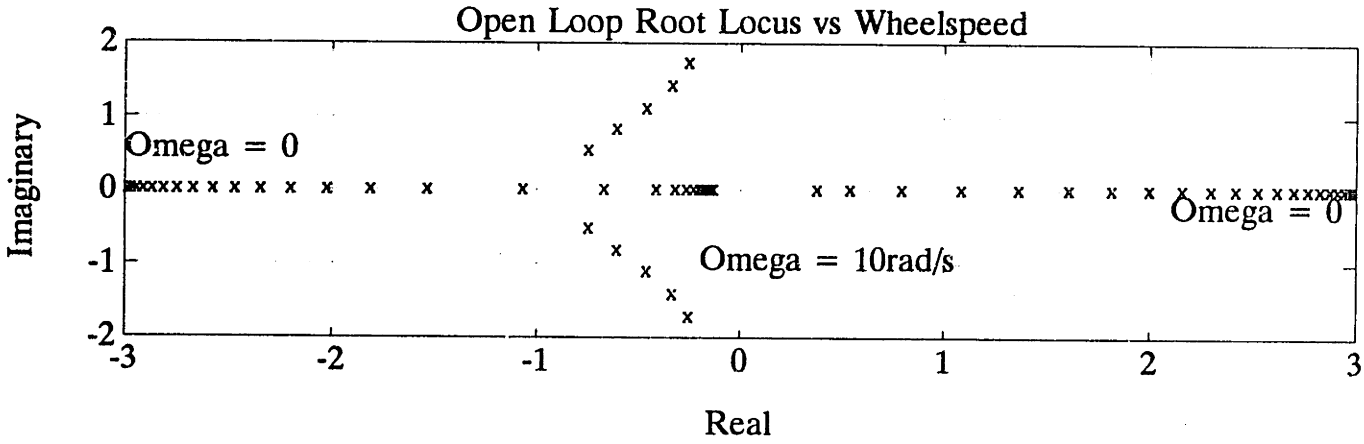

Figure 4.7. Root locus of the plant open loop dynamics as a function of wheelspeed over the range $\Omega(t)\epsilon(0,10]$. The LTI'ing control is to achieve LTI performance over this range of speeds for arbitrary changes in wheelspeed.

The correct LTI'ing control law of equation (99) including the regulating control law $\nu = -\mathbf{K}_z\mathbf{z}$, may be written in system coordinates as

$$u = \frac{m_{22}}{n_t}\{ (\frac{-k_1 g}{k_2 \Omega} + \frac{I_2^w \Omega}{m_{22}})\dot{\phi} + \frac{f_{\dot{\psi}}}{m_{22}} \dot{\psi} - \frac{\dot{\Omega}}{\Omega} \dot{\psi} - \frac{m_{11}}{k_2 \Omega} [K_0 \, K_1 \, K_2] z \}$$

$$= \frac{m_{22}}{n_t} (\frac{-k_1 g}{k_2 \Omega} + \frac{I_2^w \Omega}{m_{22}} - \frac{m_{11}}{k_2 \Omega} K_1) \dot{\phi} + \frac{m_{22} m_{11}}{n_t \, k_2 \Omega} (-K_0 - K_2 \frac{k_1 g}{m_{11}}) \phi$$

$$+ \frac{m_{22}}{n_t} (\frac{f_{\dot{\psi}}}{m_{22}} - K_2 - \frac{\dot{\Omega}}{\Omega}) \dot{\psi}$$

$$= -[G_{\dot{\phi}} \mid G_{\phi} \mid G_{\dot{\psi}}] \, x(t) \qquad (101)$$

where the *correct* regulator gains in system coordinates are determined as

$$G_{\dot{\phi}}(\Omega) = -\frac{m_{22}}{n_t} (\frac{-k_1 g}{k_2 \Omega} + \frac{I_2^w \Omega}{m_{22}} - \frac{m_{11}}{k_2 \Omega} K_1) \qquad (102a)$$

$$G_{\phi}(\Omega) = -\frac{m_{22} m_{11}}{n_t \, k_2 \Omega} (-K_0 - K_2 \frac{k_1 g}{m_{11}}) \qquad (102b)$$

$$G_{\dot{\psi}}(\Omega, \dot{\Omega}) = -\frac{m_{22}}{n_t} (\frac{f_{\dot{\psi}}}{m_{22}} - K_2 - \frac{\dot{\Omega}}{\Omega}) \qquad (102c)$$

Notice that the effect of the feedback LTI'zation is to add the term $\frac{m_{22}\dot{\Omega}}{n_t \Omega}$ to the yaw rate control gain which the feedback linearizing control law yields.

Gain Scheduling: Slowly Varying *Closed Loop* Dynamics & Arbitrary Parameter Changes

The previous section dealt with design of a time varying gain scheduled control law which yields LTI behavior of the closed loop system in transformed coordinates (**z**–space). Using the results of equation (62), it is possible to allow the closed loop

dynamics to vary with parameter value, whilst still maintaining stability of the closed loop system. In the case of the unicycle, it is not reasonable to expect similar closed loop bandwidth at low speed and at high speed, since this places physically unachievable requirements on the actuators. The closed loop dynamics are thus scheduled to be lower bandwidth for small Ω and vice versa. Figure 4.8 shows the root locus vs Ω of the closed loop dynamics for the gain scheduled design. This is simply an LQR design with the control penalty (arbitrarily) decreased linearly with increasing wheelspeed. The resulting controller gains are plotted vs Ω in the same figure.

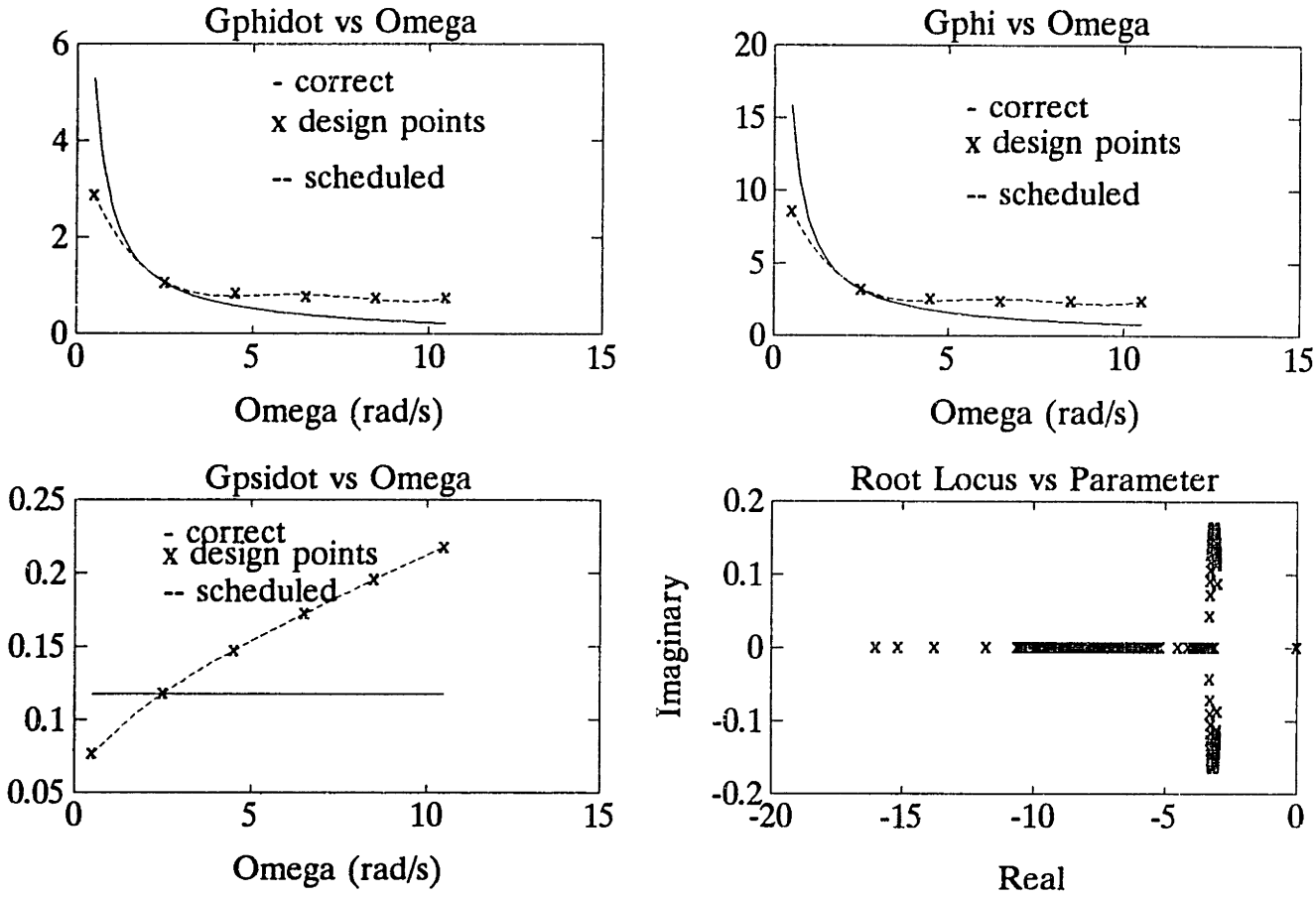

Figure 4.8a. System space gains achieving slowly varying closed loop dynamics for the gain scheduled system designed in system space. Lower bandwidth at small Ω reduces load on the actuators. The eigenvalues of the design done in system space at Ω=2.5rad/s are the reference values used for the pole placement design in z–space which when transformed back to system space, yields the "correct" gains (solid lines) shown. The dashed line shows the scheduled gains which are curve fits through the design points (×). Also shown is the root locus of closed loop eigenvalues of the gain scheduled design, vs Ω.

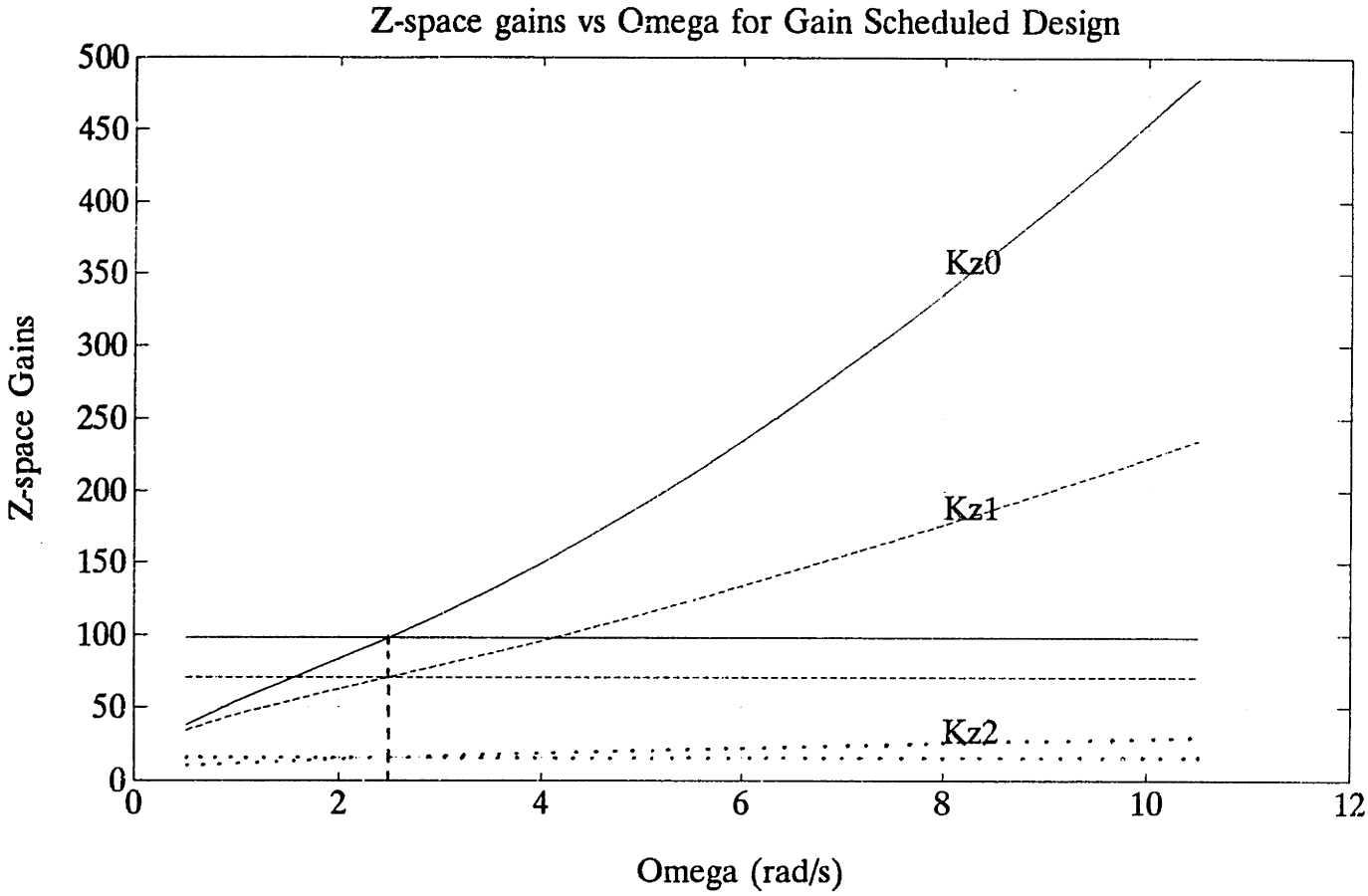

Figure 4.8b. The **z**–space gains for the gain scheduled designs of figure 4.8a (designs done in system space) vary with Ω in order to yield slowly varying closed loop dynamics as a function of the parameter Ω. The *correct* control law is for constant eigenvalues at all values of Ω, designed in this example to be the same as the eigenvalues of the gain scheduled design at Ω=2.5rad/s. The variation of the **z**–space gains must satisfy the Lipschitz condition (62) in order to guarantee stability for this system.

The criterion for stability with slowly changing closed loop dynamics (equation 23) is repeated here, for the (not strictly correct) least conservative case of $\tau_l=\tau_{max}$,

$$K_l \leq \frac{\epsilon}{\|\Delta \hat{P}_{max}\|[1-e^{-\tau_{max}/\tau_p}]}$$

with $\Delta\hat{\mathbf{P}}_{max}$ the maximum expected parameter change away from the present value, and τ_p and τ_{max} the slowest parameter variation and closed loop system time constants respectively. The smallest allowable gain change (represented by ϵ) for instability is easily determined for this example by the Circle Criterion.

The characteristic equation for the example is given by

$$s^3 + K_2 s^2 + K_1 s + K_0 = 0 \tag{103}$$

for the system evaluated at the slowest wheelspeed (Ω=0.5 rad/s) where the closed loop dynamics are the slowest (hence the gains K_{z_i} are the smallest) with eigenvalues

$$\lambda_1 = -3.01+j0.088 \qquad \lambda_2 = -3.01-j0.088 \qquad \lambda_3 = -4.125 \tag{104}$$

the z–coordinates gains are (solved by pole–placement)

$$\mathbf{K}_z = [K_0 \;\; K_1 \;\; K_2] = [37.4233 \;\; 33.9111 \;\; 10.1465] \tag{105}$$

Applying the Circle Criterion to the system (A_{cl} is Hurwitz, and [A_{cl},C] observable, [A_{cl},B] controllable)

$$\dot{\mathbf{z}}(t) = \begin{bmatrix} 0 & 1 & 0 \\ 0 & 0 & 1 \\ -K_0 & -K_1 & -K_2 \end{bmatrix} \mathbf{z}(t) + \begin{bmatrix} 0 \\ 0 \\ 1 \end{bmatrix} e(t) = A_{cl}\mathbf{z}(t) + Be(t) \tag{106}$$

$$e(t) = -\delta K_0 \, y(t) \tag{107}$$

$$y(t) = [1 \;\; \frac{K_1}{K_0} \;\; \frac{K_2}{K_0}]\mathbf{z}(t) = C\,\mathbf{z}(t) \tag{108}$$

where

$$\delta K_1 = \frac{K_1}{K_0}\delta K_0 \qquad \text{and} \qquad \delta K_2 = \frac{K_2}{K_0}\delta K_0 \tag{109}$$

For the time varying nonlinearity $\phi=\delta K_0(t)$ assumed in the sector $[-\rho,\rho]$, the disk $D(a,\beta)$ is then of radius $1/\rho$. From the Nyquist plot (figure 4.9) of the system of equations (106,108) above, $g(j\omega)=C[sI-A_{cl}]^{-1}B$ always lies inside the circle (centered at the origin) of radius $\frac{1}{\rho} \geq 0.034232$, thus the bound on the nonlinearity is

$$|\delta K_0| \leq 29.2 \tag{110}$$

and, hence, the other acceptable gain variations are

$$|\delta K_1| = \frac{K_1}{K_0}\delta K_0 = 26.5 \qquad \text{and} \qquad |\delta K_2| = \frac{K_2}{K_0}\delta K_0 = 7.9 \tag{111}$$

and for ϵ the smallest allowable single gain change for stability,

$$\epsilon = 7.9 \tag{112}$$

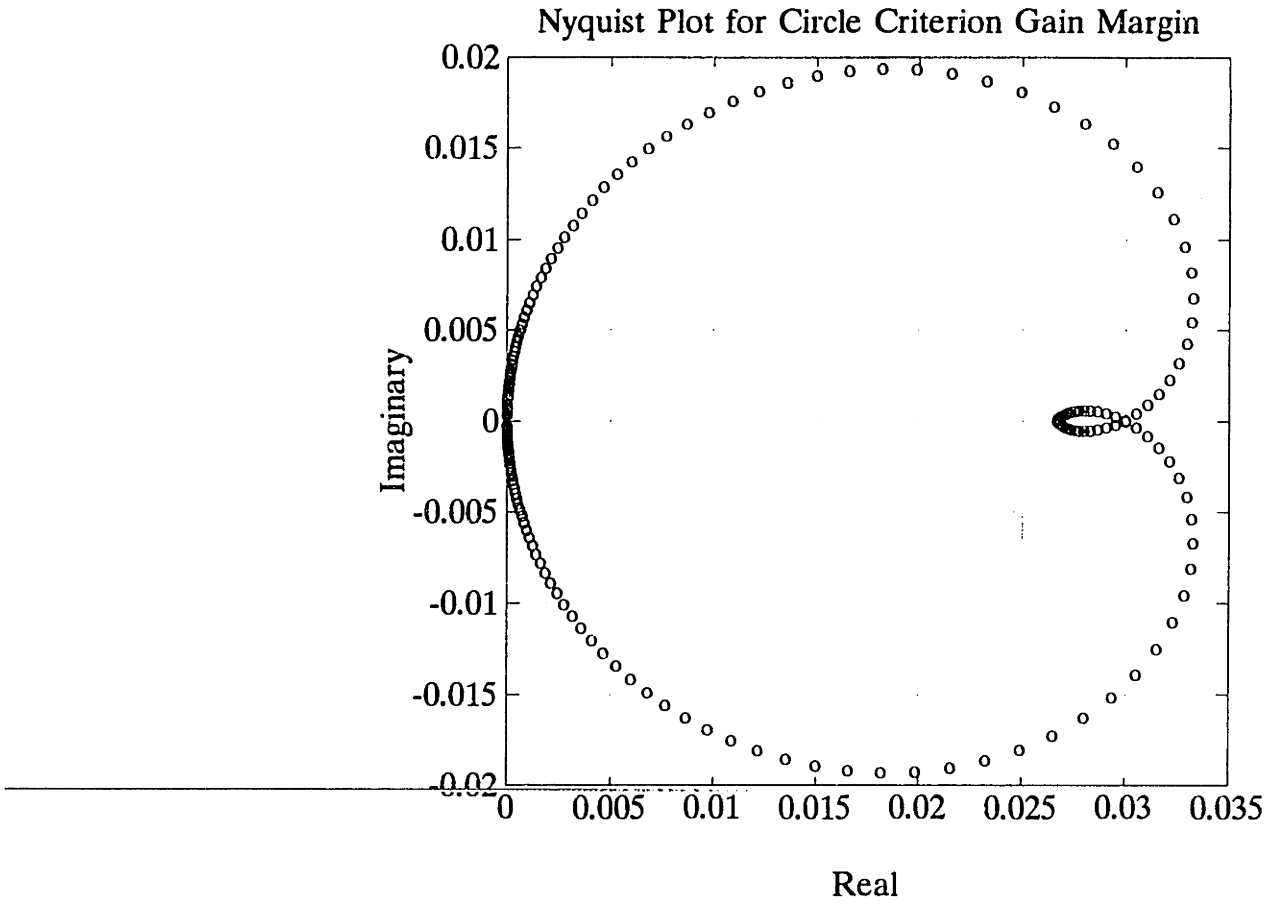

Figure 4.9. Nyquist plot of system of (LTI) equations (106,108) for determining gain margins by means of Circle Criterion for arbitrary time variation of each gain within the determined bounds whilst maintaining stability. With this known, the Lipschitz constant of equation (62) may be determined to evaluate the allowable (while guaranteed stable) variation in *closed loop dynamics* of the gain scheduled system.

The Lipschitz constant K_l may be determined (conservatively) for all gains simultaneously using the expression of equation (62). For the closed loop system, $\tau_{max}=1/3$ second, $\tau_p=2$ seconds and $\Delta\hat{P}_{max}=5$ rad/s (these values are accurate representations of the actual unicycle capabilities), then

$$K_l \leq \frac{\epsilon}{\|\Delta\hat{P}_{max}\|[1-e^{-\tau_{max}/\tau_p}]}$$

$$= \frac{7.9}{5(1-\exp(-1/6))}$$

$$= 10.3 \qquad (113)$$

Evaluation of figure 4.8 showing the z–space gains vs parameter (Ω), indicates that the gain gradients do not satisfy this condition everywhere.

A less conservative estimate for the Lipschitz constant is determined by evaluating each gain individually over the parameter range as mentioned in remark 4) of equation (62). In this case, the individual Lipschitz constants are evaluated as

$$K_{l_0} \leq \frac{\delta K_{z0}}{\|\Delta\hat{P}_{max}\|[1-e^{-\tau_{max}/\tau_p}]} = \frac{29.2}{5(1-\exp(-1/6))} = 38.0 \qquad (114a)$$

$$K_{l_1} \leq \frac{\delta K_{z1}}{\|\Delta\hat{P}_{max}\|[1-e^{-\tau_{max}/\tau_p}]} = \frac{26.5}{5(1-\exp(-1/6))} = 34.5 \qquad (114b)$$

$$K_{l_2} \leq \frac{\delta K_{z2}}{\|\Delta\hat{P}_{max}\|[1-e^{-\tau_{max}/\tau_p}]} = \frac{7.9}{5(1-\exp(-1/6))} = 10.3 \qquad (114c)$$

Comparing these Lipschitz constants with the local gradient (i.e. at Ω=0.5) of z–space gain with respect to wheelspeed of figure 4.10 indicates that the condition is satisfied not only at Ω=0.5, but up to wheelspeeds of Ω=2.0rad/s. Re–evaluating the Lipschitz constants at each design point, noting that for higher bandwidths the Nyquist plot fits inside a ball of smaller radius, shows that the design easily meats the local Lipschitz conditions everywhere in the operating range $\Omega\epsilon$[0.5,5.0]. Note that for the

evaluation at Ω=0.5rad/s, the nonlinearity satisfies $\delta K_0(t) \in [0,\beta]$, such that condition (2) of the circle criterion may be used to conclude stability for any increase in $\delta K_0(t)$.

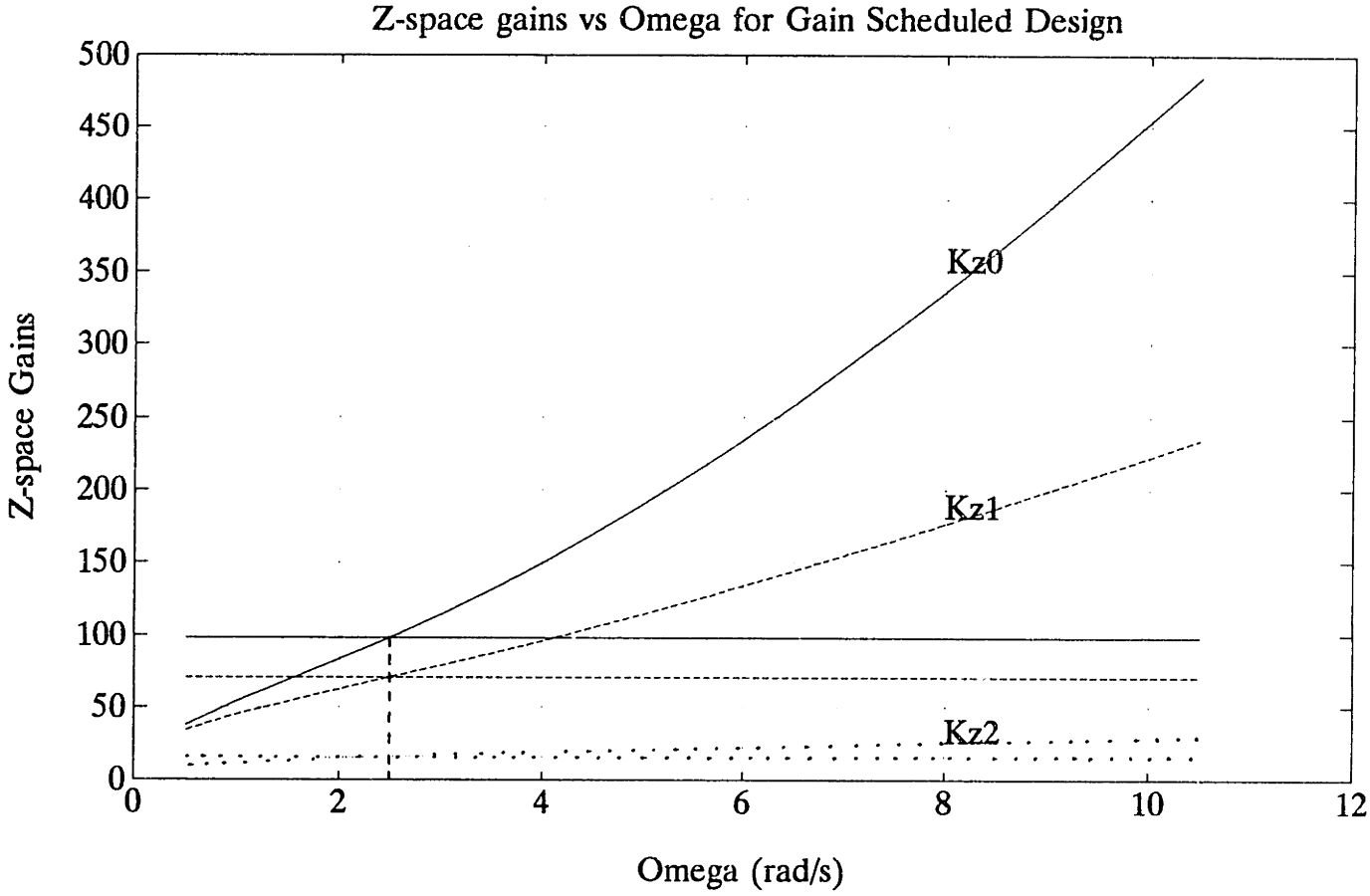

Figure 4.10. Z–space gains of gain scheduled design vs unicycle wheelspeed. Note that the Lipschitz constants determined above (equation (89)) are satisfied for $\Omega \in [0.5,2.0]$. Further evaluation at each design point (at 0.5rad/s intervals) shows that the local Lipschitz condition is met across the full range $\Omega \in [0.5,5.0]$. Since this evaluation is done assuming $\tau_1 = \tau_{max}$ in the Lipschitz constant, strictly speaking stability is not guaranteed, but practically, the system will be stable, as shown in simulation.

Ignoring the Parameter Rate Dependent Term

The control laws of equation (48) for the Feedback LTI'd case, where closed loop

eigenvalues are constant regardless of parameter value, and equation (53) where the closed loop eigenvalues vary slowly with parameter value, include the parameter rate of change term to ensure stability regardless of rate of change of the parameter. In this section the Circle Criterion is used to determine when the $\dot{P}$ terms in the feedback LTI'ing control law may be dropped.

Autonomous Control Law Excluding $\dot{P}$ term

In this case, the control law is that of equation (48) with $\mathbf{K}_z$ constant. The closed loop system with the control law *ignoring* the parameter rate of change term which is simply the feedback linearizing law (as opposed to the feedback LTI'ing control law) yields the extra $\dot{P}$ terms which are thus not canceled. For

$$u = \frac{m_{22}}{n_t}\{ (\frac{-k_1 g}{k_2 \Omega} + \frac{I_2^{yy}\Omega}{m_{22}})\dot{\phi} + \frac{f_{\dot{\psi}}}{m_{22}}\dot{\psi} + \frac{m_{11}}{k_2\Omega}\nu \} \tag{115}$$

with

$$\nu = -\mathbf{K}_z \mathbf{z}(t)$$

The resulting closed loop dynamics in transformed coordinates ($\mathbf{z}$–space) are then represented by the characteristic equation with the $\frac{\dot{\Omega}}{\Omega}$ terms *not* canceled by the control law, thus

$$s^3 + (K_2 - \frac{\dot{\Omega}}{\Omega})s^2 + K_1 s + (K_0 + \frac{k_1 g}{m_{11}}\frac{\dot{\Omega}}{\Omega}) = 0 \tag{116}$$

rewrite the system as

$$\dot{z}(t) = \begin{bmatrix} 0 & 1 & 0 \\ 0 & 0 & 1 \\ -K_0 & -K_1 & -K_2 \end{bmatrix} z(t) + \begin{bmatrix} 0 \\ 0 \\ 1 \end{bmatrix} e_1(t) = A_{cl_1} z(t) + B_1 e(t) \qquad (117)$$

$$e_1(t) = -\frac{\dot{\Omega}}{\Omega} y(t) \qquad (118)$$

$$y(t) = [\frac{k_1 g}{m_{11}} \; 0 \; -1] z(t) = C_1 z(t) \qquad (119)$$

Noting that the observability and controllability conditions are met with this output function, the Circle Criterion yields (refer to the Nyquist plot of figure 4.11 for the gains evaluated at Ω=0.5rad/s, K_z=[37.4233 33.9111 10.1465], the disk D(−5.6657,3.8536) of radius $1/\rho$=0.218 which entirely encircles the transfer function plot, thus

$$-5.6657 \leq \frac{\dot{\Omega}}{\Omega} \leq 3.8536 \qquad (120)$$

For the unicycle, the parameter change occurs mostly in a first order sense in normal transition from one steady speed to another and otherwise arises in a sinusoidal form for the station keeping case.

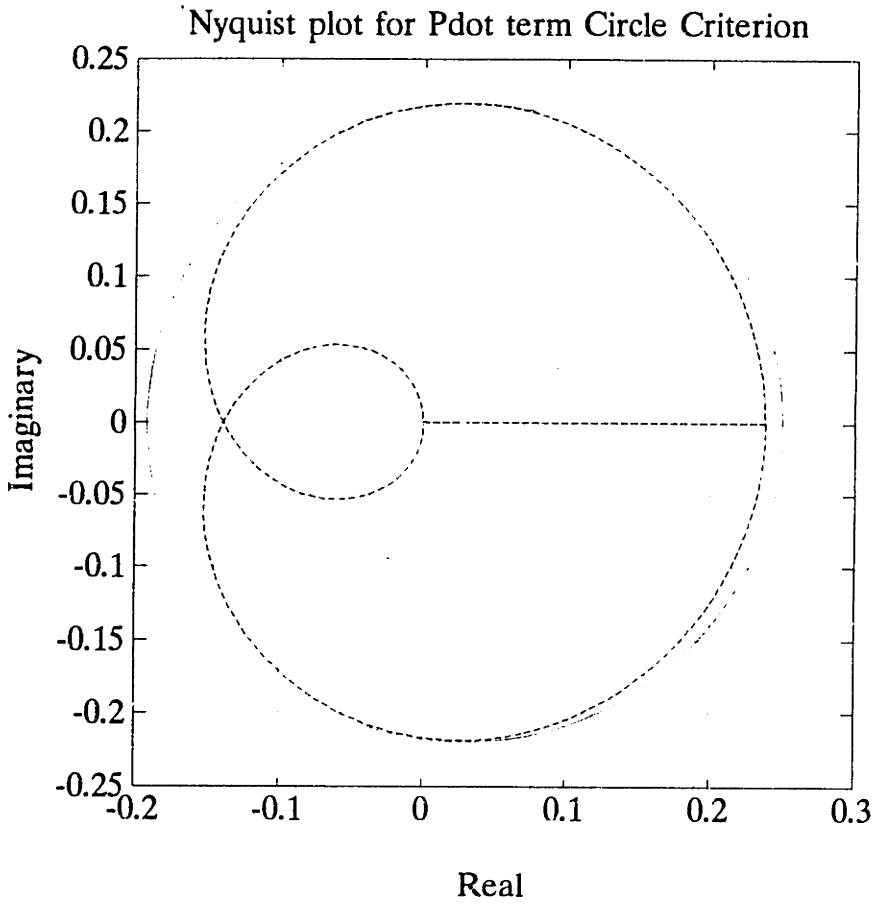

Figure 4.11. Nyquist plot for determining the bounds of equation (120). The loop transfer function plot falls inside the disk D(−5.6657,3.8536) of radius $1/\rho$=0.218 for all frequencies, thus satisfying the stability criterion if the nonlinearity is bounded according to (120).

First Order Wheelspeed Changes

In this case, the parameter (Ω) changes approximately according to the first order response

$$\Omega(t) = \Omega_{ref}(1-e^{-t/\tau_p}) + \Omega_0 \qquad (121)$$

with the derivative

$$\dot{\Omega}(t) = \frac{\Omega_{ref}}{\tau_p} e^{-t/\tau_p} \tag{122}$$

then, the term of interest is

$$\frac{\dot{\Omega}}{\Omega} = \frac{e^{-t/\tau_p}}{\tau_p[1-\exp(-t/\tau_p)+\Omega_0/\Omega_{ref}]} \tag{123}$$

Physically, the unicycle never operates at a steady speed of less than Ω_{min}=0.5rad/s, and the top speed is Ω_{max}=5.0rad/s, such that the maximum effective value of $\frac{\dot{\Omega}}{\Omega}$ may be determined to be (evaluate at t=0, where $\frac{\dot{\Omega}}{\Omega}$ is maximum)

$$\left\{\frac{\dot{\Omega}}{\Omega}\right\}_{max} = \frac{e^0}{2[1-\exp(0)+0.5/5.0]}$$

$$= 5.0 > 3.8536 \text{ (from equation (120))} \tag{124}$$

The Circle Criterion is thus violated for this specific change of parameter, but the Circle Criterion is extremely conservative in the sense that it allows arbitrary time histories for the nonlinearity $\frac{\dot{\Omega}}{\Omega}$ and is extremely sensitive to the initial parameter value Ω_0. If, e.g. Ω_0=1, then $\left\{\frac{\dot{\Omega}}{\Omega}\right\}_{max}$ = 2.5, well within the allowable sector bounds. Another simple solution is to design the closed loop system to be of higher bandwidth. For example, setting the nominal feedback gains to K_z=[68.8 53.8 13.3] yields closed loop eigenvalues

$$\lambda_1 = -7.07 \quad \lambda_2 = -3.11+j0.16 \quad \lambda_3 = -3.11-j0.16 \tag{125}$$

The Nyquist plot of figure 4.12 shows the disk D(–8,7.576), which intersects the real axis at $1/a$=–0.125 and $1/\beta$=0.132, completely contains the plot. The stability range for $\frac{\dot{\Pi}}{\Pi}$ is thus

$$-8 < \frac{\dot{\Pi}}{\Pi} < 7.576 \tag{126}$$

So it may be concluded that this system can safely be operated without inclusion of the parameter rate dependent term for this type of parameter change.

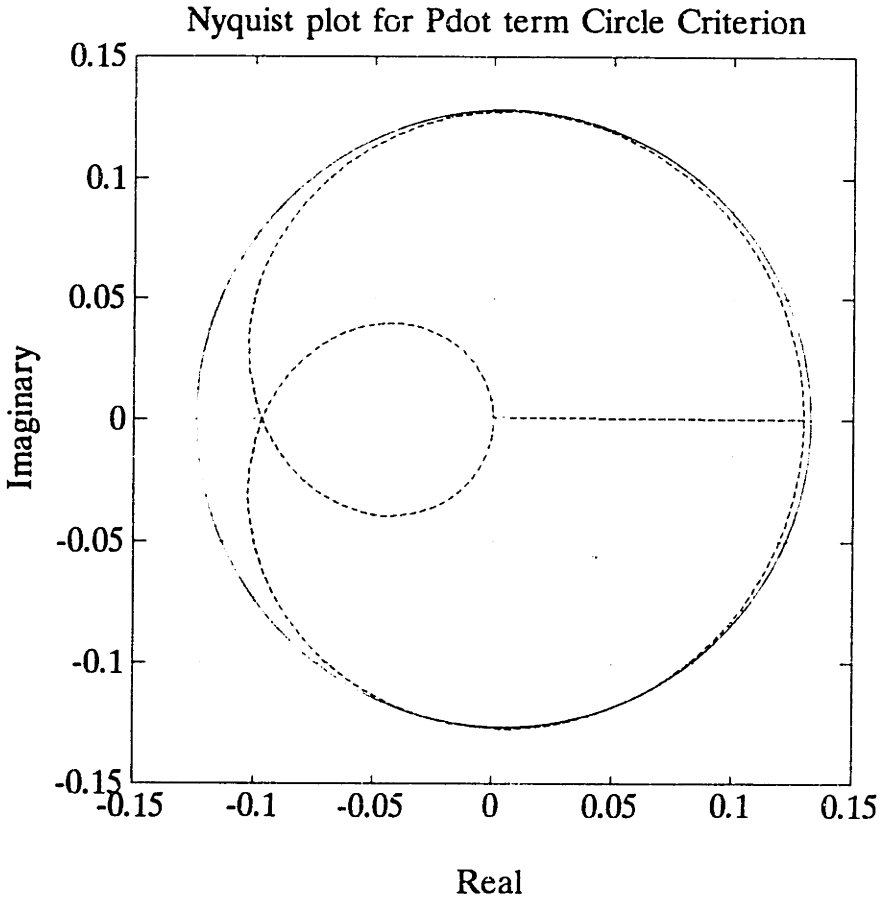

Figure 4.12. Nyquist plot for similar evaluation as in figure 4.11, but for higher bandwidth closed loop system. In this case, the loop transfer function easily fits inside the disk D(–8,7.576) which intersects the real axis at $1/a$=–0.125 and $1/\beta$=0.132,

allowing greater range of variation of the nonlinearity whilst maintaining stability.

It is possible to view this situation a little more generically, by considering three cases: 1) closed loop time constants approximately one tenth of parameter change time constant, i.e. $\tau_{max} \approx \tau_p/10$, or 2) $\tau_{max} \approx \tau_p$, or 3)$\tau_{max} \approx 10\tau_p$. Then

$$\left.\frac{\dot{\Omega}}{\Omega}\right|_{\tau_{max}} = \frac{e^{-\tau_{max}/\tau_p}}{\tau_p[1-\exp(-t_{max}/\tau_p)+\Omega_0/\Omega_{ref}]}$$

$$\approx \left[\begin{array}{ll} \dfrac{0.000045}{\tau_p[0.99+\Omega_0/\Omega_{ref}]} & \text{for } \tau_{max} \approx 10\tau_p \\ \dfrac{0.368}{\tau_p[0.63+\Omega_0/\Omega_{ref}]} & \text{for } \tau_{max} \approx \tau_p \\ \dfrac{0.9}{10\tau_{max}[0.1+\Omega_0/\Omega_{ref}]} & \text{for } \tau_{max} \approx 0.1\tau_p \end{array}\right] \qquad (127)$$

In each of the above cases, the term may be ignored if the magnitude is smaller than the relevant sector bound of equation (120). For example, with closed loop time constants approximately 1/3second and Ω_0=0.5rad/s, required to satisfy the bounds of equation (120),

1) set τ_p=1/30seconds ($\tau_{max} \approx 10\tau_p$), then $\left.\frac{\dot{\Omega}}{\Omega}\right|_{\tau_{max}} \approx 1.2\times10^{-3} << 3.854.$ (128)

2) set $\tau_p=\tau_{max}$, then $\left.\frac{\dot{\Omega}}{\Omega}\right|_{\tau_{max}} \approx 1.51 < 3.854.$ (129)

3) set $\tau_p=10\tau_{max}$, then $\left.\frac{\dot{\Omega}}{\Omega}\right|_{\tau_{max}} \approx 1.35 < 3.854.$ (130)

In (127), it is clear that the situation becomes less tolerable for Ω_0 small and Ω_{ref} large, and vice versa, i.e. more tolerable for small changes of the parameter away from large Ω_0. Conservatively, the evaluations are only made at the lowest wheelspeed (i.e. Ω_0=0.5 rad/s) for expected changes up to the maximum achievable wheelspeed (Ω_{ref}=5 rad/s).

The above indicates that for this system with the control law ignoring $\dot{P}$ terms, first order changes of the parameter may occur with almost any time constant and the closed loop system will maintain stability. This has been the case in simulation studies. No case of instability due to first order parameter changes has been found in extensive simulation, where the control law ignores the parameter rate of change term, but follows either the feedback linearizing control law or the gain scheduling control law (where closed loop dynamics are not constant with parameter change). Figure 4.13 shows simulation results.

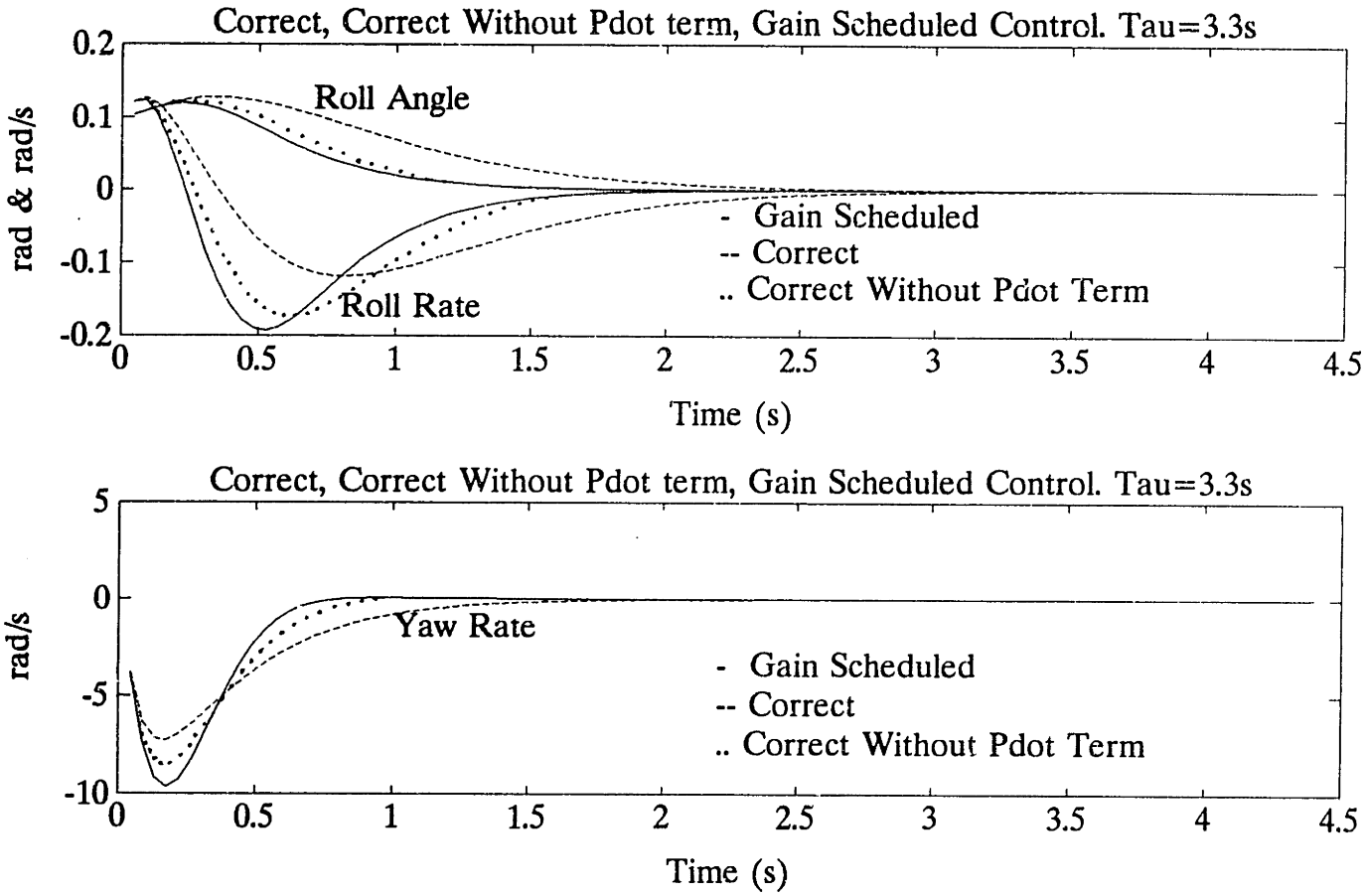

Figure 4.13a. Simulation results for first order parameter changes from Ω=0.5 to Ω=10 rad/s (physically achievable maximum speed is 5 rad/s) with various time constants. No case was found where instability occurred for this type (first order step) of parameter change.

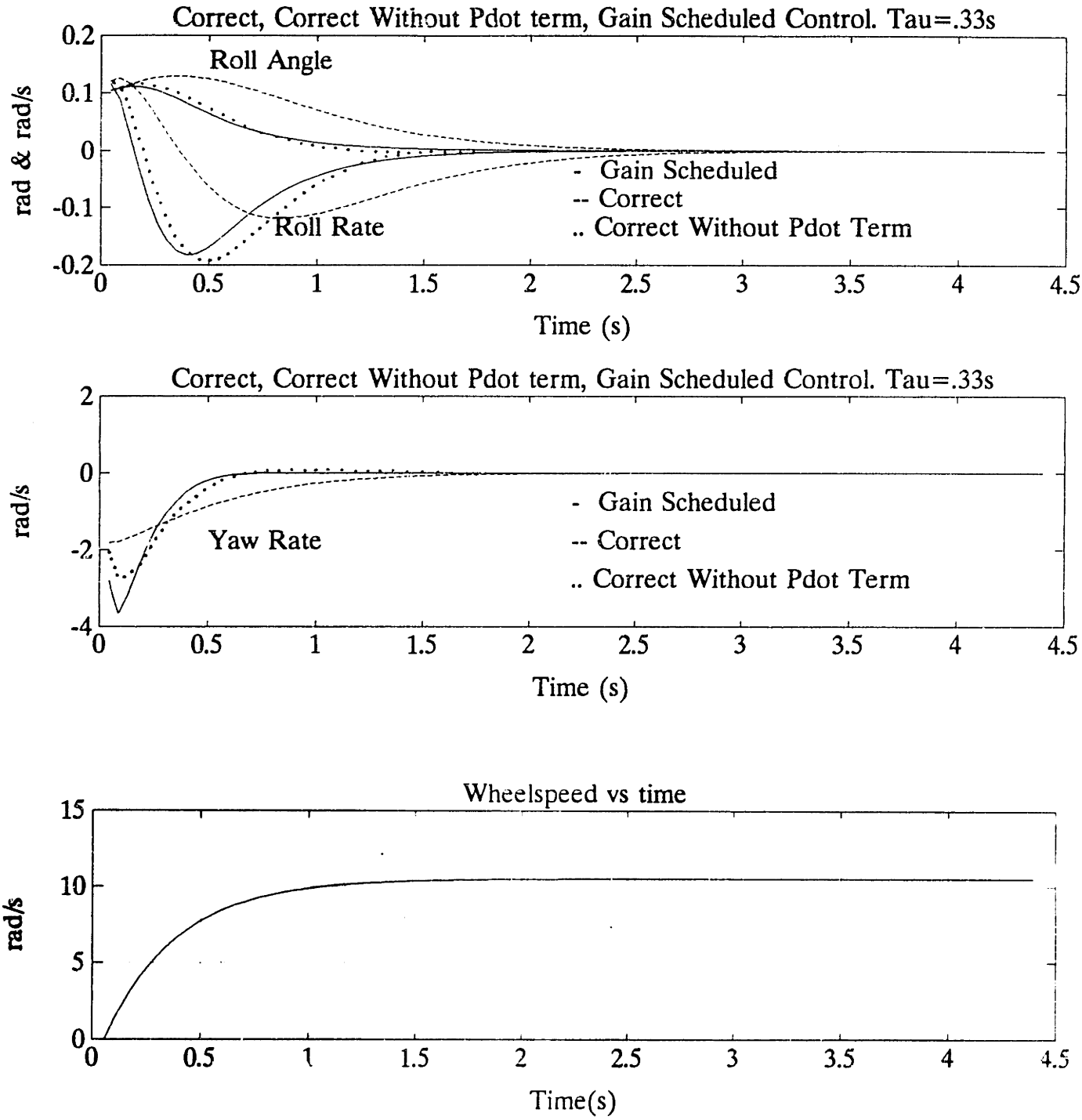

Figure 4.13b. Ω changed according to first order filter of time constant τ=0.33s which is approximately the same as the closed loop system time constants.

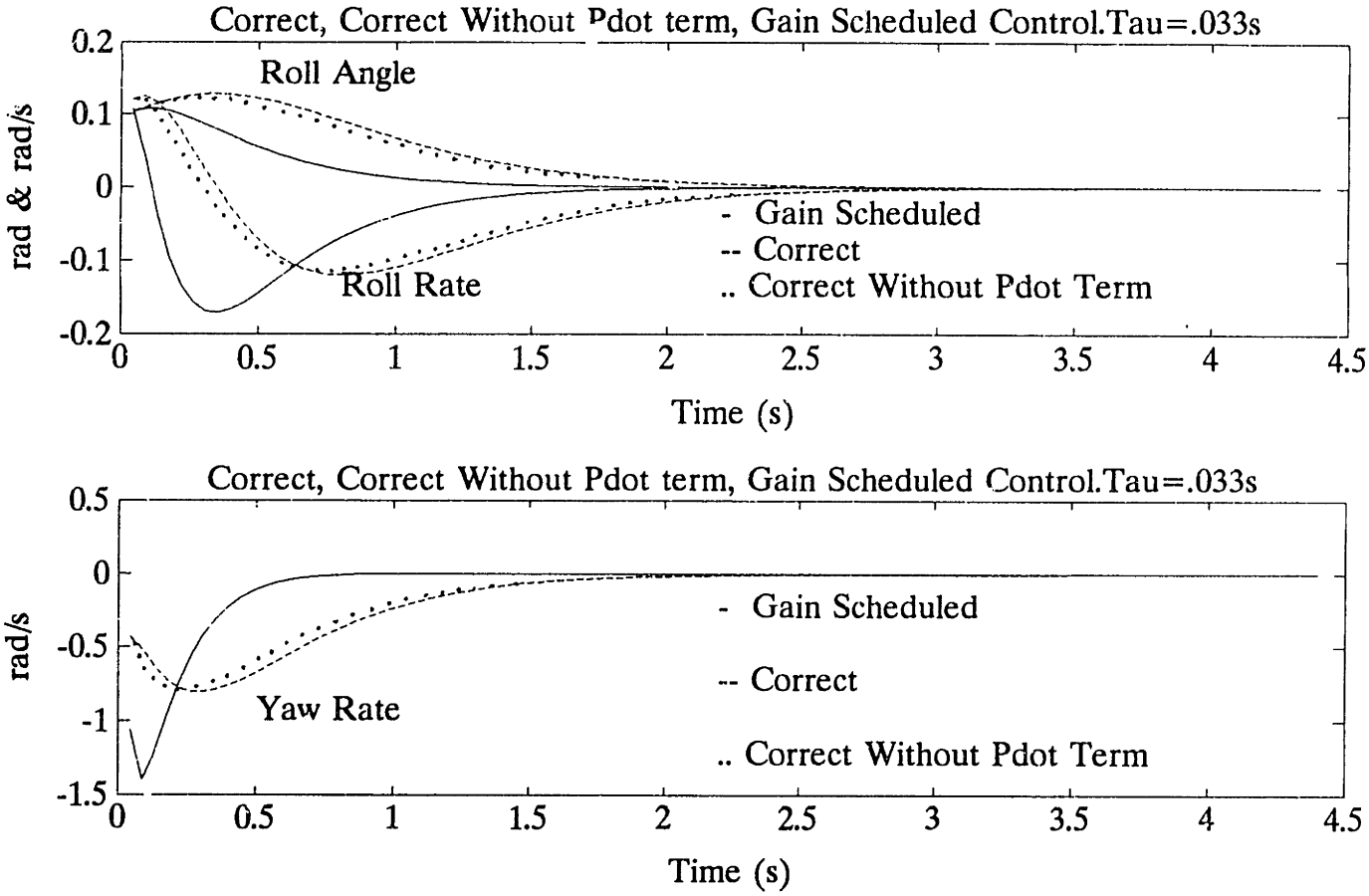

Figure 4.13c. Same as figures 4.13a and 4.13b, with tau=0.033s. In this case, the parameter change is instantaneous in the time scales of the closed loop system which has time constants of approximately 0.33s.

Sinusoidal Wheelspeed Change

For the case of sinusoidal wheelspeed changes, the frequency is of importance in determining the stability properties of the system. In this case, the nonlinear feedback element in the Circle Criterion structure is

$$\frac{\dot{\Omega}}{\Omega} = \frac{\omega\ \Delta\Omega\ \cos(\omega t)}{\Omega_0+\Delta\Omega\sin(\omega t)} \tag{131}$$

Since the nonlinearity is periodic in this case, it must lie in the sector $[-\rho,\rho]$, i.e. the disk containing the Nyquist plot is centered at the origin. The bounds of equation (120) thus become

$$\left|\frac{\dot{\Omega}}{\Omega}\right| < 3.854 \tag{132}$$

Then, for the wheelspeed varied according to $\Omega(t)=2.5+2\sin(\omega t)$, get

$$\frac{\dot{\Omega}}{\Omega} = \frac{\omega\ 2\cos(\omega t)}{2.5+2\sin(\omega t)} \qquad \leq \frac{2\ \omega}{2.5-2} \qquad \leq 3.854 \tag{133}$$

then

$$\omega \leq 0.964\text{rad/s} = 0.153\text{Hz} \tag{134}$$

Note that for $\Omega_0 >> \Delta\Omega$, the allowable frequency is much higher. These guarantees are very conservative, as demonstrated in simulation. Figure 4.14 shows the case of the unicycle with wheelspeed varied according to the function $\Omega(t)=2.1+2.0\sin(\omega t)$. For this range of parameter variation, the above analysis predicts an extremely conservative value of $\omega\leq 0.031$Hz for stability. In simulation, instability is first observed for the feedback linearized control law (<u>not</u> feedback LTI'd control law) at $\omega=0.8$Hz. Note that this frequency is close to the system roll mode closed loop natural frequency, which is $\omega=0.479$Hz.

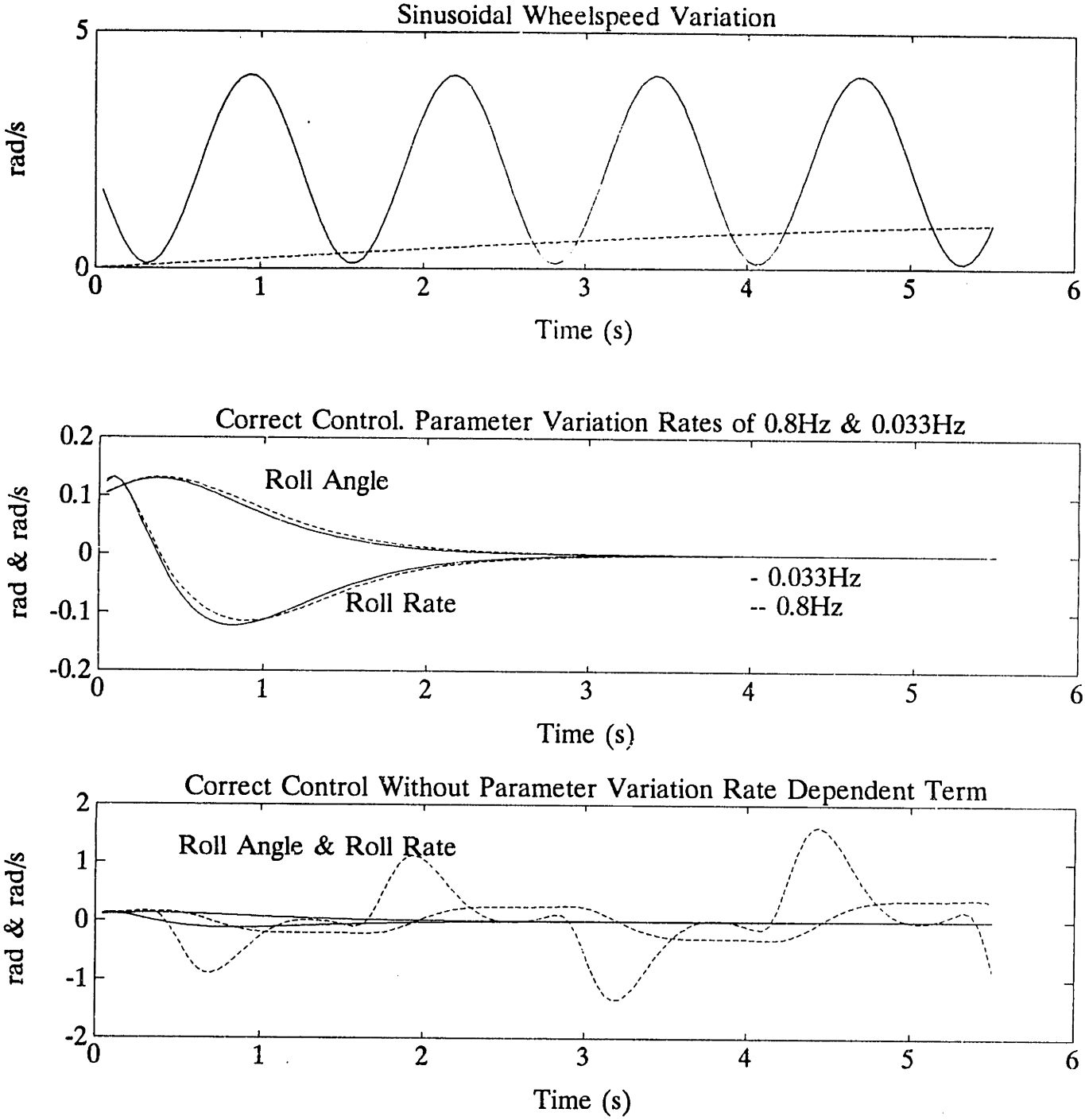

Figure 4.14a. Sinusoidal wheelspeed variation according to $\Omega(t)=2.1+2.0\sin(\omega t)$ for various frequencies. The "Correct Control" is the full *correct* control law of equation (48) including the $\dot{P}$ term. Note instability at $\omega=0.8$Hz for the feedback linearized system which ignores the $\dot{P}$ control term (even though eigenvalues are *stable, constant*

and well damped, independent of P); almost a full decade higher frequency than the conservative estimate of 0.03Hz predicted by Circle Criterion based analysis.

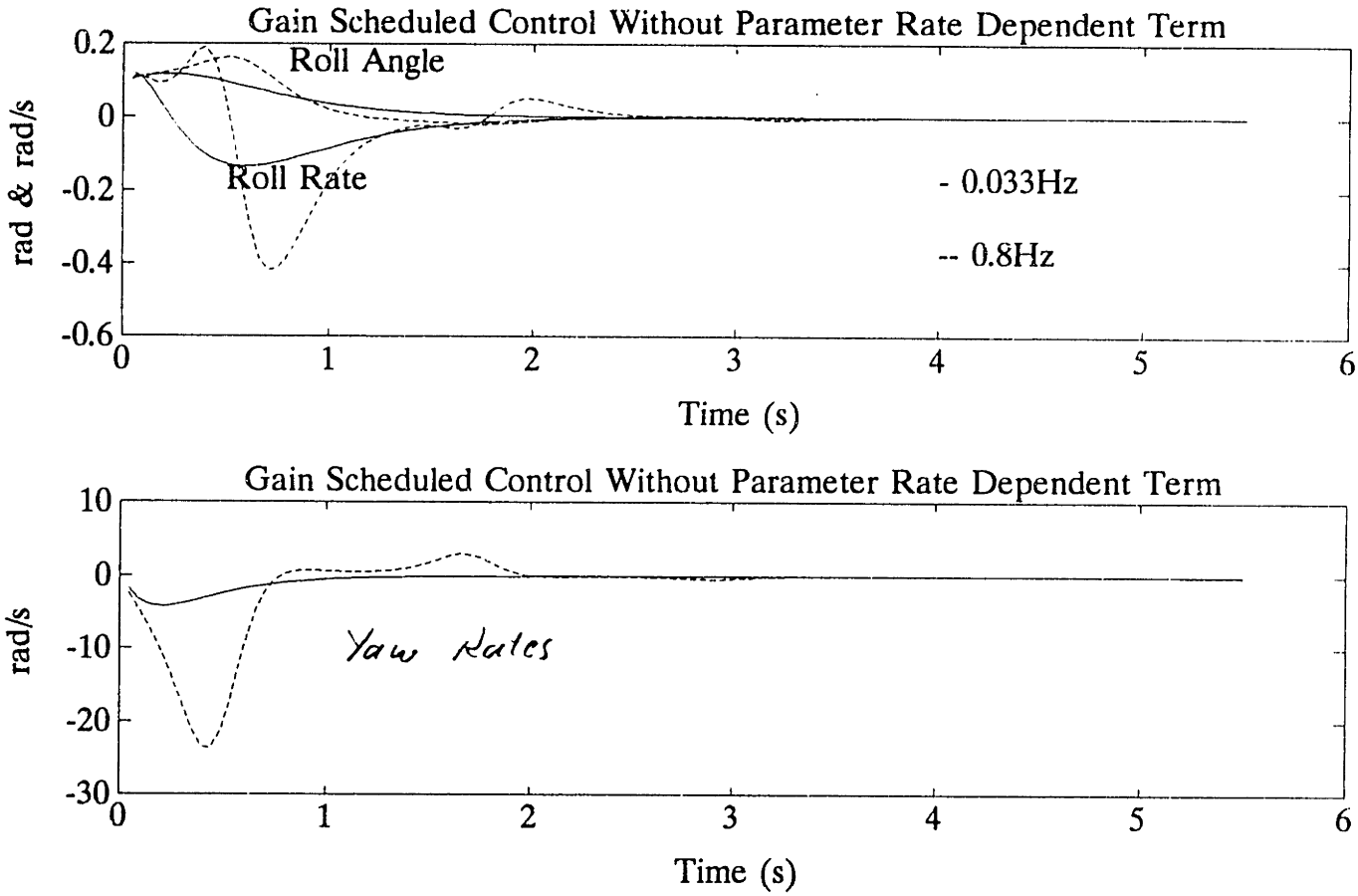

Figure 4.14b. Same as figure 4.14a, but for the gain scheduled control system with closed loop dynamics varying over the parameter range as in figure 4.8a. This control law ignores the $\dot{P}$ term, yet still manages to remain stable where the "Correct without $\dot{P}$ term" of figure 4.14a went unstable. The reason for this is probably the fact that the gain scheduled controller has much higher bandwidth at the larger values of Ω.

Output Feedback Case. Feedback LTI'd LQG Controller.

For the case of full state not accessible, the strategy as outlined previously involves defining the z–space estimator of equation (73). Assume for the unicycle example that the sensors measure only yaw rate ($\dot{\psi}$) and roll angle (ϕ). The estimator is then used to obtain optimal estimates of the full state vector $\hat{\mathbf{z}}(t)'=[\dot{\phi}(t) \;\; \phi(t) \;\; \dot{\psi}(t)]$ which are, in turn, transformed via the diffeomorphism to yield the system space estimate $\hat{\mathbf{x}}(t)=\Phi^{-1}\hat{\mathbf{z}}(t)$ for implementing the feedback LTI'ing control law.

To this end, define the output

$$y_x(t) = \begin{bmatrix} 0 & 1 & 0 \\ 0 & 0 & \Omega \end{bmatrix} \mathbf{x}(t) = C_x\mathbf{x}(t) \tag{135}$$

where the scaling of the measurement of $\dot{\psi}$ according to Ω is due to the diffeomorphism of equation (95) being dependent on Ω. The diffeomorphism and its inverse are repeated here

$$\Phi = \begin{bmatrix} 0 & 1 & 0 \\ 1 & 0 & 0 \\ 0 & \frac{k_1 g}{m_{11}} & \frac{k_2 \Omega}{m_{11}} \end{bmatrix} \qquad \Phi^{-1} = \begin{bmatrix} 0 & 1 & 0 \\ 1 & 0 & 0 \\ -\frac{k_1 g}{k_2 \Omega} & 0 & \frac{m_{11}}{k_2 \Omega} \end{bmatrix} \tag{136}$$

The equivalent measurement matrix in z–space is

$$\mathbf{y}_x(t) = \mathbf{y}_z(t) = C_x\Phi^{-1}\mathbf{z}(t) = \begin{bmatrix} 1 & 0 & 0 \\ -\frac{k_1 g}{k_2} & 0 & \frac{m_{11}}{k_2} \end{bmatrix} \mathbf{z}(t) = C_z\mathbf{z}(t) \tag{137}$$

with the z–space measurement now *independent* of the parameter Ω. This allows designing of an LTI estimator independent of, and thus valid for all, parameter and $\dot{P}$

values.

For the z–space plant, with process white noise w(t) and sensor white noise v(t)

$$\begin{aligned} \dot{\mathbf{z}} &= A_z\mathbf{z} + B_z w \\ \mathbf{y}_z &= C_z\mathbf{z} + v \end{aligned} \tag{138}$$

The noises are all assumed uncorrelated and, in typical LQG fashion, the noise covariances are chosen as design parameters to yield the desired (fast) closed loop estimator dynamics. Thus, for

$$E(ww') = 1 \qquad E(vv') = \begin{bmatrix} 1\times10^{-4} & 0 \\ 0 & 1\times10^{-3} \end{bmatrix} \tag{139}$$

solve for the Kalman filter gains

$$H_{kf} = \begin{bmatrix} 5.5953 & -0.4595 \\ 16.709 & -1.1526 \\ 48.804 & 27.601 \end{bmatrix} \tag{140}$$

which yield the estimator closed loop dynamics with $\mathbf{K}_z$ as in equation (105) for the regulator structure ($\mathbf{y}_{ref}=\mathbf{0}$) (note that the estimator is driven directly by the system space measurements $\mathbf{y}_x(t)$)

$$\dot{\hat{\mathbf{z}}} = [A_z - B_zK_z - H_{kf}C_z]\,\hat{\mathbf{z}} + H_{kf}\mathbf{y}_x \tag{141}$$

and

$$\lambda_i\{[A_z - B_z K_z - H_{kf} C_z]\} = \left\{ \begin{array}{l} -146.33\text{rad/s} \\ -6.1911\text{rad/s} \\ -3.0038\text{rad/s} \end{array} \right\} \tag{142}$$

These closed loop dynamics are not sufficiently fast as to yield good estimates for use in the regulator as is apparent in the pole at −3rad/s which is the same (approximately) as the regulator closed loop bandwidth. This problem cannot be overcome due to the non minimum phase nature of the unicycle robot, and simply has to be tolerated if full state measurement is not applied. The system space control law is implemented using the transformed state estimate

$$\begin{aligned} \hat{\mathbf{x}}(t) &= \Phi^{-1}\hat{\mathbf{z}}(t) \\ &= \begin{bmatrix} \hat{z}_2 \\ \hat{z}_1 \\ \frac{k_1 g}{k_2 \Omega}\hat{z}_1 + \frac{m_{11}}{k_2 \Omega}\hat{z}_2 \end{bmatrix} = \begin{bmatrix} \dot{\hat{\phi}} \\ \hat{\phi} \\ \dot{\hat{\psi}} \end{bmatrix} \end{aligned} \tag{143}$$

thus the control law is finally

$$u = -[\, G_{\dot{\phi}} \,|\, G_{\phi} \,|\, G_{\dot{\psi}} \,]\, \hat{\mathbf{x}}(t) \tag{144}$$

where the gains G_i are as defined in equation (102) including the Ω terms. Figure 4.15 shows simulation performance of the LTI'd LQG control system for the parameter Ω varied according to the function $\Omega(t)=2\sin(\omega t)+2.1$ for $\omega=0.5$ Hz, approximately system closed loop modal frequencies.

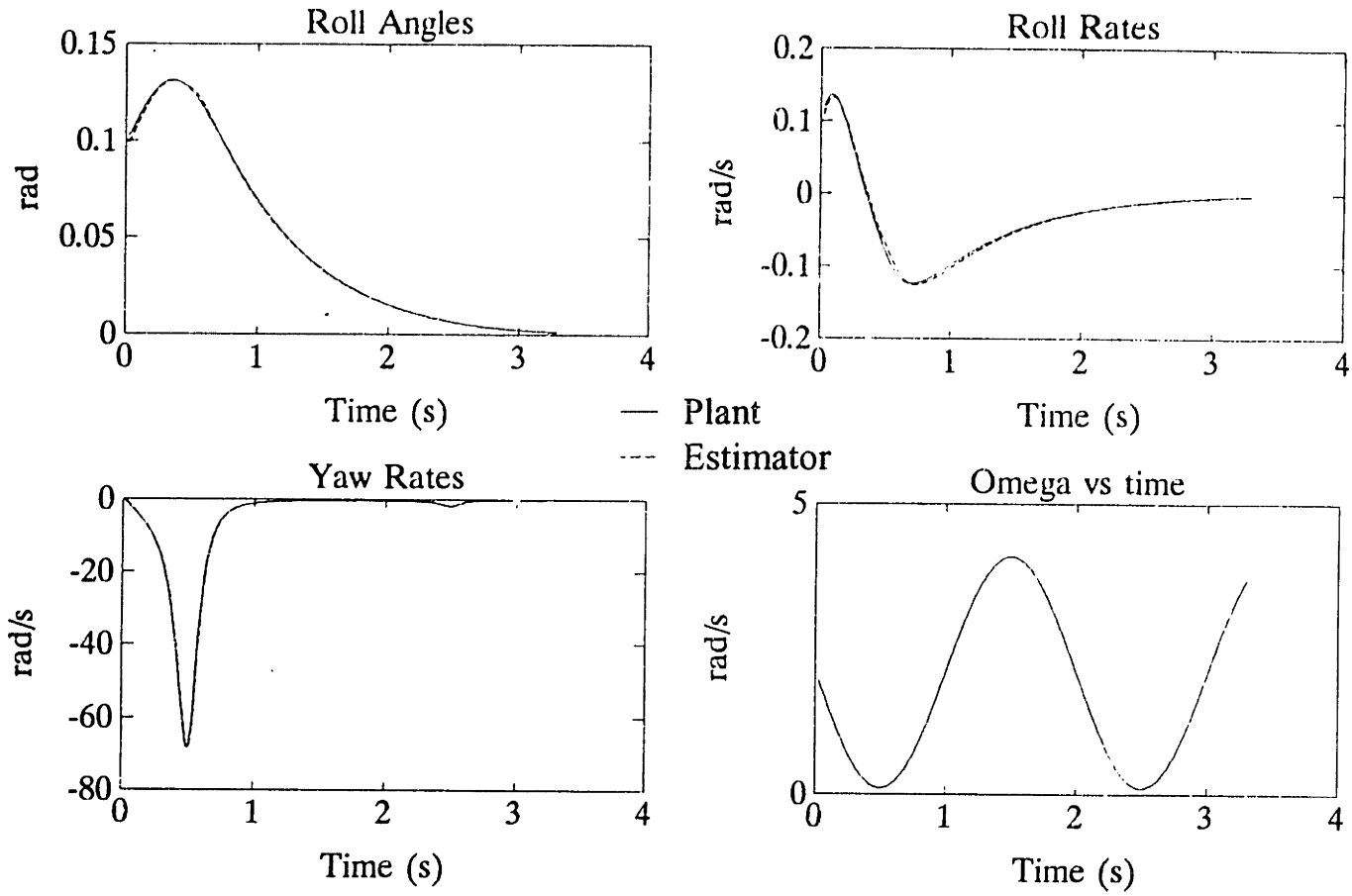

Figure 4.15. LTI'd LQG control system including $\dot{P}$ term, applied to the unicycle simulation. The wheelspeed (parameter) is varied according to $\Omega(t)=2\sin(\omega t)+2.1$ for $\omega=0.5$ Hz (3.14rad/s). Compare with figure 4.14.

IMPLEMENTATION ON ACTUAL UNICYCLE ROBOT

The gain scheduled control laws derived here are implemented on the unicycle robot with great success. The implementation includes the parameter rate of change term in the control law for stability when fast parameter changes occur, as well as design with

the closed loop dynamics slowly varying as a function of the parameter (wheelspeed).

Performance of the gain scheduled system is shown in the many experimental data plots of chapter 2. These are all for the system with full state accessibility. For the case of the full state not measured, with the observer as designed in the previous section, the performance is shown in figure 4.16. Note the relatively poor roll performance due to the phase lag incurred through the observer. Although the observer is designed and implemented in z–space, the non minimum phase zeros still limit the closed loop observer bandwidth, such that in the unicycle example, it is not possible to achieve an observer with closed loop dynamics 4–5 times faster than the regulator dynamics. In fact, the closed loop bandwidth is essentially the *same* for both the regulator and the observer, resulting in significant phase lag in the estimate obtained. This serves once again to illustrate that it is not possible to avoid the non minimum phase issue by transformation or other means; that in the final implementation, these zeros will always be there to degrade the system performance. This is an artifact of the physical system and cannot be avoided.

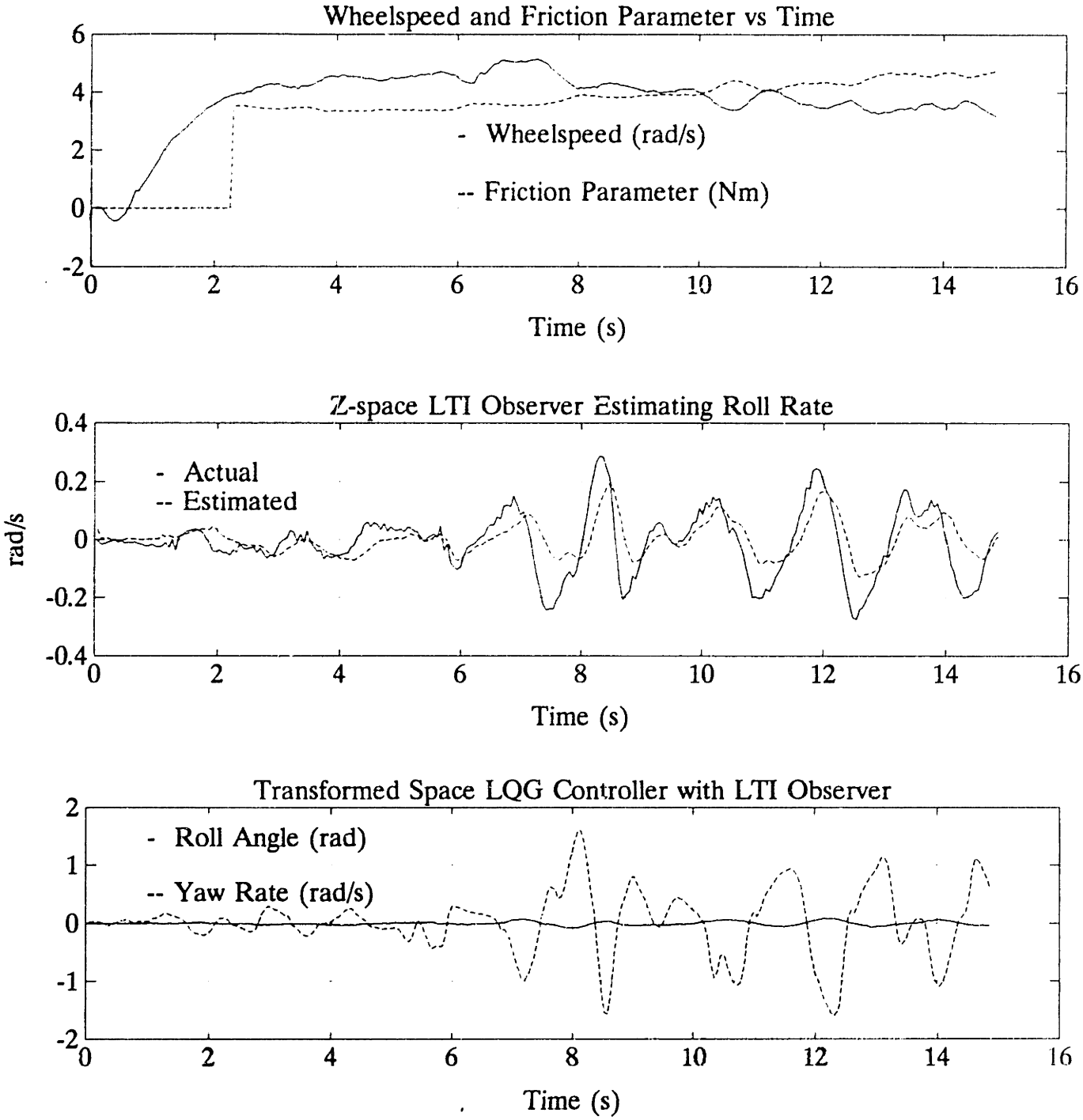

Figure 4.16. LTI'd LQG controller implemented on actual unicycle robot. The inherent phase lag due to the closed loop bandwidth of the observer being limited by the non minimum phase zeros of the lateral dynamics is apparent in the roll rate estimate plot. This phase lag significantly degrades performance of the closed loop system. This data is for the closed loop system including the adaptive friction

compensation scheme (adaptive switching controller) as defined in chapter 3.

CONCLUSION

In this chapter, the gain scheduled control problem has been formally addressed resulting in a clearer understanding of the design procedure than previously known. The basis of evaluation of such parameter dependent systems is to transform the system into a locally (about the equilibrium point of concern) tangent space to the system manifold by means of suitable feedback linearizing control law and a diffeomorphism which is smooth in state variables. Extending this further to the case of suitable feedback LTI'zation, the transformed system is LTI for all parameter, P, and rate of change of parameter, $\dot{P}$, values and analysis and synthesis of controllers may then proceed in the vast world of linear control theory.

The gain scheduled control system must include parameter rate of change dependent terms in order to guarantee stability for any value of, or rate of change of the parameters. The old notion that the parameters must vary slowly for stability is only valid in the case where the $\dot{P}$ term is ignored in the control law, which is the case for these types of controllers designed in the traditional fashion of curve fitting through the gains of LTI controllers designed at various points in the operating envelope. An easy to evaluate means of quantifying how fast the parameters may vary if the $\dot{P}$ term is ignored is described, based on the Circle Criterion applied to the transformed space system.

Since it is often desirable to have the closed loop dynamics slowly varying as a function of the parameters, a measure of how fast this may be done is given. The

simple expression involves both system closed loop time constants and fastest expected parameter change time constants, yielding a Lipschitz constant according to which the (transformed coordinates) gains must be locally Lipschitz continuous in transformed space, to satisfy stability margins determined by another (different to the case of evaluating stability for fast parameter changes) application of the Circle Criterion

Finally, for the case of the full state not accessible, an "LTI'd LQG" design methodology is defined, resulting in an LTI estimator implemented in *transformed coordinates* and driven by the physical system measurements, which gives least squares optimal estimates in **z**–space. The estimates $\hat{\mathbf{z}}$ are then transformed to system space via the feedback linearizing diffeomorphism to yield system state estimates for use in the feedback LTI'ing (gain scheduled) control law which includes the regulator designed in transformed coordinates.

All of the techniques defined are applied to the unicycle robot example and also implemented on the actual robot. Performance is as expected, as is demonstrated by the results presented in chapter 2, in which the feedback LTI'd control law or gain scheduling control law with slowly varying closed loop dynamics as derived in this chapter, is implemented.

CHAPTER 5. SUMMARY AND CONTRIBUTIONS

Contributions

Feedback linearization is extended to explicitly account for the parameter dependent case, where parameters vary in a known fashion. Stability conditions are defined for two cases: 1) the closed loop dynamics are LTI and 2) closed loop dynamics slowly varying with parameter value. Use of the circle criterion for stability to determine conditions on the parameter variation for which the $\dot{P}$ terms may be ignored from the control law, is demonstrated. This is the traditional gain scheduled controller case.

For the case of output feedback (full state inaccessible), under assumptions of 1) scaling of the measurement matrix allows the z–space measurement to be independent of the parameter value (P) and 2) the diffeomorphism may be represented arbitrarily well by a first order Taylor expansion in a neighborhood of the equilibrium point, the gain scheduling technique is extended to an LQG setting with stability guarantees. The (single design point) observer, which runs in z–space, is valid for any parameter value and rate of change.

Necessary implementation extensions to standard Model Reference Adaptive Control techniques applied to friction compensation are determined. The problem to which this is applied is the friction arising in yaw between the tire and surface. The strategies are: 1) Tracking error reset, where the Reference Model trajectory is periodically reset to equal the system response, prevents the traditional "blowing–up" problem of these algorithms. 2) Bounding of the friction model parameters to within physically reasonable values prevents parameter drift in conditions of reduced

persistence of excitation and thus improves stability robustness. 3) Implementing the friction compensation in an adaptive dither setting achieves remarkable performance improvement for this type of friction problem, where the nominal operating condition is zero yaw rate. 4) Finally, for fast operating condition changes, the friction model parameters are not constant and the standard MRAC parameter update laws are not valid. Memorizing (through previous testing) a nominal model of the friction dependence on operating condition solves this problem, since the adaptive control algorithm then only has to adapt on the error between the nominal model and the correct model, which is typically a constant error approximately independent of operating condition, hence the adaptive parameter estimation laws are valid.

Implementing all of these strategies together, yields an extremely well performing adaptive friction compensating controller.

Unicycle Robot Performance Capabilities

The unicycle is routinely operated with all of the discussed control strategies active. The gain scheduled lateral controllers include all parameter rate of change ($\dot{P}$) terms and the adaptive friction compensation algorithm includes the discussed error reset, parameter bounding, memorized nominal model, and adaptive dither strategies.

The robot is capable of stable operation over a range of speeds and surface conditions. Speed ranges for which successful operation has been demonstrated, are from Ω=0.5rad/s (forward speed of $\approx$ 0.12m/s) up to 5.7rad/s (forward speed of $\approx$ 1.37m/s). The top speed is limited by saturation of the A/D converter measuring wheelspeed; this is obviously easily alleviated by suitable scaling of the signal from the tachometer. Minimum speed is limited by the lack of roll controllability at

wheelspeed of zero. Good, stiff performance is maintained for speeds down to $\Omega \approx 0.5$rad/s. At slower speeds, the actuators easily saturate in the attempts to maintain stability.

Performance of the adaptive friction compensation has been demonstrated on a number of surfaces. For steady speed of approximately 3rad/s, the robot has driven between surfaces of polished tiled laboratory floor and 1/4 inch rubber mat as well as between a pebbled paving surface and the same rubber mat, with failure rate of approximately one in eleven attempts. Failure being that the system destabilizes due to the friction adaptation not achieving suitable friction compensation timeously. The unicycle has been operated over the full range of speeds on surfaces of tiled laboratory floor, dry asphalt paving, wet asphalt paving and pebbled paving (pebbles of 3/4 inch mean diameter in concrete matrix). The adaptive friction compensation maintained good stability and performance with exactly the same adaptive algorithms active in all cases.

The gain scheduled controller capability has been well tested, with transition from the minimum speed to the maximum speed through step wheelspeed commands to the longitudinal controller. If, however, the initial conditions are unsuitably far from the nominal equilibrium point (vertical upright balanced condition), i.e. if roll errors are initially greater than 6^o to 8^o, even with roll rates very small (<0.1rad/s), the system may not recover and instability may result. This is more the case for transition from low speed to high speed, than from high speed to low speed due to the lower bandwidth of the lateral controller at low speed.

Pitch stability robustness is very good. The pitch controller has been successfully operated with the turntable removed (turntable mass is 23kg located 0.5m above the

nominal C of G, with system total mass (including turntable) of 50kg and nominal C of G position at 0.9m above ground contact point) and is easily able to recover from 10^0 pitch angle errors. When failure in pitch occurs, it has always been due to saturation of the motor current amplifier cards.

Table 5.1 shows a summary of a series of sixteen test runs in a parking lot of approximately 100 yards by 60 yards dimensions. Surface conditions varied from very wet (puddles of water) asphalt to semi–dry asphalt with the accompanying range of dips and bumps and lose gravel common to any parking lot. Three failures occurred due to an as yet unknown reason, which has been conjectured to be due to temperature cut–out of the actuator amplifier cards. On six occasions, the run was aborted due to turntable spinning up to too high a speed, which leads to strong gyroscopic coupling between the lateral and longitudinal dynamics, for which the controllers are not designed. All other runs (seven) ended as a result of running to the edge of the parking lot. These tests were done for the system commanded straight ahead at nominal wheelspeed setting of 3.3rad/s, although drift in the yaw rate sensor lead to drift in heading and the undulating nature of the surface caused the unicycle to operate over the wheelspeed range of approximately $\Omega \in (1,4.5)$ rad/s.

Future Work

The output feedback case of the gain scheduled controller may be extended to not require the assumption of linearizability of the diffeomorphism in a neighborhood of the equilibrium point. [*Cro Granito–Valavani–Hedrick*] have done similar work, where the strategy is based on Input–Output linearization of the system.

The remaining major goal is to realize a control strategy capable of stable station

keeping. This involves for–aft periodic oscillation of the unicycle in order to maintain lateral controllability for part of the for–aft cycle and thus the ability to recover roll errors.

The unicycle also remains an interesting testbed for further control algorithm research, whether nonlinear, linear or non–parametric regression based.

Duration	End of Run	Comments
37sec	t/table spinup	15deg left at 4sec 20deg left at 12sec t/table spinup at 23sec
23.5sec	t/table spinup	20deg left at 10sec, downhill
36.5sec	roll over	20deg left at 2 & 11sec
22.6sec	t/table spinup	smooth throughout
29.6sec	end of park	10deg left at 10sec
27sec	end of park	70deg left at 2sec 30deg left at 15sec
24sec	t/table spinup	10deg left at 2sec
21sec	end of park	10deg left at 2sec
25sec	t/table spinup	20deg left at 3sec
31sec	end of park	70deg left at 15sec
23sec	t/table spinup	60deg zig-zag at 3sec
38sec	roll over	5deg left at 15 & 25sec
35sec	end of park	generally straight ahead
35sec	end of park	30deg right at 7sec 30deg left at 13sec
23sec	end of park	slow left drift to edge of park
39sec	roll over	30deg zig-zag at 26sec & 35sec

Table 5.1. Summary of autonomous test runs in open parking lot (≈100×60 yds). Setpoint values: steady forward speed (Ω_{ref}=3.3rad/s) and steady heading.

REFERENCES

Aggarwal, J.K. and E.F. Infante, "Some Remarks on the Stability of Time–Varying Systems", IEEE Trans. Aut. Control, Vol AC–13, pp722–723, December 1968.

Anderson, B. D. O., R. R. Bitmead, C. R. Johnson, Jr., P. V. Kokotovic, R. L. Kosut, I. M. Y. Mareels, L. Praly, B. D. Riedle, "Stability of Adaptive Systems: Passivity and Averaging Analysis", MIT Press, Cambridge, MA, 1986.

Åström, K. J. and B. Wittenkark, "Adaptive Control", 1989, Addison–Wesley, New York.

Åström, K. J. and T. Hägglund, "Practical Experiences of Adaptive Techniques", No. TP3 2:30, Proceedings of American Control Conference, 1990.

Aikeson, C. G., C. H. An and J. M. Hollerbach, "Model–Based Control of a Robot Manipulator", MIT Press, Cambridge, Massachusetts, 1988.

Brockett, R.W., "Feedback Invariants for Nonlinear Systems", 7th IFAC World Congress, pp 1115–1120, Helsinki, Finland, 1978.

Bryson, A. E. Jr., and Yu–Chi Ho, "Applied Optimal Control", Hemisphere Publishing Corporation, New York, 1975.

Canudas, C., K. J. Åström and K. Braun, "Adaptive Friction Compensation in DC–Motor Drives", IEEE Journal of Robotics and Automation, Vol. RA–3, No. 6, December 1987.

Canudas de Wit, C. A., "Adaptive Control for Partially Known Systems", Elsevier science Publishers, B. V., Amsterdam, 1988.

Cro Granito, J.A., L. Valavani and J.K. Hedrick, "Servo Design for Nonlinear Systems with Output Feedback",

Fu, L–C., "A New Approach for solving Model Reference Adaptive Control Problem for Fast Time–Varying Unknown Plants with Relative Degree One", American Control Conference paper no. TA3 8:30, 1990.

Guez, A., J. Eilbert and M. Kam, "Neuromorphic Architectures for Fast Adaptive Control", Drexel University, Philadelphia, PA, IEEE paper no. CCH2555, 1988.

Haber, R., L. Keviczky and H. Unbehauen, "Application of Adaptive Control on Nonlinear Dynamic Processes – A Survey on Input–Output Approaches", IFAC 10th Triennial World Congress, Munich, FRG, 1987.

Hatwell, M. S., B. J. Oderkerk, C. Ari Sacher and G. F. Inbar, "The Development of a Model Reference Adaptive Controller to Control the Knee Joint of Paraplegics", IEEE Trans. Aut. Control, Vol. 36, No. 6, June 1991.

Hauser, J., S. Sastry and G. Meyer, "On the Design of Nonlinear Controllers for Flight Control Systems", AIAA paper # 89–3489–CP, 1989.

Hunt, L.R., R. Su and G. Meyer, "Global Transformations of Nonlinear Systems", IEEE Trans. Aut. Control, Vol. AC–28, No. 1, January 1983.

Hunt, L.R., R. Su and G. Meyer, "Design for multi–input nonlinear systems in Differential Geometric Control Theory, R.W. Brockett, R.S. Millman and H.S. Sussmann, eds., pp268–297, Birkhäuser, Boston, MA, 1983.

Isidori, A., "Nonlinear Control Systems", 1989, Springer–Verlag, New York.

Jabbari, A., M. Tomizuka and T. Sakaguchi, "Robust Nonlinear Control of Positioning Systems with Stiction", American Control Conference paper no. TA4 8:30, 1990.

Jordan, M. I. and D. Rumelhart, "Forward Models: Supervised Learning with a Distal Teacher", submitted to "Cognitive Science", July 1990.

Kailath, T., "Linear Systems", Prentice–Hall, Englewood Cliffs, NJ, 1980.

Kanellakopoulos, I. and P. V. Kokotovic, "Adaptive Control Design for a Class of Nonlinear Systems", American Control Conference paper no. TP6 5:00, 1990.

Kang, H., G. Vachtsevanos and F. L. Lewis, "Lyapunov Redesign for Structural Convergence Improvement in Adaptive Control", IEEE Trans. Aut. Control, Vol. 35, No. 2, Feb 1990.

Kokotovic', P.V., I. Kanellakopoulos and A.S. Morse, "Adaptive Feedback Linearization of Nonlinear Systems", Lecture Notes in Control and Information Sciences Vol 160, M. Thoma and A. Wyner, eds., Springer–Verlag, Berlin, 1991.

Krener, A.J., "On the Equivalence of Control Systems and the Linearization of

Nonlinear Systems", SIAM J. Control, Vol 11 No. 4, November 1973.

Kubo, T., G. Anwar and M. Tomizuka, "Application of Nonlinear Friction Compensation to Robot Arm Control", IEEE paper no. CH2282–2/86/0000/0722, 1986.

Kwakernaak, H. and R. Sivan, "Linear Optimal Control Systems", Wiley–Interscience, John Wiley & Sons, 1972, New York.

La Salle, J.P., "Some Extensions of Liapunov's Second Method", IRE Trans. on Circuit Theory, Vol. CT–7, December 1960.

Landau, Y. D., "Adaptive Control", Marcel Dekker Inc., New York, 1979.

Lawrence, D. A. and W. J. Rugh, "On a Stability Theorem for Nonlinear Systems with Slowly Varying Inputs", IEEE Trans. Aut. Control, Vol. 35. No. 7, July 1990.

Lefschetz, S., "Stability of Nonlinear Control Systems", Academic Press, New York, 1962.

Maron, J. C., "Identification and Adaptive Control of Mechanical Systems with Friction", IFAC Adaptive Systems in Control and Signal Processing, Glasgow, UK, 1989.

Marino, R. and P. Tomei, "Global Adaptive Observers and Output–Feedback Stabilization for a Class of Nonlinear Systems", Lecture Notes in Control and Information Sciences Vol. 160, Springer–Verlag, Berlin, Heidelberg, 1991.

McRuer, D., I. Ashkenas and D. Graham, "Aircraft Dynamics and Automatic Control", Princeton University Press, Princeton, New Jersey, 1973.

Meyer, G., R. Su and L.R. Hunt, "Application of Nonlinear Transformations to Automatic Flight Control", *Automatica*, Vol 20, No. 1, pp103–107, 1984.

Narendra, K.S. and J.H. Taylor, "Frequency Domain Criteria for Absolute Stability", Academic Press, New York 1973.

Nguyen, D. H. and B. Widrow, "Neural Networks for Self–Learning Control Systems", IEEE Control Systems Magazine, Vol. 10, No. 3, April 1990.

Niemi, A.J., "Invariant Control of Variable Flow Processes", 8th IFAC World Congress, Kyoto, Japan, 1981, pp2687–2692.

Nijmeijer, H. and A.J. van der Schaft, "Nonlinear Dynamical Control Systems", Springer–Verlag, New York, 1990.

Papadopoulos, J. "Discussion of Bicycle–Tire Modelling", Internal Note, Cornell University, Cornell, NY, 1987.

Radcliffe, C. J. and S. C. Southward, "A Property of Stick–Slip Friction Models which Promotes Limit Cycle Generation", American Control Conference paper no TA6 11:00, 1990.

Rohrs, C. E., L. Valavani, M. Athans and G. Stein, "Robustness of Adaptive Control Algorithms in the Presence of Unmodeled Dynamics", Proceedings of 21st IEEE

CDC, 1982.

Rohrs, C. E., L. Valavani, M. Athans and G. Stein, "Some Design Guidelines for Discrete Time Adaptive Controllers", *Automatica*, Vol. 20, No. 5, 1984.

Rugh, W. J., "Analytical Framework for Gain Scheduling", Proceedings of 1990 American Control Conference, pp1688–1694.

Rumelhart, D. E. and J. L. McLelland and the PDP Research Group, "Parallel Distributed Processing", MIT Press, Cambridge, MA, 1986.

Schoonwinkel, A. "Design and Test of a Computer Stabilized Unicycle", PhD Thesis, Stanford University, Palo Alto, 1987.

Shamma, J. S. and M. Athans, "Stability and Robustness of Slowly Time–Varying Linear Systems", Proc. of 26th CDC, Los Angeles, CA, December 1987, pp434–439.

Shamma, J. S. and M. Athans, "Analysis of Gain Scheduled Control for Nonlinear Plants", IEEE Trans. Aut. Control, Vol. 35, No. 8, August 1990.

Slotine, J–J. E. and W. Li, "Theoretical Issues in Adaptive Manipulator Control", The Fifth Yale Workshop on Applications of Adaptive Systems Theory, May 1987.

Slotine, J–J. E. and W. Li, "Applied Nonlinear Control", Prentice–Hall, Englewood Cliffs, NJ, 1991.

Su, R., "On the linear equivalents of nonlinear systems", Systems and Control

Letters, Vol. 2, No. 1, July 1982, pp48–52.

Teel, A., R. Kadiyala, P. Kokotovic and S. Sastry, "Indirect Techniques for Adaptive Input Output Linearization of Nonlinear Systems", American Control Conference paper no. WA3 11:45, 1990.

Townsend, W. T. and J. K. Salisbury Jr., "The Effect of Coulomb Friction and Stiction on Force Control", IEEE paper no. CH2413–3/87/0000/0883, 1987.

Vidyasagar, M., "Nonlinear Systems Analysis", Prentice–Hall Englewood Cliffs, New Jersey, 1978.

Vos, D.W., "Dynamics and Nonlinear, Adaptive Control of and Autonomous Unicycle", S.M. thesis, MIT dept. of Aeronautics and Astronautics, May 1989.

Vos, D. W. and A. H. von Flotow, "Dynamics and Nonlinear Adaptive Control of an Autonomous Unicycle: Theory and Experiment", AIAA Dynamics Specialist Conference, Long Beach, CA, 1990.

Vos, D. W., L. Valavani and A. H. von Flotow, "Intelligent Model Reference Nonlinear Friction Compensation using Neural Networks and Lyapunov Based Adaptive Control", IEEE Int. Symposium on Intelligent Control, 1991.

Vos, D. W., W. Baker and P. Millington, "Learning Augmented Gain Scheduling Control", AIAA GNC Conference paper no. AIAA 91–2717, 1991.

Vos, D. W. and L. Valavani, "Input–Output Linearization using Model Reference

Adaptive Control Techniques", IEEE CDC, Brighton, U.K., 1991.

von Flotow, A. H. and P. R. Williamson, "Deployment of a Tethered Satellite into Low Earth Orbit for Plasma Diagnostics", JAS Vol. 34 no. 1, Jan–March 1986, pp 65–90.

Wu, M.Y., "A Note on Stability of Linear Time–Varying Systems", IEEE Trans. Aut. Control, Vol. AC–19, April 1974.